

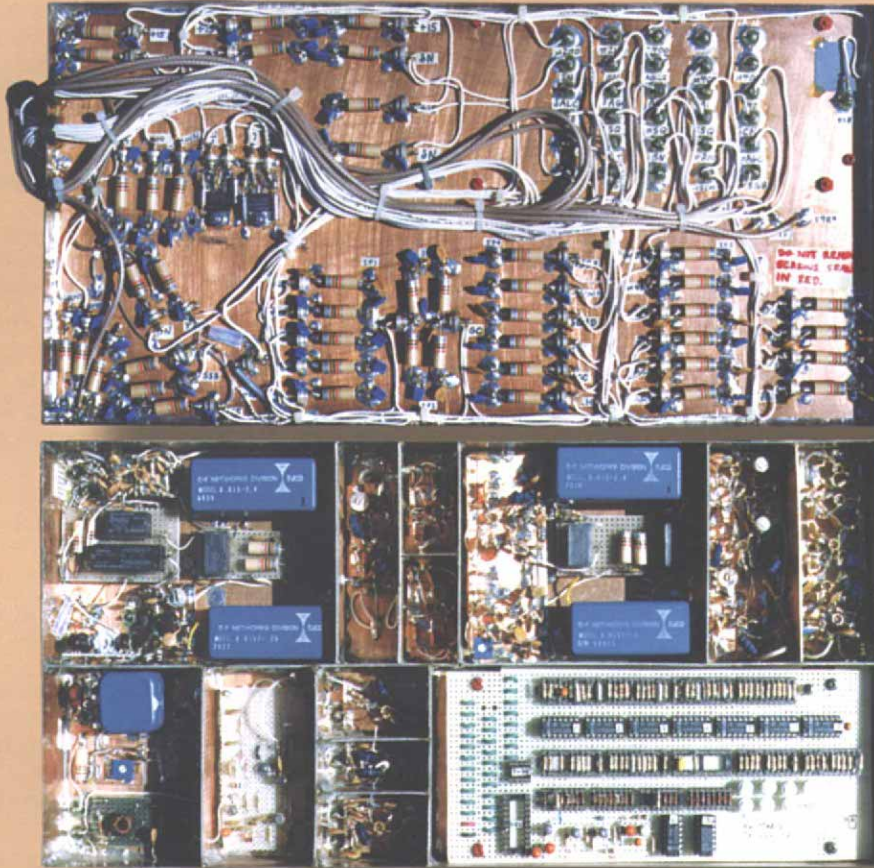
QEX

September/October 1999

\$5



Forum for Communications Experimenters



More of the High-Performance Homebrew Transceiver

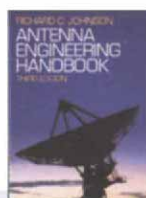
QEX: Forum for
Communications Experimenters
American Radio Relay League
225 Main Street
Newington, CT USA 06111-1494

TECHNICAL BOOKS

the antennas & propagation collection



Microstrip Antennas
David M. Pozar and Daniel H. Schaubert
 430 pages of antenna designs, theoretical and practical techniques for microstrip antennas. Covers element types, feed systems, polarization, bandwidth improvement and more.



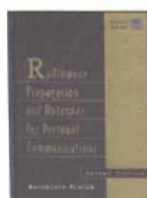
Antenna Engineering Handbook
Richard C. Johnson, editor
 The most widely-used reference for antenna engineering from VLF to microwaves, covering all standard antenna types and more. Each chapter written by an expert contributor.
MH-4 \$120.00



Introduction to Radio Propagation for Fixed and Mobile Communications
John Doble
 Basic insight into fixed-link and mobile radio propagation effects. Includes data on in-building systems and diversity techniques.
AH-48 \$69.00



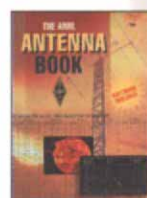
Antennas
John Kraus
 A classic text by an important researcher and teacher, required for any antenna design reference library. Has a good combination of strong theory and practical applications.
MH-14 \$89.00



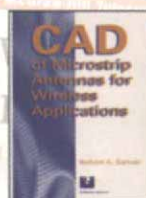
Radiowave Propagation and Antennas for Personal Communications
Kazimierz Siwiak
 A thorough review of propagation in mobile environments, antenna types and their performance. Includes a program disk.
AH-7 \$89.00



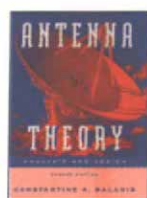
Phased Array Antennas
R.C. Hansen
 Detailed coverage of both practice and theory in the design and analysis of antenna arrays, from sidelobe considerations to superdirectivity and HTS antennas.



The ARRL Antenna Book
Gerald L. Hall, editor
 A practical guide to the design and construction of antennas for HF through microwave, valuable data for amateur and professional designers and experimenters.
AR-2 \$30.00



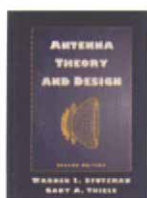
CAD of Microstrip Antennas for Wireless Applications
Robert A. Sainati
 Provides understanding of microstrip antennas and supplies the tools for design work. Written for engineers who are not antenna specialists.
AH-59 \$89.00



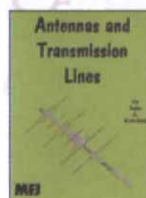
Antenna Theory: Analysis & Design, Second Edition
Constantine A. Balanis
 Emphasis on design, with a solid theoretical foundation. Excellent coverage of antenna terminology and performance parameters.
JW-11 \$103.00



Ionospheric Radio
Kenneth Davies
 An especially well-written and understandable text on radiowave propagation. A complete summary of all aspects of solar-terrestrial interaction and its effects.
IN-1 \$88.00



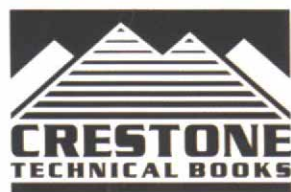
Antenna Theory and Design, Second Edition
Warren L. Stutzman and Gary A. Thiele
 New edition covers resonant, broadband and aperture antennas, lines and feeds, arrays, systems and electromagnetic modeling.
JW-29 \$100.00



Antennas and Transmission Lines
John A. Kuecken
 A handy collection of short, to-the-point chapters with the basic design equations for various antennas, matching, self-impedance, noise and radio range prediction.
MF-2 \$20.00

THE POWER OF INFORMATION

www.noblepub.com



Crestone Technical Books
 Division of Noble Publishing Corp.
 4772 Stone Drive
 Tucker, GA 30084
 Tel: 770-908-2320
 Fax: 770-939-0157

Order today by phone, fax or on the web, using your VISA, Mastercard or American Express!

QEX

QEX (ISSN: 0886-8093) is published bimonthly in [January '99](#), [March '99](#), [May '99](#), [July '99](#), [September '99](#), and [November '99](#) by the American Radio Relay League, 225 Main Street, Newington CT 06111-1494. Subscription rate for 6 issues to ARRL members is \$22; nonmembers \$34. Other rates are listed below. Periodicals postage paid at Hartford, CT and at additional mailing offices.

POSTMASTER: Form 3579 requested. Send address changes to: QEX, 225 Main St, Newington, CT 06111-1494
Issue No 196

David Sumner, K1ZZ
Publisher

Doug Smith, KF6DX
Editor

Robert Schetgen, KU7G
Managing Editor

Lori Weinberg
Assistant Editor

Zack Lau, W1VT
Contributing Editor

Production Department

Mark J. Wilson, K1RO
Publications Manager

Michelle Bloom, WB1ENT
Production Supervisor

Sue Fagan
Graphic Design Supervisor

David Pingree, N1NAS
Technical Illustrator

Joe Shea
Production Assistant

Advertising Information Contact:

Robin Mickett, N1WAL, *Advertising*
American Radio Relay League
860-594-0207 direct
860-594-0200 ARRL
860-594-0259 fax

Circulation Department

Debra Jahnke, *Manager*
Kathy Capodicasa, N1GZO, *Deputy Manager*
Cathy Stepina, *QEX Circulation*

Offices

225 Main St, Newington, CT 06111-1494 USA
Telephone: 860-594-0200
Telex: 650215-5052 MCI
Fax: 860-594-0259 (24 hour direct line)
e-mail: qex@arrl.org

Subscription rate for 6 issues:

In the US: ARRL Member \$22,
nonmember \$34;

US, Canada and Mexico by First Class Mail:
ARRL member \$35, nonmember \$47;

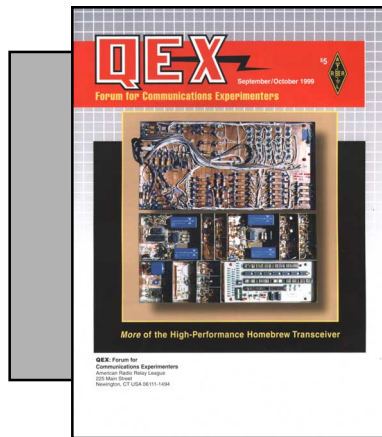
Elsewhere by Surface Mail (4-8 week delivery):
ARRL member \$27,
nonmember \$39;

Elsewhere by Airmail: ARRL member \$55,
nonmember \$67.

Members are asked to include their membership control number or a label from their QST wrapper when applying.

In order to ensure prompt delivery, we ask that you periodically check the address information on your mailing label. If you find any inaccuracies, please contact the Circulation Department immediately. Thank you for your assistance.

Copyright ©1999 by the American Radio Relay League Inc. For permission to quote or reprint material from QEX or any ARRL publication, send a written request including the issue date (or book title), article, page numbers and a description of where you intend to use the reprinted material. Send the request to the office of the Publications Manager (permission@arrl.org)



Go inside the high-performance homebrew transceiver in Part 2 of the series. K5AM's article begins on [page 3](#).



Features

3 A High-Performance Homebrew Transceiver: Part 2
By Mark Mandelkern, K5AM

9 The Bedford Receiver: A New Approach
By Rodney Green, VK6KRG

24 Parabolic Dish Feeds—Phase and Phase Center
By Paul Wade, W1GHZ

36 Basics of Digital-Receiver Design
By Brad Brannon, N4RGI

45 Narrow-Band Doppler Spectrum Techniques for Propagation Study
By Peter Martinez, G3PLX

52 Underground HF Antennas
By Grant Bingeman, KM5RG

55 Current Sources
By Parker R. Cope, W2GOM/7

Columns

57 RF *By Zack Lau, W1VT*

64 Strays

63 Upcoming Technical Conferences

64 Next Issue in QEX

59 Letters to the Editor

Sept/Oct 1999 QEX Advertising Index

American Radio Relay League: [Cov III](#),
[Cov IV](#)
Communications Specialists, Inc: [64](#)

Crestone Technical Books: [Cov II](#)
Tucson Amateur Packet Radio Corp: [35](#)
Z Domain Technologies, Inc: [51](#)



The American Radio Relay League, Inc. is a noncommercial association of radio amateurs, organized for the promotion of interests in Amateur Radio communication and experimentation, for the establishment of networks to provide communications in the event of disasters or other emergencies, for the advancement of radio art and of the public welfare, for the representation of the radio amateur in legislative matters, and for the maintenance of fraternalism and a high standard of conduct.

ARRL is an incorporated association without capital stock chartered under the laws of the state of Connecticut, and is an exempt organization under Section 501(c)(3) of the Internal Revenue Code of 1986. Its affairs are governed by a Board of Directors, whose voting members are elected every two years by the general membership. The officers are elected or appointed by the Directors. The League is noncommercial, and no one who could gain financially from the shaping of its affairs is eligible for membership on its Board.

"Of, by, and for the radio amateur," ARRL numbers within its ranks the vast majority of active amateurs in the nation and has a proud history of achievement as the standard-bearer in amateur affairs.

A bona fide interest in Amateur Radio is the only essential qualification of membership; an Amateur Radio license is not a prerequisite, although full voting membership is granted only to licensed amateurs in the US.

Membership inquiries and general correspondence should be addressed to the administrative headquarters at 225 Main Street, Newington, CT 06111 USA.

Telephone: 860-594-0200
Telex: 650215-5052 MC1
MCIMAIL (electronic mail system) ID: 215-5052
FAX: 860-594-0259 (24-hour direct line)

Officers

President: RODNEY STAFFORD, W6ROD
5155 Shadow Estates, San Jose, CA 95135

Executive Vice President: DAVID SUMNER, K1ZZ

The purpose of *QEX* is to:

- 1) provide a medium for the exchange of ideas and information among Amateur Radio experimenters,
- 2) document advanced technical work in the Amateur Radio field, and
- 3) support efforts to advance the state of the Amateur Radio art.

All correspondence concerning *QEX* should be addressed to the American Radio Relay League, 225 Main Street, Newington, CT 06111 USA. Envelopes containing manuscripts and letters for publication in *QEX* should be marked Editor, *QEX*.

Both theoretical and practical technical articles are welcomed. Manuscripts should be submitted on IBM or Mac format 3.5-inch diskette in word-processor format, if possible. We can redraw any figures as long as their content is clear. Photos should be glossy, color or black-and-white prints of at least the size they are to appear in *QEX*. Further information for authors can be found on the Web at www.arrl.org/qex/ or by e-mail to qex@arrl.org.

Any opinions expressed in *QEX* are those of the authors, not necessarily those of the Editor or the League. While we strive to ensure all material is technically correct, authors are expected to defend their own assertions. Products mentioned are included for your information only; no endorsement is implied. Readers are cautioned to verify the availability of products before sending money to vendors.

Empirically Speaking

We're seeing a lot of good receiver articles and discussion lately. This is encouraging; it's an area where both new and old technologies can enhance the enjoyment and use of our resources. Elegance in design implies maximizing performance-to-cost ratios; receivers are certainly no exception to this.

The order of the scientific method—measure, formulate, theorize—tends to reverse when we are wishing for something better than what we have. That's all right as long as we finally get down to the nitty-gritty. Let me work it in its normal direction, though, as I add my two cents worth.

I find that not all receivers have very high dynamic range (DR). Further, I find those that have it tend to cost more. Seeking a formula for the relation between performance and cost, I make a graph and find it somehow exponential; at some point, the cost increases much faster than the performance. I ask myself "Why?" and come up with the same answer as did many *QEX* correspondents. I see that many receiver sections must be simultaneously improved to move up the DR performance curve. I conclude it is tougher than it initially seems.

So the challenge is: Exactly what new circuits and techniques do you have that will help us get past the curve? *QEX* is the ideal medium for showing how you broke through.

In This *QEX*

Mark Mandelkern, K5AM, returns with the second installment about his homebrew transceiver. We've had the overview, now it is time to dive into the subsystem details. Mark's 9-MHz IF strip includes his optimized AGC, "non-crunch" noise blanker and an RF speech clipper for maximum intelligibility under difficult conditions.

Our recent international flavor continues as **Rodney Green, VK6KRG**, contributes the "Bedford" receiver. This architecture is new as far as we know. It holds the promise of flexibility and high performance for home-brewers and working engineers alike. Check it out.

Paul Wade, W1GHZ, takes a close look at phasing effects in parabolic dish feeds and explains the concept of "phase center." It's surprising what variations in gain and beamwidth are produced with small changes in feed location. Why not get that extra decibel or more? P3D proponents take note.

Brad Brannon, N4RGI, brings the perspective of an ADC designer into our discussion of receiver topologies. He focuses on dynamic-range issues facing those of us using DSP to reduce the cost and complexity of equipment. The advantages and limitations of state-of-the-art data-acquisition techniques are thoroughly examined. Brad puts it all together by defining a set of realistic performance expectations that foretell the immediate future of digital-radio strategies. Thanks to *EDN* and Michael Markowitz for reprint permission.

Peter Martinez, G3PLX, examines another use for those extremely narrow (25 mHz!) DSP filters: mapping of propagation media with "dopplergrams." Here is a field of research open to amateurs that can now be explored with minimal investment in equipment. Many thanks to *RadCom* and our RSGB friends once again.

Grant Bingham, KM5KG, looks at antenna performance from a different viewpoint: underground. **Parker Cope, W2GOM/7**, has some notes on current regulators along with some circuit examples. In his "RF" column, Zack builds a low-loss impedance transformer for 450:50 Ω.—73, **Doug Smith, KF6DX**; kf6dx@arrl.org □□

A High-Performance Homebrew Transceiver: Part 2

Let's begin our look inside this transceiver with the IF board. It contains the IF amplifier, AGC, noise-blanker and RF speech clipper circuits.

By Mark Mandelkern, K5AM

Part 1 gave a general description of the K5AM homebrew transceiver, built for serious DX work and contest operating.¹ This article gives complete circuit details for the IF board. While obtaining gain at 9 MHz is routine, care is taken to ensure optimal AGC performance, non-crunch noise blanking and QRM-piercing transmit audio.

The IF board in any radio is perhaps its most crucial component. While the other parts of the radio are certainly important, converting to the IF—and later to audio—are essentially trans-

lation functions. The IF board must provide most of the gain; it must control this gain automatically and smoothly, provide all of the selectivity, blank out noise and also process the transmitted signals.

IF-Board Features

The IF board is shown in [Fig 1](#). Relay-switching of the SSB and CW filters avoids diode-generated distortion. This also reduces “blow-by,” resulting in high ultimate attenuation. Sharp filters are used near the IF amplifier’s output, as well as at the input. This improves the signal-to-noise ratio.

Other features include:

- A high-performance, no-pop, no-click, hang-AGC circuit²
- A non-crunching noise blanker³

- A sensitive integrating squelch circuit (see [Reference 2](#))
- RF speech clipping for transmitted SSB with a punch
- Special operating features (discussed in [Part 1](#))

The Circuit

A general description of the IF board has been given in [Part 1](#). The IF board consists of the IF amplifier, noise blanker and AGC section. The block diagram in [Fig 2](#) shows the arrangement of the three sections as well as the individual stages of the IF amplifier. An explanation of the terminal designations is given in [Table 1](#). The attenuator pads at the input and output of each crystal filter provide proper out-of-band terminations,

¹Notes appear on [page 8](#).

reduce distortion and improve the skirt and ultimate selectivity. The 9-dB pad before the second SSB filter compensates for the additional loss of the CW filter, and assures proper performance of the RF speech clipper (see below). Fig 3 shows the IF-amplifier schematic diagram. The various control lines are provided by the logic board.

RF Speech Clipper

A general description of the RF speech clipper, including microphone calibration and operating instructions, was given in Part 1. The clipper has three sections. The DSB amplifier, Q8, controls the amount of RF clipping by adjusting the input level to the IF amplifier, using the **CLIPPING** control on the front panel. When receiving, or when transmitting in the carrier modes (CW, AM, FM), the DSB amplifier (Q8), the clipping meter amplifier (Q9) and the SSB output buffer (Q10) are disabled by control line β SSB. The clipper proper consists of the two diodes in the drain circuit of Q4. The third section of the RF speech-clipping system provides metering on the front panel. It consists of amplifier Q9 and two op amps; see Figs 2 and 5. Clipping-meter amplifier Q9 parallels Q4, with a detector at the output rather than clipping diodes. This detector provides an output that tracks the amount of conduction in the clipping diodes. The detector output is amplified by a peak-indicating circuit, shown in Fig 5, and displayed on meter M1. The peak-indicating circuit gives the operator true indications of RF speech clipping level.

One special element in the clipper circuit is crucial for proper performance. Credit for it is due to Robert Sherwood, NC0B, and it was communicated to me by Paul Kollar, W8CXS. This crucial element is the isolation between the clipping diodes and the following SSB filter. Rob conducted extensive tests on the CX7 clipping circuit—which had no isolation. He found that the clipping circuit caused distortion because it was an inadequate termination for the filter. The necessary isolation may be provided by either a pad or a buffer stage. In this circuit, an additional 9-dB pad is added ahead of the SSB filter. The pad also conveniently compensates for the extra loss of the CW filter. The resultant 12 dB of attenuation provides a stable load for clipping stage Q4 as well as proper termination for the filter.

Noise Blanker

The noise blanker has been described in Reference 3. When not in use, the noise blanker is switched completely out of the signal path by relay K1, at the input to the IF amplifier. This avoids any possible signal degradation by the blanker gate diodes. The noise-channel gain is set by the front-panel **BLANKER** control through control line δ N and the op-amp circuit shown in Fig 5.

A tap on the noise amplifier provides a signal to feed an external monitor scope via the **SCOPE** (output) jack on the rear panel. A scope is very useful for locating nearby power-line noise. Attempts to locate such noise by watching the S-meter indication while rotating the antenna are doomed; the meter only shows the aggregate noise peak. A scope, on the other hand, can be used to determine the direction of the individual noise sources, since each noise source tends to have a distinctive oscillograph signature.

This precise information can then be relayed to the local power company.

An AGC Update

More experience on the 160-meter band with extremely weak DX signals under high-atmospheric-noise conditions has led to a further AGC improvement. Under such conditions, it is best to use zero hang time, in the **FAST** mode. The modification is simple. Look at Fig 8 in Reference 2, disconnect the Fast Adjust trimmer from terminal F of the **AGC HANG TIME** switch; then connect terminal F to the collector of the discharge transistor, Q304.

Construction

The general method of construction was described in Part 1, where the need for careful shielding and lead filtering was emphasized. Each power and control lead to the IF board passes through a π -section filter (two 10-nF bypass capacitors and a 1-mH choke) and a 1-nF feed-through capacitor.

Table 1

Terminals on the diagrams are labeled according to the function of the signal or control line. The characteristic of each line is indicated by an initial Greek letter, according to the following scheme:

α	alpha	Line keyed to ground, such as PTT and Keyline
β	beta	Control line that switches nominally from +15 to -15 V
δ	delta	dc control line
ι	iota	Local oscillator injection voltage for a mixer
ρ	rho	Rheostat or potentiometer control line
σ	sigma	Signal
μ	mu	Control line that switches nominally from 0 to -15 V
ϕ	phi	RF voltage obtained from an oscillator

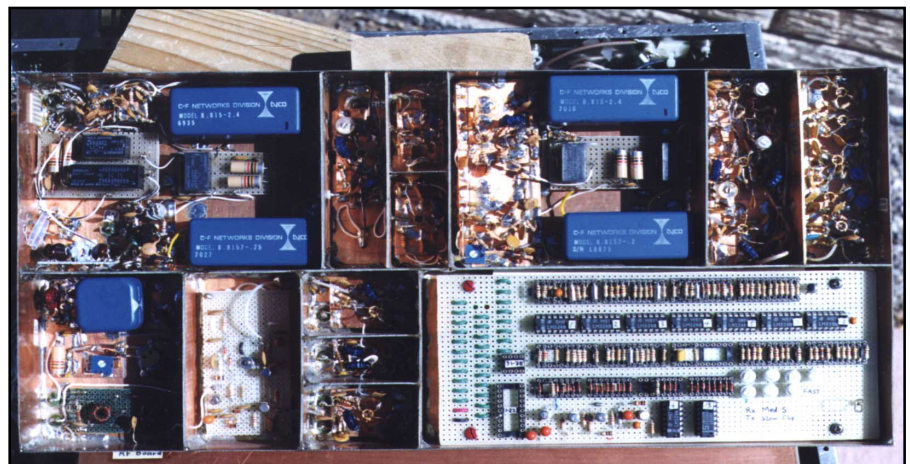


Fig 1—Top view of the IF board in the K5AM homebrew transceiver. Several shielding-compartment covers have been removed for this photo. The IF amplifier is at the top, with signals traveling left to right. The noise blanker and AGC sections are below, on the left and right, respectively. (Photo by Lisa Mandelkern.)

In passing signals to and from the board, it is important to avoid any signal leakage. Teflon-insulated miniature coax, type RG-178B, facilitates good connections because it allows safe use of a soldering iron. Simply drill a hole (# 51 bit) through the circuit board, remove the cable's outer jacket and solder the braid to both sides of the board.

The board's bottom surface is shown in Fig 6. Each IF stage is built dead-bug style on a sub-board mounted inside its separate compartment. Power and control leads connect to the feed-through capacitors on the floor of the main board. Coax cables run through the floor and up to the sub-boards. The AGC sub-board is constructed using wire-wrap methods on perf-board.

Alignment

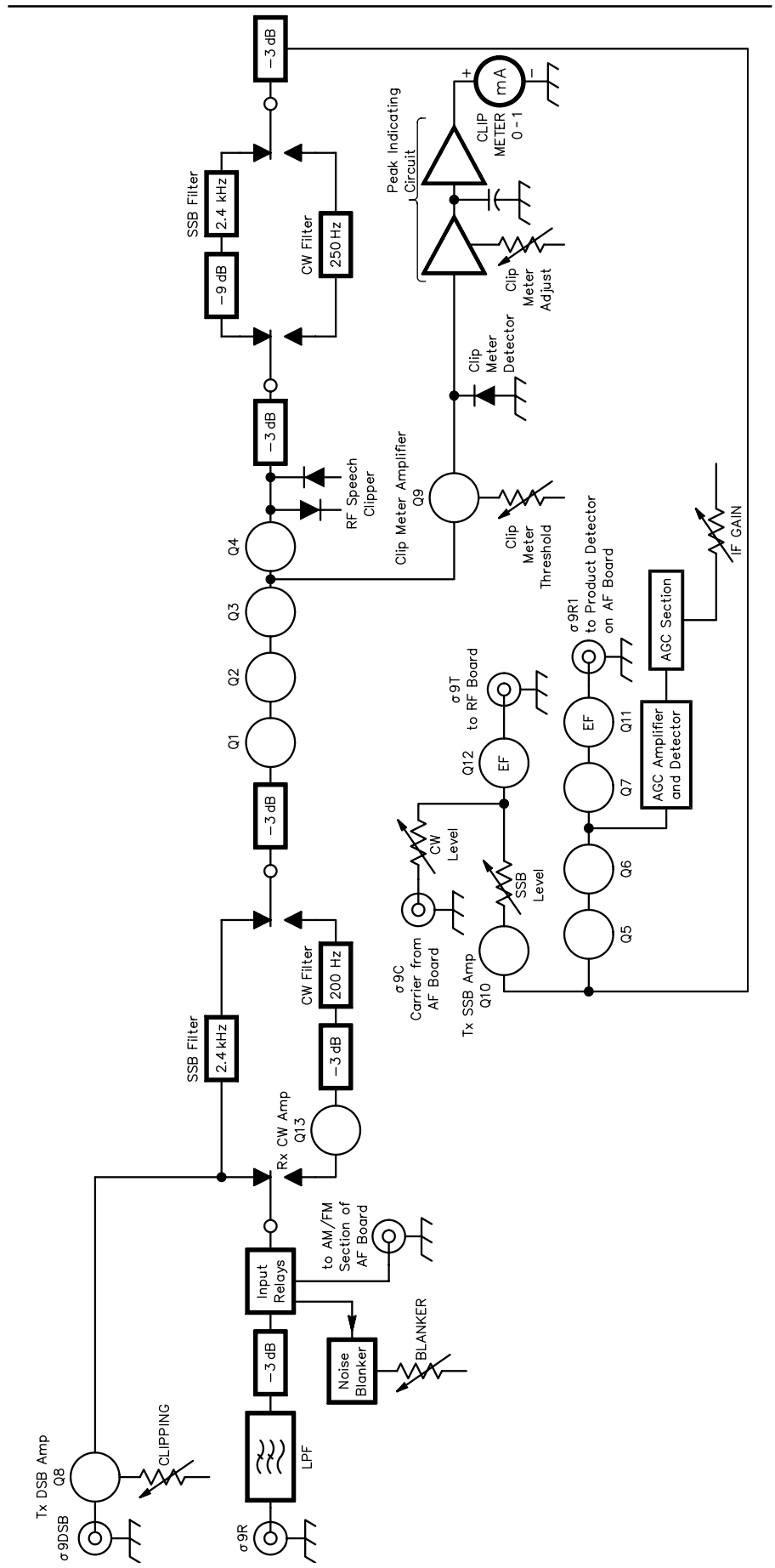
The IF amplifier operates at a gain of 90 dB overall, between terminals $\sigma 9R$ and $\sigma 9R1$. First, the no-signal AGC line level is set to 2.0 V by the Rx Gain Adjust trimmer in the AGC section (see Fig 7 in Reference 2).

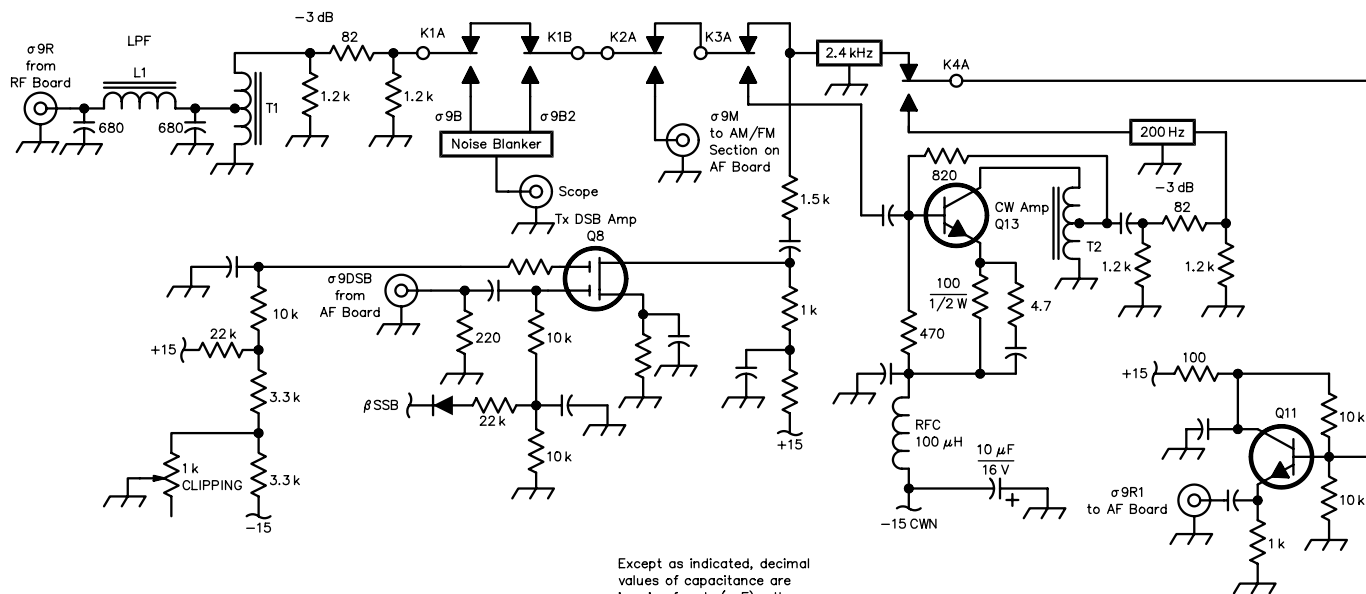
Then, with the AGC off, and an input at $\sigma 9R$ of -100 dBm, adjust the IF Gain Adjust trimmer at Q7 for an output at $\sigma 9R1$ of 200 mV (P-P, -10 dBm).

The output level of the IF amplifier with the AGC on is set by the AGC Adjust trimmer (see Fig 6 in Reference 2). With a -70 dBm signal at terminal $\sigma 9R$, adjust the trimmer for 200 mV (P-P) output at terminal $\sigma 9R1$.

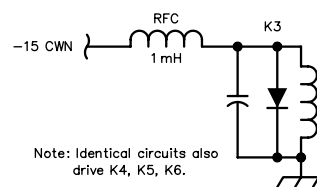
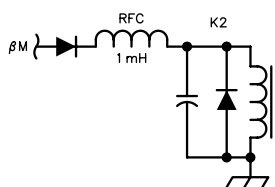
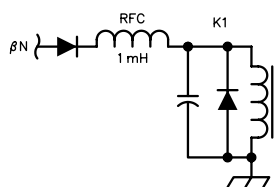
The S-Meter Adjust trimmpot, shown in Fig 9 of Reference 2, sets the full-scale S-Meter reading at 100 dB above the AGC threshold. The S-Meter threshold is the same as the AGC threshold. The S-Meter is calibrated directly, from 0 to 100 dB above the

Fig 2—IF board block diagram. This shows the individual stages of the 9 MHz IF amplifier. The AGC section has been described in Reference 2, and the noise blanker in Reference 3. Potentiometers labeled in all capital letters are front panel controls; others are circuit-board trimmers for internal adjustment. The transistors shown are all small-signal, dual-gate, VHF-type MOSFETs, except Q13, a strong bipolar, and the small bipolar emitter followers labeled "EF." The gain of the Q13 stage compensates for the additional loss of the CW filter. The triangles indicate op amps. When receiving, the input is at terminal $\sigma 9R$; the output is at terminal $\sigma 9R1$. For transmitting SSB, the input is at terminal $\sigma 9DSB$. For transmitting in the carrier modes (CW, AM, FM), the input is at terminal $\sigma 9C$. Terminal $\sigma 9T$ is the transmitting output.





Except as indicated, decimal values of capacitance are in microfarads (μF); others are in picofarads (pF); resistances are in ohms; k=1,000.



Note: Identical circuits also drive K4, K5, K6.

Fig 3—IF amplifier schematic diagram. Each resistor is a $1/4$ -W carbon-film type. The diodes are all small-signal silicon types, such as 1N4148. The unlabeled coupling and bypass capacitors are all 10-nF disc ceramic types. Also, each control and power terminal has a bypass capacitor that is not shown. The trimmer capacitors are 5 to 18-pF miniature ceramic types. The crystal filters, salvaged from an irreparable CX7, have an impedance of 220 Ω ; the attenuators and transformers are designed accordingly. Potentiometers labeled in all capital letters are front-panel controls; others are circuit-board trimmers for internal adjustments. Certain other simplifications have been incorporated in this schematic to save space and improve clarity. In the MOSFET stages, the gate-2 isolation resistors, source resistors and drain-circuit decoupling resistors are all unlabeled; each is 100 Ω . Note that there is no bypass capacitor directly at gate 2; the resistor serves as a parasitic suppressor, which is more effective than a ferrite bead. As a further simplification, circuit elements for stages Q2 through Q7 that are identical to those of the preceding stage are omitted. An obvious exception: The drain circuit of Q5 is the same as that of Q1. Not shown on this diagram is the additional filtering at each terminal; it is described in the text under “Construction.” The noise blanker was described in Reference 3; some additional details are given in Fig 4. The AGC section was described in Reference 2; the AGC amplifier and detector circuits, located in the IF-amplifier section, are shown in Fig 6 of Reference 2. The clipping-level circuit requires only a single lead to the front panel, and provides a range of -0.6 to $+2.0$ V for gate 2 of Q8; this allows a 25-dB gain variation. The tuned circuits at the inputs to stages Q1 and Q5 provide a voltage gain. On the other hand, the inductors in all the drain circuits are untuned, and function simply as chokes. The R/T line disables Q5 through Q7 during transmission; it switches from 0 to -15 V. The squelch circuit (part of the AGC section) disables Q7 by control line βSQ . The 1- μF capacitor in this muting circuit is a monolithic ceramic type.

K1—Low-loss, high-isolation RF DIP relay; DPDT, 12-V dc. Omron #G5Y-254P-DC12; Digi-Key #Z704 (Digi-Key Corp, tel 800-344-4539, 218-681-6674, fax 218-681-3380; www.digikey.com).

K2-K6—Low-loss, high-isolation RF DIP relay; SPDT, 12-V dc. Omron #G5Y-1-DC12; Digi-Key #Z724.

L1—0.7 μH , 15 turns #26 enameled wire on a T-37-6 powdered-iron toroidal core.

L2-L8—14 μH , 16 turns #26 enameled wire on an FT-37-61 ferrite toroidal core. L2 and L6 are tapped 4 turns from the cold end.

Q1-Q10—Small-signal VHF-type dual-gate MOSFET. Type 3N140 is used here, but any similar type may be substituted.

Type NTE 221 is available from Hosfelt Electronics Inc, tel 800-524-6464, 740-264-6464, fax 800-524-5414, fax 740-264-5414.

Q11-Q12—2N2222A.

Q13—2N5109.

T1-T3—8 bifilar turns #26 enameled wire on an FT-37-61 ferrite toroidal core.

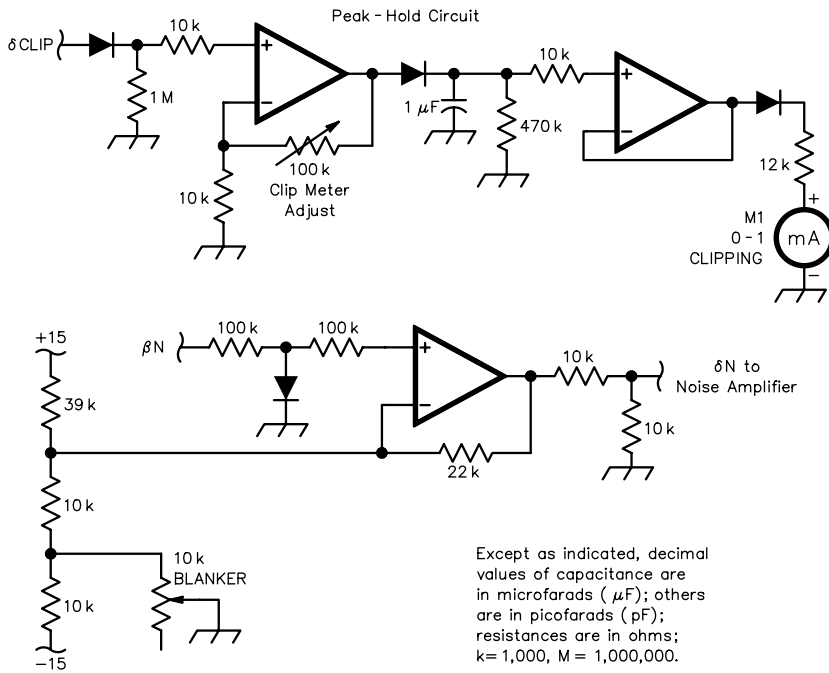


Fig 5—Control-section schematic diagram. Each op amp is one section of an LM324N, powered from the $\pm 15\text{-V}$ rails. The $1\text{-}\mu\text{F}$ capacitor in the peak-hold circuit is a monolithic ceramic type. The blanker gain circuit, requiring only a single lead to the front panel, provides a range of -3 to $+2$ V for the gate-2 leads of the noise-amplifier MOSFETs. The circuit also disables the noise amplifier when not in use, by means of control line βN . For general notes on the schematic, refer to the caption for Fig 3. This control section occupies a portion of the AGC sub-board.

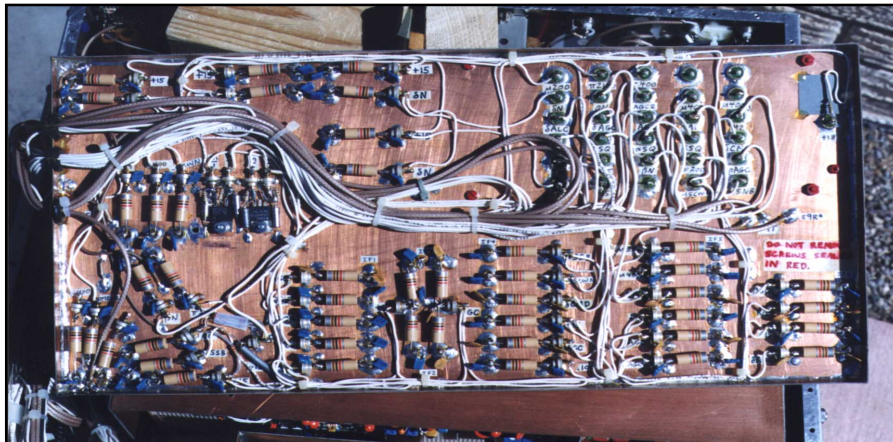


Fig 6—Bottom view of the IF board. Effective filters are installed at each terminal, and coax cables are soldered directly to the double-sided circuit board (see text). To minimize connector troubles, the board is hard-wired to the radio; a 12 inch long bundle of wires and cables allows the board to be easily lifted and serviced. The IF amplifier has unusually high gain, and operates at an unusually low signal input level. This is done as a gain-distribution method to achieve high dynamic range. The stages ahead of the sharp SSB and CW crystal filters can operate at relatively low gain and are not easily overloaded. The stages after the filters are shielded from signals outside the filter passband. The high gain of the IF amplifier makes it vulnerable to stability problems. The low signal input level makes it vulnerable to entrance of BFO energy. These vulnerabilities create the necessity for exceptional filtering and shielding of the IF strip and account for the large number of RF chokes, bypass capacitors and feed-through capacitors on the bottom of this board. The careful filtering and shielding also contributes to the effective ultimate attenuation of the filters. (Photo by Lisa Mandelkern.)

AGC threshold. The AGC threshold at terminal $\sigma 9\text{R}$ is -100 dBm. The threshold is -110 dBm at the 40-MHz input on the RF board, and nominally -130 dBm at the antenna. The MDS (bandwidth = 2 kHz) at terminal $\sigma 9\text{R}$ is -116 dBm. The MDS at 40 MHz is -126 dBm, and nominally -138 dBm at the antenna.

Setting the Clip-Meter Threshold trimmer requires a means of precisely determining the point at which clipping begins. This is done with a dual-trace scope by monitoring the IF amplifier signal level at the input to Q4, and at the transmit-output terminal, $\sigma 9\text{T}$. With the front-panel CLIPPING control set to minimum, the two-tone audio test oscillator and MIKE controls are set to obtain 1 dB of compression at the output; the Clip Meter Threshold trimmer is then adjusted for a 10% meter indication. The CLIPPING control is now advanced to obtain a 20-dB increase at the input to Q4, and the Clip Meter Adjust trimmer in the control section, Fig 5, is adjusted for a full-scale indication. Finally, a meter calibration chart is made, so the operator may select a desired degree of RF compression. For normal use, 3 dB is adequate and pleasant sounding. For extreme conditions, 10 dB may be used effectively.

When transmitting, the DSB input level at terminal $\sigma 9\text{DSB}$ is nominally 200 mV P-P; the carrier input level at terminal $\sigma 9\text{C}$ is 500 mV P-P. The SSB Level and CW Level trimmers are adjusted to obtain 200 mV P-P output at terminal $\sigma 9\text{T}$. The AGC sub-board reduces the gate-2 voltage of the MOSFETs to about 1.2 V during each transmission; this can be varied as required by a trimmer in the AGC section (see Fig 7 in Reference 2).

Summary

This article gives a complete description of the 9-MHz IF board in a high-performance homebrew transceiver. The board is designed for optimal performance; it includes sharp filters for SSB and CW, a high-performance hang-AGC circuit, a non-crunching noise blanker and a powerfully effective RF speech clipper.

References

1. M. Mandelkern, K5AM, "A High-Performance Homebrew Transceiver: Part 1," *QEX*, March/April 1999, pp 16-24.
2. M. Mandelkern, K5AM, "A High-Performance AGC System for Home-Brew Transceivers," *QEX*, Oct 1995, pp 12-22.
3. M. Mandelkern, K5AM, "Evasive Noise Blanking," *QEX*, Aug 1993, pp 3-6. □

The Bedford Receiver: A New Approach

Look at this new Australian receiver design. It offers continuously variable bandwidth and very great dynamic range.

By Rodney Green, VK6KRG

This new receiver is neither direct-conversion nor superheterodyne, but uses both phasing and heterodyne techniques in a unique design embodying the following features:

- High dynamic range¹
- Continuously variable selectivity from 600 Hz to 3 kHz
- Filtering shape factors from 1.5 at 600 Hz to 1.1 at 3 kHz
- Phasing techniques replace filters to eliminate ringing
- No specialized test equipment is required for set up
- The bandwidth can be counted directly on a frequency counter

Basic Receiver Operation

The text below assumes the reader is familiar with the phasing method of

receiving single sideband. If you are unfamiliar with the subject, refer to *The ARRL Handbook*, where the subject is discussed in detail.²

Fig 1 is a basic block diagram of the receiver. The first block seen by an incoming signal is a phasing-type SSB receiver. The output of this section is shown graphically as the zero-IF response in Fig 1. Notice how quickly the frequency response rolls off below 300 Hz and the unwanted-sideband level is greatly reduced. However, the response above 2.7 kHz rolls off at a much slower rate. There are two reasons for the fast roll-off below 300 Hz. Firstly, there are an infinite number of octaves between 300 Hz and 0 Hz. This means that even a very simple high-pass filter must have an infinite roll off over this range. For instance, even a single RC network will not couple dc.

The second reason for the sharp roll off is that as the beat frequency crosses over 0 Hz to the other sideband, it is strongly rejected, since this is a phasing type SSB receiver. Thus, the low-frequency selectivity of this

type of receiver is very good indeed. However, between 2.7 kHz and 9 kHz there are only about two octaves. A filter with a 30-dB-per-octave roll-off will be 60 dB down at 9 kHz. The rapid roll-off below 300 Hz is used a second time to improve the high-frequency skirt dramatically, as shown below.

Brick-Wall Variable Band-Pass Filter

The above-mentioned 0- to 9-kHz signal is now passed on to a phasing-method SSB generator at a convenient frequency. In this case, the signal is translated to the frequency range of 7.8 to 16.8 kHz with a local-oscillator frequency of 7.8 kHz. This is shown graphically as the translated SSB signal in Fig 1. Notice that the filter in this section removes some of the unwanted spectrum, shown dotted. This translated signal is now sent to a second tunable phasing-type SSB receiver. This receiver inverts the sideband, and it can be viewed as seeing a spectrum between 7.8 and 10.8 kHz. The local oscillator in this receiver is tunable between 8.3 and 11.8 kHz. With this

¹Notes appear on [page 23](#).

receiver, frequencies above the local oscillator fall on the rejected sideband, and are canceled. Since the previous section has shaped the roll off below 7.8 kHz, and frequencies above that of the local oscillator in this section are also rejected, the overall effect is that of a variable-bandwidth filter with extraordinary selectivity and no ringing. The bandwidth is the difference between the second and third local-oscillator frequencies. The selectivity is equally sharp on both ends of the frequency response. This is shown graphically as the audio response in Fig 1.

In the above discussion, I did not mention which sideband was being dealt with, to avoid confusion. However, note that one sideband inversion process is used in this system. This simply means that to receive upper sideband, the first section should be set to receive lower sideband, and *vice versa*, to get two sideband inversions, which is equivalent to none at all.

I take advantage of the fact that the bandwidth is the difference between the second and third local-oscillator frequencies by mixing the two frequencies and sending the difference frequency to a frequency counter. The counter then displays bandwidth directly. The counter could be switched between frequency readout and bandwidth.

No Filter Ringing

Because of the lack of sharp filters in this system, there is a complete lack of filter ringing, even at the narrowest bandwidth setting. The audio quality from this receiver is therefore excellent. This should make the unit well suited to data reception.

Maintaining High Dynamic Range

Because of a larger number of mixers than usual in this system, mixers with very high dynamic range and extremely good intermodulation characteristics are required. Using 4053 CMOS switches in an op amp circuit proved easily equal to the task. The mixers were designed to have IMD products of less than -60 dBc at 20 V (P-P) input and output. These mixers are described in detail later.

Design Details

The radio is divided into 10 subassemblies on PC boards (PCB). This facilitates easy changes where necessary. The more-detailed block diagram in Fig 2 shows all of the modules and their interconnections. The subassemblies are detailed below.

Front End³—(Refer to Fig 3.) Signals from the antenna feed a 3.5-4 MHz band-pass filter comprising C1, C2, L1, L2, C4 and C5, to attenuate signals

outside the 80-meter band. This filter also acts as a matching network between the 50-Ω antenna and the 750-Ω input resistance of the two first mixers. These are IC1 and IC3, a pair of NE602s. They are fed with phase-quadrature local-oscillator signals from the VFO board and in-phase signals from the antenna, which together convert signals in the 3.5 to 4.0-MHz band to audio (zero IF). The gain of each of the mixers is about 15 dB. Also on this board are high-gain first (audio) IF amplifiers (SSM2017s), with their gain set at 33 dB by resistors R1 and R4 for IC2 and IC4, respectively. These devices are worthy of special mention, since they have noise figures of only 1 dB, and distortion figures of 0.01% at a gain of 60 dB. These amplifiers produce two quadrature audio signals for the audio phase-shift board. See Note 1

Fig 2—(See right) Detail of module interconnections. Power wiring and ground-pin numbers for shielded cables have been omitted to simplify the drawing. The PC board pins do not correspond to the physical connections. Consult the schematics and PC overlays for pin and ground locations (See Note 7). The audio, AGC and power-amplifier module is available as a complete kit with double-sided, silk-screened PC board with plated through holes and green solder mask. It includes an exhaustive manual.

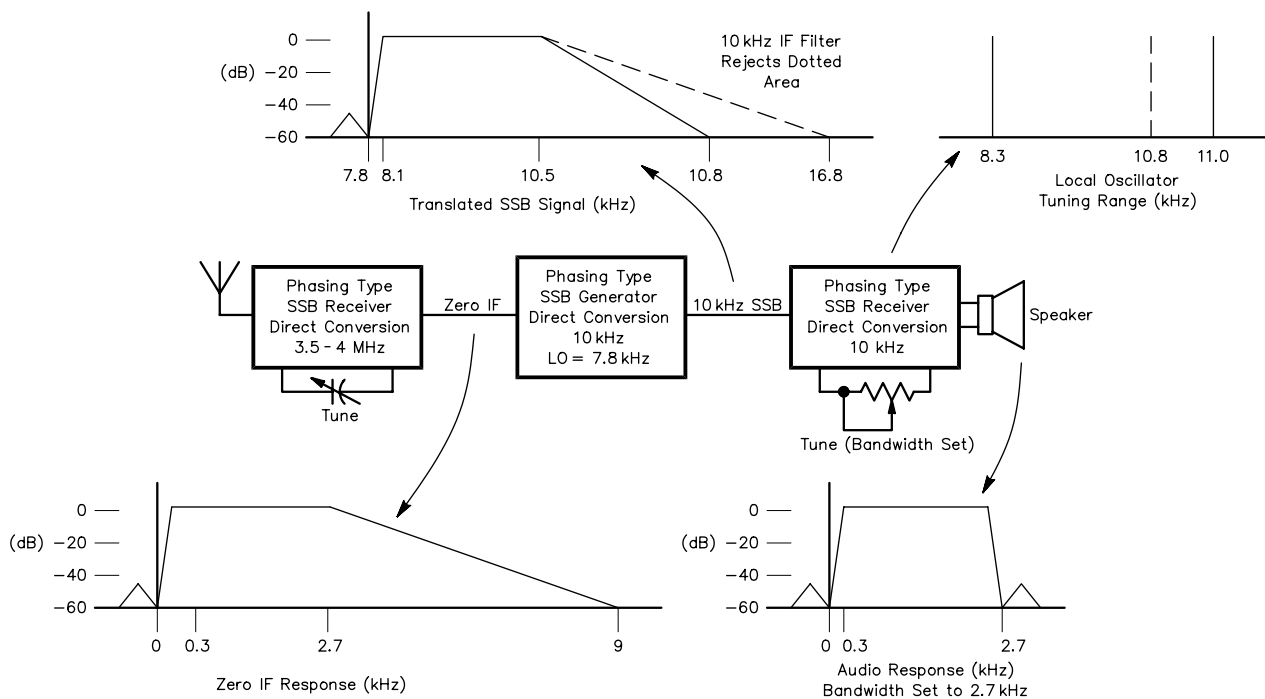
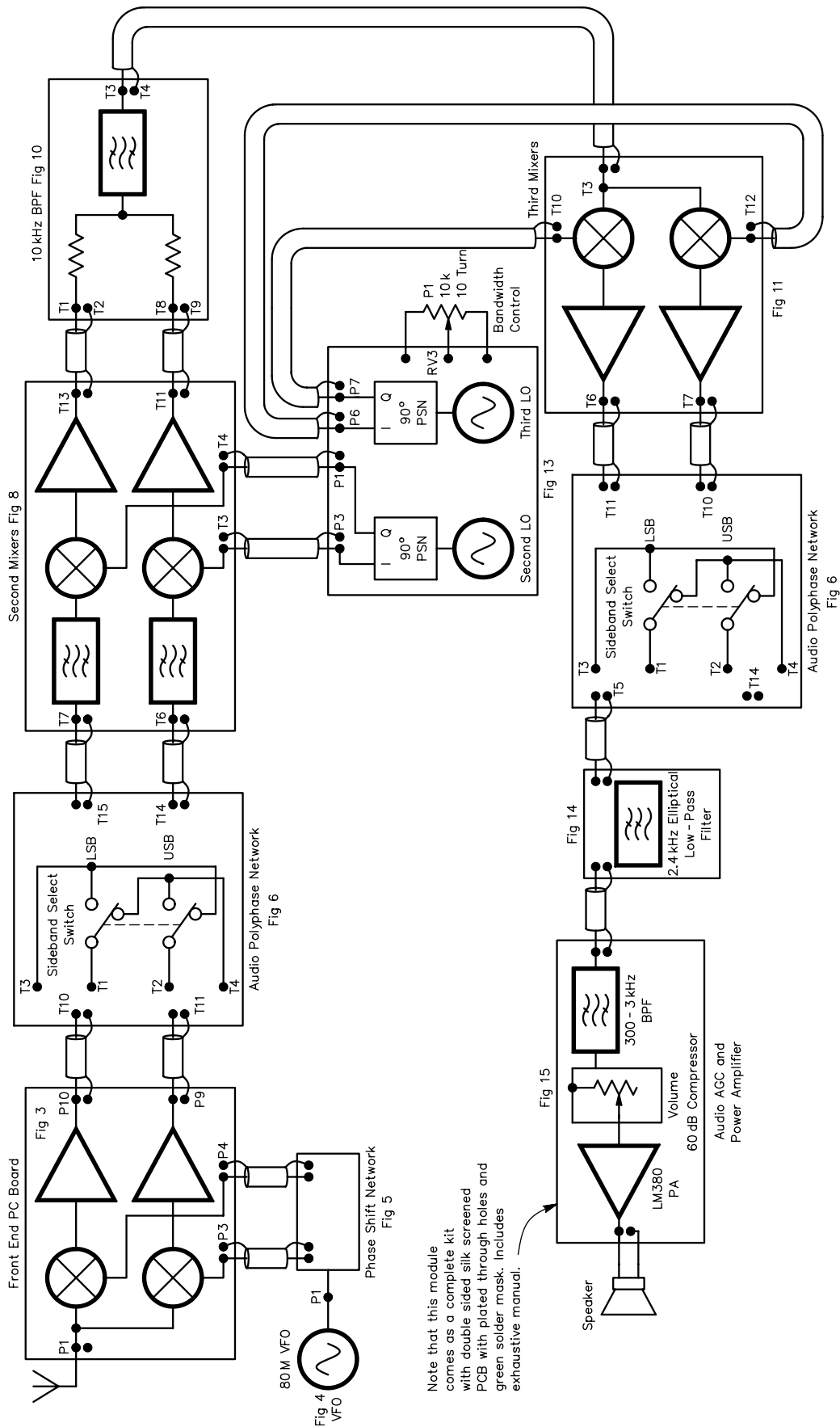


Fig 1—Receiver block diagram. The system bandwidth is equal to the difference between the second and third LO frequencies. The dashed line at 10.8 kHz in the LO Tuning Range detail indicates the LO frequency for 2.7 kHz bandwidth.



Note that this module comes as a complete kit with double sided silk screened PCB with plated through holes and green solder mask. Includes exhaustive manual.

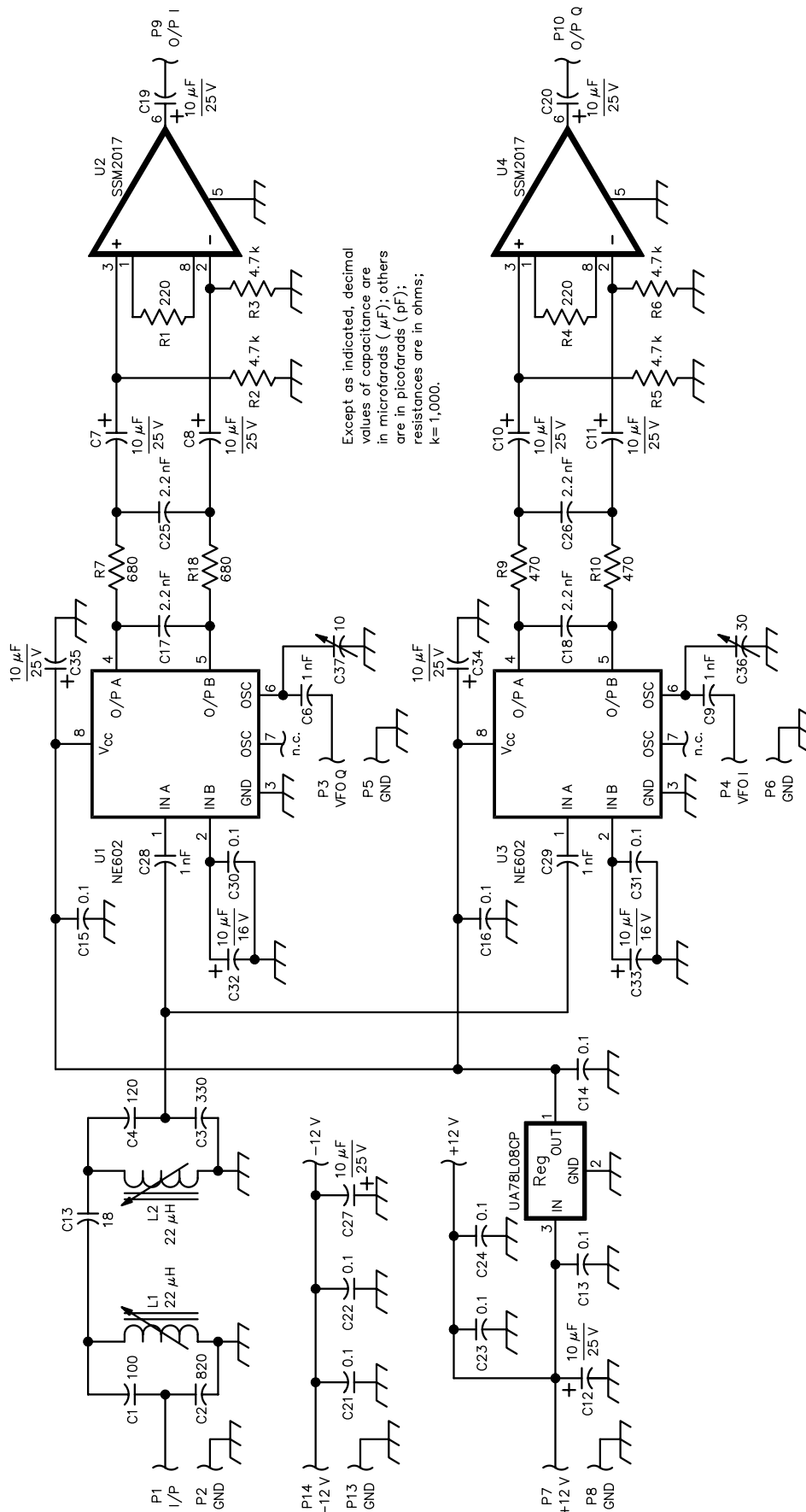
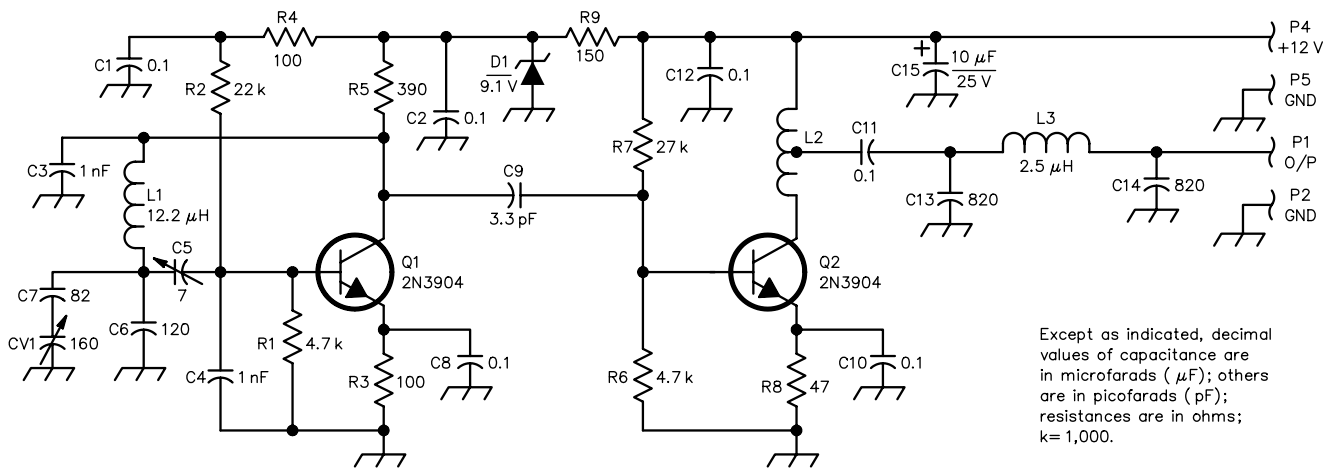


Fig 3—Front-end module schematic diagram. Some part designations differ from ARRL style in order to comply with the author's materials.



Except as indicated, decimal values of capacitance are in microfarads (μF); others are in picofarads (pF); resistances are in ohms; k=1,000.

Fig 4—VFO schematic diagram. Some part designations differ from ARRL style in order to comply with the author’s materials. L2—13 turns on a ferrite bead with a tap at 6 turns.

regarding the dynamic range of the NE602.

VFO: (See Fig 4.) This contains a Vackar VFO (3.5 to 4.0 MHz), with Q1 as the oscillator transistor. The operating frequency is set mainly by inductor L1 and capacitors C6, CV1 and C7. Capacitors C4 and C3 are relatively large in value and shunt most of the circulating current away from the transistor, thus decoupling it from the tuned circuit. Small variable capacitor C5 is adjusted until the circuit only just oscillates reliably over the required band. Q2 is the buffer stage, and its output is taken from auto-transformer L2. C11 is the dc-blocking capacitor. The output is low-pass filtered by C13, L3 and C14. A two-pole polyphase quadrature network follows, providing tight 90° phase-shifted outputs over the frequency range. On the prototype, this section was mounted on a small PCB, but it could just as easily have been mounted with the rest of the VFO components. The network—shown in Fig 5—consists of four capacitors, four resistors, input transformer T1 and two output transformers T2 and T3.

Audio Phase-Shift Board⁴: (See Fig 6.) The two quadrature outputs from the Front End are inverted by IC1A and IC1D. Similarly, IC1B and IC1C are used for the other (quadrature) input. Trimpot RV1 is adjusted to ensure that the two paths from the front end are equal in amplitude; good cancellation of the unwanted sideband is thereby obtained. The four outputs from IC1 have a relative phase relationship of 0°, 180°, 270° and 90°. These four signals are now fed to a

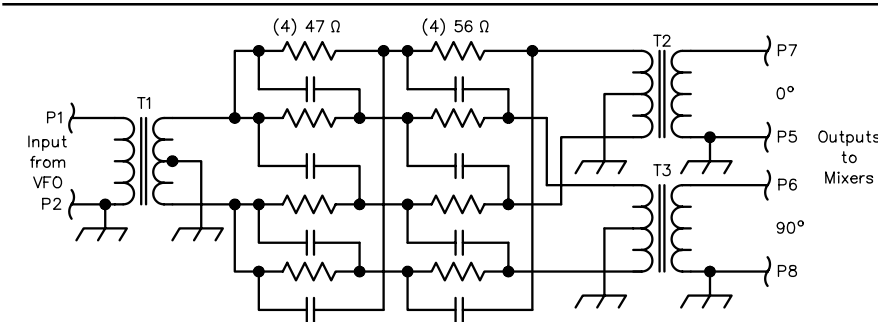


Fig 5—A two-pole, quadrature polyphase network for VFO. All capacitors are 1.0 nF MKT style. T1-T3—6 trifilar turns on a ferrite EMI-suppression bead.

nine-pole polyphase network that gives a tight 90° phase shift over the 300 Hz to 8 kHz range. This is shown as block PH1 in Fig 6; the circuit is shown in Fig 7. The four outputs from the polyphase network are amplified by IC2A-D. Only two of the outputs are used to drive the next board, but I have made all four outputs available for experiments. Notice that this network cancels the wrong sideband, and the outputs don’t need to be combined, as is required by some other networks. It is also noteworthy that the same audio appears on each output, but in quadrature. This is useful, as it avoids the need for a phase-shift network at the inputs of the second mixers. The extra-wide bandwidth (beyond 3 kHz) of this network is used to allow the following circuitry to greatly attenuate any unwanted signals above about 3 kHz before the polyphase network runs out of range. The desired sideband can be selected on this board by swapping inputs to the polyphase network. Links

are provided on the board to accommodate a sideband select switch, if required. They are T1, T2, T3 and T4.

Tuning and setup are covered later under the “Construction Notes, Tuning and Adjustment” subheading. At this point, builders can choose to connect an output from this board to the six-pole elliptical 3-kHz low-pass filter and then to the AGC and audio power amplifier board for a truly superb receiver. Alternatively, use two outputs from this board to connect to the second mixer and continue to the best part of all.

Variable-Bandwidth “Brick-Wall” Low-Pass Filter Section

Second Mixers: The schematic is shown in Fig 8, and the block diagram is shown in Fig 9. This board is fed from the audio phase-shift board by two signals in quadrature. Each of these signals is fed to a two-pole, 300-Hz high-pass filter consisting of IC3A and surrounding components. IC2A and associated components form

the same filter for the quadrature path. Following this is a five-pole, 3-kHz low-pass filter, consisting of IC3B, C and D and surrounding components; IC2B, C and D and surrounding components are used for the quadrature path. These filters are all of the maximally flat, equal-component Sallen-and-Key type. The signals are then fed to two double-balanced mixers, consisting of R27, R16 and $\frac{1}{3}$ of IC5. R6, R17 and $\frac{1}{3}$ of IC5 are for the quadrature path. IC3D feeds a signal into R16, and an inverted version from IC1A feeds R27. IC5 acts essentially as a changeover switch, switching pin 14 between pins 12 and 13. The current in these resistors is thus alternately switched to the input of IC6A at the clock rate of 7.8 kHz. This is, in fact, a double-balanced mixer operation. Similarly, R6, R17, pins 1, 2 and 15 of IC5, and IC6B form the same for the quadrature path. These mixers

have a very good dynamic range, as the FETs in IC5 only switch current with very little voltage drop across them.

The mixers have logic-level quadrature oscillator inputs at a frequency of 7.8 kHz. The outputs of these mixers are summed into the 10-kHz band-pass filter that follows. The phasing of the 7.8-kHz oscillators and of the quadrature audio inputs is such that upper sideband is selected. The following 10-kHz filter is good enough to give reasonable lower-sideband rejection on its own, but the addition of the phasing circuits gives very good suppression indeed.

10-kHz Band-Pass Filter: (Refer to Fig 10.) The two outputs of the second mixers enter this board via T8 and T1. Then they are summed into U3A via RV5, R29 and R2. Trimpot RV5 is set to combine the two inputs equally for optimum unwanted-signal attenuation. The combined signal is now

filtered in a four-pole band-pass filter. This filter has a 2-dB dip at mid-band and a bandwidth of 2.7 kHz at 3 dB, which, along with the second mixer quadrature outputs, is more than sufficiently selective to filter the upper-sideband signal. As shown on the circuit diagram, the filter uses op amps and passive components. Thus, it is easily duplicated and inexpensive. The circuit used is the bi-quad type and consists of four single-tuned circuits. Looking at Fig 10, the first tuned circuit consists of U3A, U3B and U4. The other three follow in a similar manner starting at U1A, etc.

There are only two frequencies to set up, as these are two cascaded two-pole filters. Note the test points TP1, TP2, TP3 and TP4. Each is connected to the input of one of the filters. The alignment frequency can be injected into these test points to allow adjustment of each stage without affecting the other

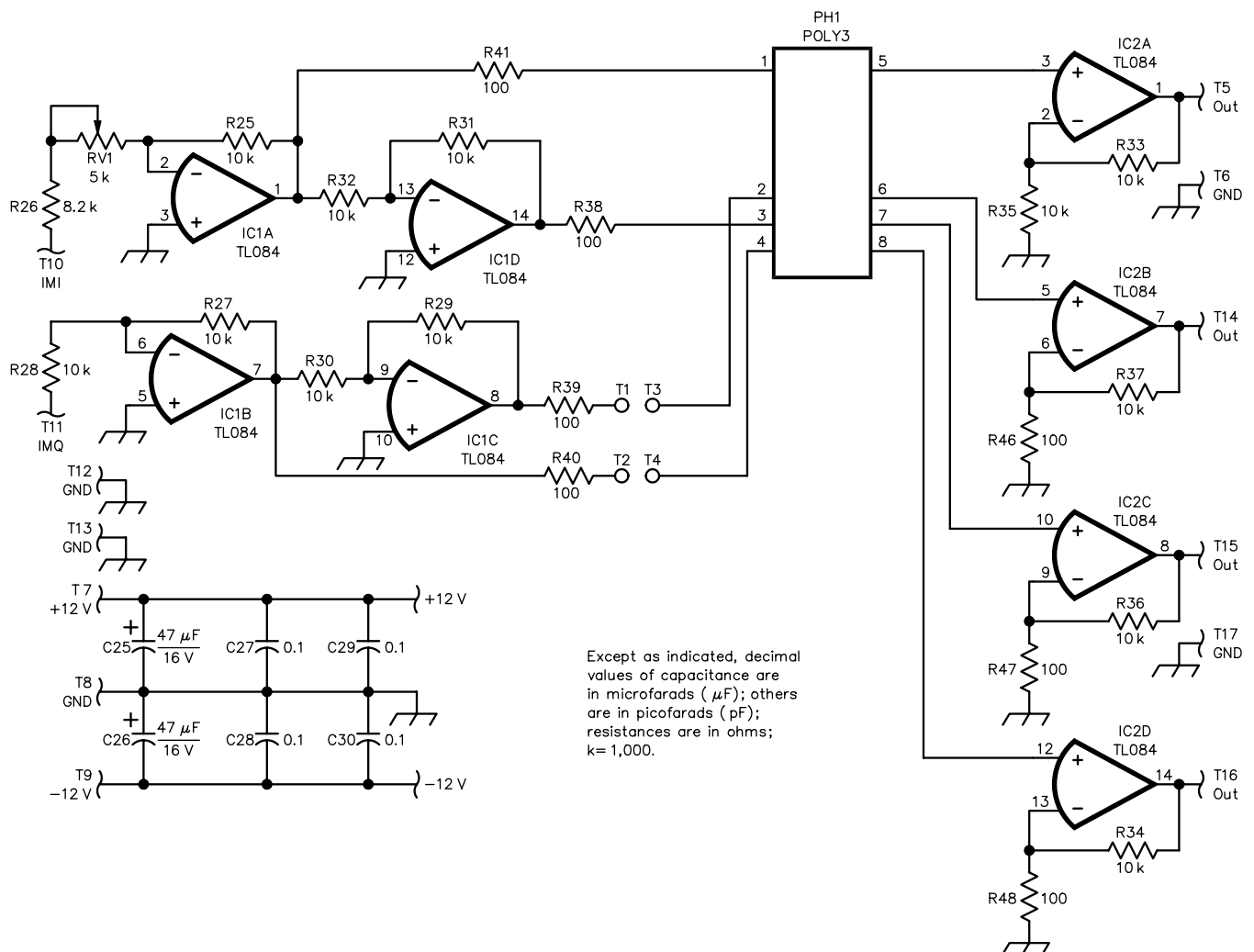


Fig 6—Audio phase-shift board schematic diagram. Some part designations differ from ARRL style in order to comply with the author's materials.

stages, and without the need to disconnect anything on the board. More on adjustment is found below. Each of the four tuned circuits has an adjustment trimpot with a tuning range of only a few percent for easy tuning. After setting up the prototype, the filter was swept on a spectrum analyzer, but no further tuning was required.

Third Mixers: This board could also be called the product detector, as it is the final mixing process. The schematic is shown in Fig 11, and the block diagram in Fig 12. The signal from the 10-kHz band-pass filter now feeds two high-level, single-balanced mixers using the 4053 CMOS switch IC. The FETs in the 4053 switch the signal currents coming from R6 and R7 between the virtual-ground inputs of IC2A and IC2B and earth. Since resistors R6 and R7 have high values compared to the switch FET on resistances, the FETs operate only over a very small part of their characteristic curves. Thus, these mixers have a very high dynamic range. The 4053 ICs have some output capacitance; low-value resistors R4 and R8 are placed between the 4053 outputs and the inputs of IC2—this is to prevent IC2 from generating high-frequency noise. These mixer-input signals are not in quadrature, but are in phase, so that the inputs are tied together. As for the front end, this is another direct-conversion receiver. In addition, as in the front end, the local oscillator is fed in quadrature to the two mixers. The os-

illator inputs, however, must be logic-level square waves, as in the second mixers. The oscillator frequency feeding this mixer pair is variable and is used to set the system bandwidth as previously described. The outputs of these mixers are fed to a final audio-polyphase network, which is identical to the first audio-phase-shift board already described.

Second and Third Oscillators: (See Fig 13.) This board generates the quadrature oscillator signals for the second and third mixers. The second oscillator is tuned to 31.2 kHz, and the signal emerges in quadrature at P1 and P3 at 7.8 kHz. Q1 and its neighboring components form the second oscillator. It is a Vackar circuit, with L1, C5 and C12 controlling the frequency. The output is taken from collector load R5, buffered and converted to CMOS levels by IC3A and IC3B. From here, the signal passes to the quadrature generator made up of IC4A and IC4B. This is a standard arrangement and is described in *The ARRL Handbook*. Suffice it to say here that the signal emerges from IC4 in quadrature and at one-quarter of the input frequency.

The third oscillator needs to have external frequency control, and so a good-quality voltage-controlled oscillator IC was used. I used an XR2206 since I had one in the junk box. I think a number of substitutes are available. This IC also has a built-in double-bal-

anced mixer that is used to mix the second- and third-oscillator frequencies, producing the difference frequency for direct-bandwidth reading on a frequency counter. More work needs to be done on this. IC3D was to buffer this output, but the level from IC2's mixer output was not sufficient for the purpose.

Audio Phase-Shift Board: This board is fed from the third mixers and is identical to that of Fig 6; it is set to permanently receive lower sideband. One of the four outputs is sent to the 2.4-kHz elliptical low-pass filter. Adjustment is described later.

2.4-kHz Elliptical Low-Pass Filter⁵: (See Fig 14.) This filter consists of an op amp, IC1, with trimpot VR1 to set the gain. Resistor R3 terminates the input of the filter in 680 Ω , the correct terminating impedance for this filter. Inductors L1, L2, L3 and capacitors C1 through C7 form the filter. The capacitors across the inductors C5 through C7 tune the filter so that it has a steep notch at the band-pass edge. This filter has a 680- Ω output-terminating resistor also. Unlike the other boards, this filter was built on readily available etched copper-strip board such as "Vero-Board." This filter existed before the brick-wall-filter option was added; it may be deleted, although this has not been tried. The next stages also contain adequate low-pass filtering.

AGC and Audio Power Amplifier Board: (Refer to Fig 15.) The signal

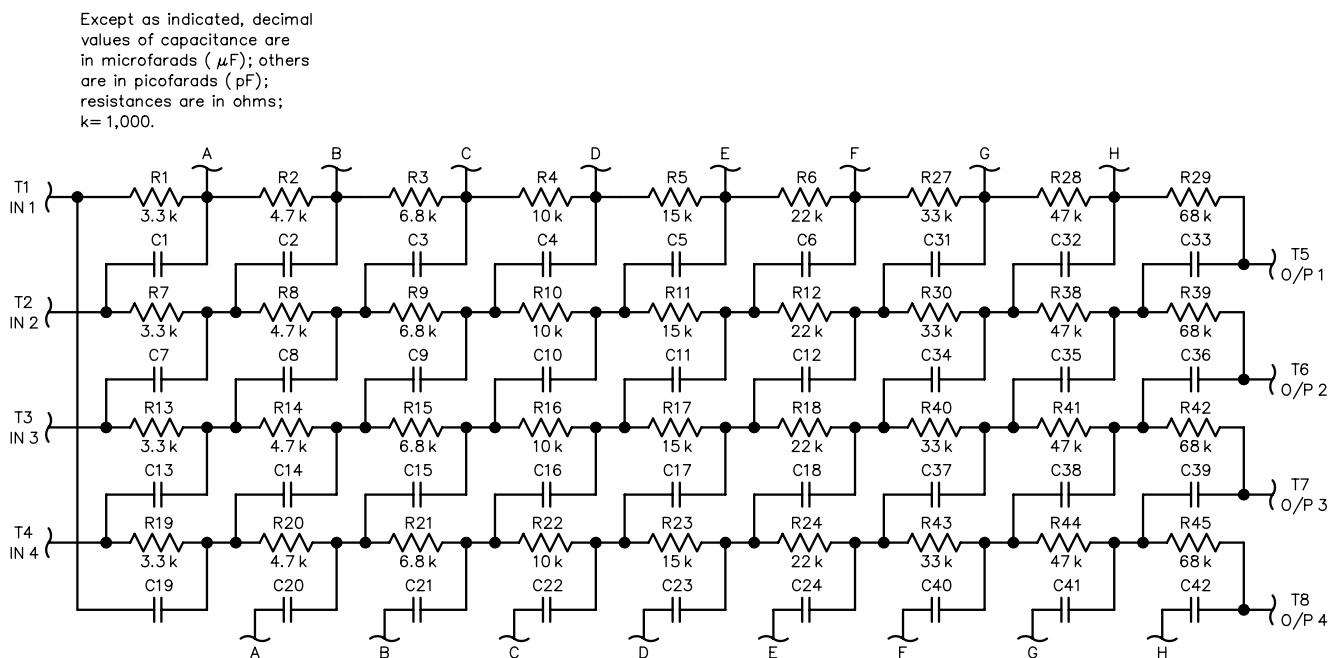


Fig 7—A nine-pole polyphase network. All capacitors are 10 nF.

Fig 8

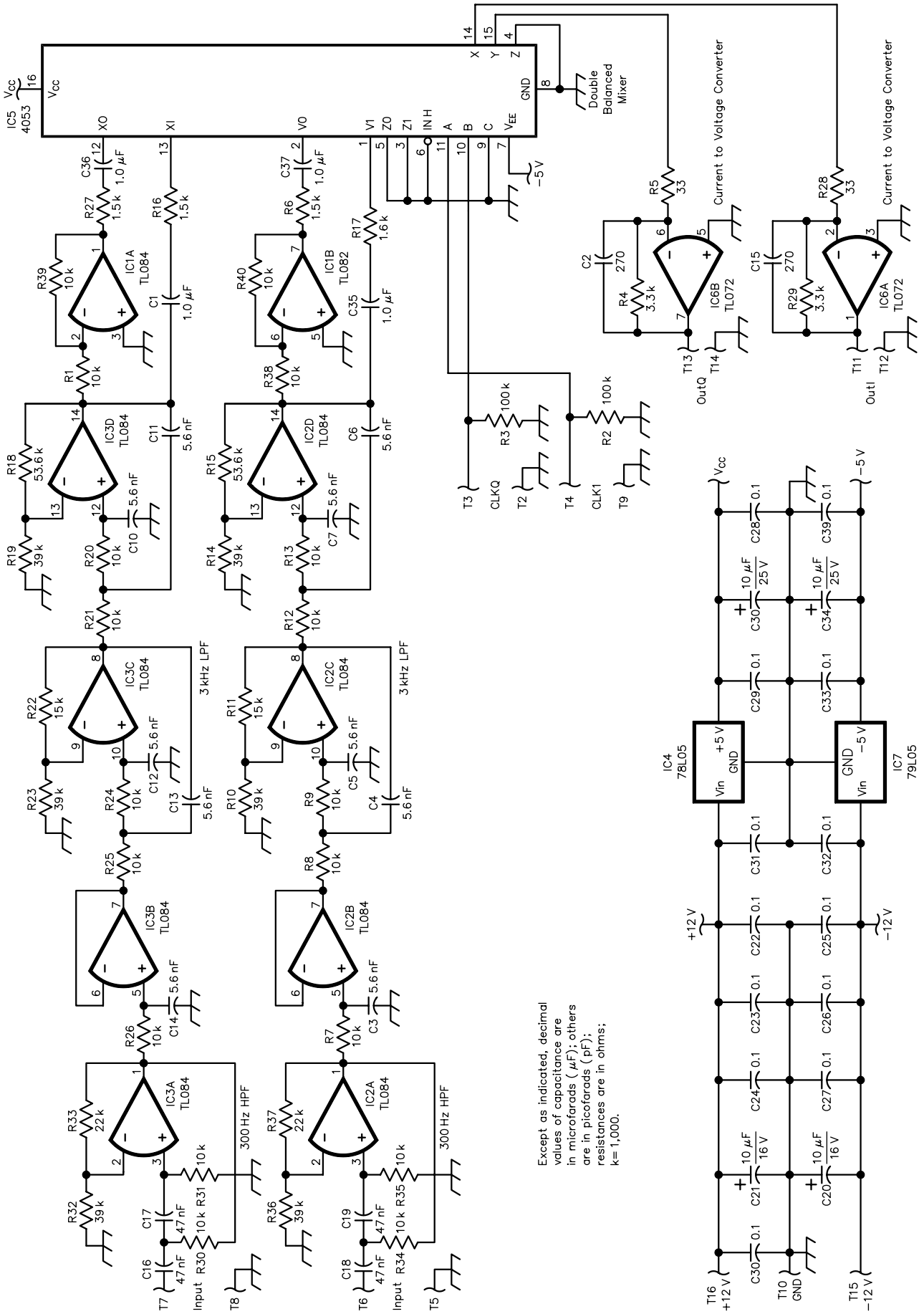
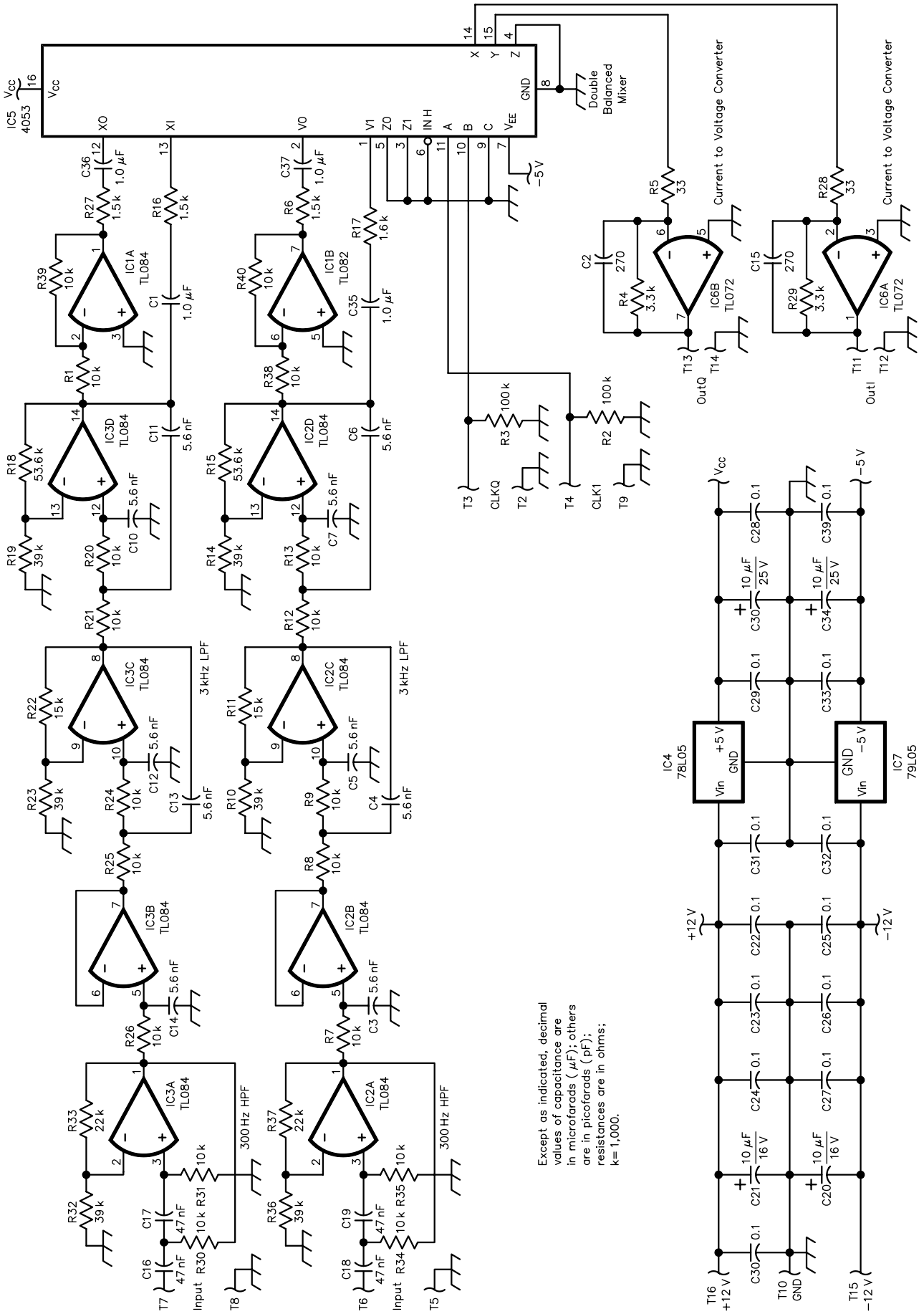


Fig 8—(See left) Variable-bandwidth brick-wall filter section schematic diagram. Some part designations differ from ARRL style in order to comply with the author's materials.

from the 2.4-kHz elliptical low-pass filter is fed to this board. It contains a five-pole, 3-kHz low-pass filter, a gain-control cell, AGC rectifier and a 2-W audio amplifier.

The five-pole low-pass filter consists of IC3A to D and associated components. The components were chosen such that the filter has a maximally flat frequency response.

The filter output feeds the AGC circuit consisting of Q1, IC1, Q2 and surrounding components. In a no-signal condition, FET Q1 is an open circuit, and a signal can pass through R1 and R2 into the op amp IC1. An applied signal is amplified by IC1 and rectified by Q2, which is set up as a combination rectifier and dc amplifier. The dc voltage from the collector of Q2 is proportional to the audio-signal amplitude. This voltage is fed to the gate of FET Q1 and causes its drain-source resistance to be lowered, thus shunting some of the signal from R1 to ground. The stronger the signal, the

more of it is shunted to ground. The effect is to make the loudness of the signal from the speaker vary only 1.5 dB for an input range of 60 dB.

The gain-reducing action of Q1 must happen quickly to avoid distortion of strong signals by the loudspeaker amplifier. R1 limits the current that can flow into the rectifier output-storage capacitor, C1. Note that the value of this resistor is low when compared to the value across C1, which discharges that capacitor slowly over a few seconds. The charging time for C1 must not be too short, or the AGC unit will overcompensate, and momentary complete signal cut off will result between bursts of strong signals, or even noise pulses. The slow return of gain via the slow discharge of C1 is to prevent gain variation between syllables, as this will cause severe audio distortion.

The controlled signals now pass on to the audio power amplifier, an LM380. This device has been around for a couple of decades and has stood the test of time, because it is easy to use and reliable. Volume control RV2 is front panel mounted, and a shielded cable runs back to pins on the PCB. The maximum output power from this IC is about 2 W. This board has been

used as a stand-alone AGC kit for direct-conversion receivers.

Construction Notes, Tuning and Adjustment

All of the modules are constructed on double-sided, plated-through-hole PCB with silk-screened legends. These can be made if quantities of 50 or more are required. However, the prototypes were simply made at home with the artwork negative and etch-resist-coated PC-board stock. This is an easy exercise, which can be done by anyone with care and cleanliness. The prototypes were simply soldered on both sides of the boards where required. Although I would not recommend this project for a beginner, it should not pose any problems for the experienced constructor. If building the whole project, it can be done in stages. Start with the Audio/AGC unit, as this can be used to test other stages. Next, build the front end and VFO, then the two audio phase-shift boards. The second and third oscillators and mixers should be built last. Fig 2 shows how all of the boards are interconnected. Use this as a guide to install each PCB when you are happy that each one is working on its own.

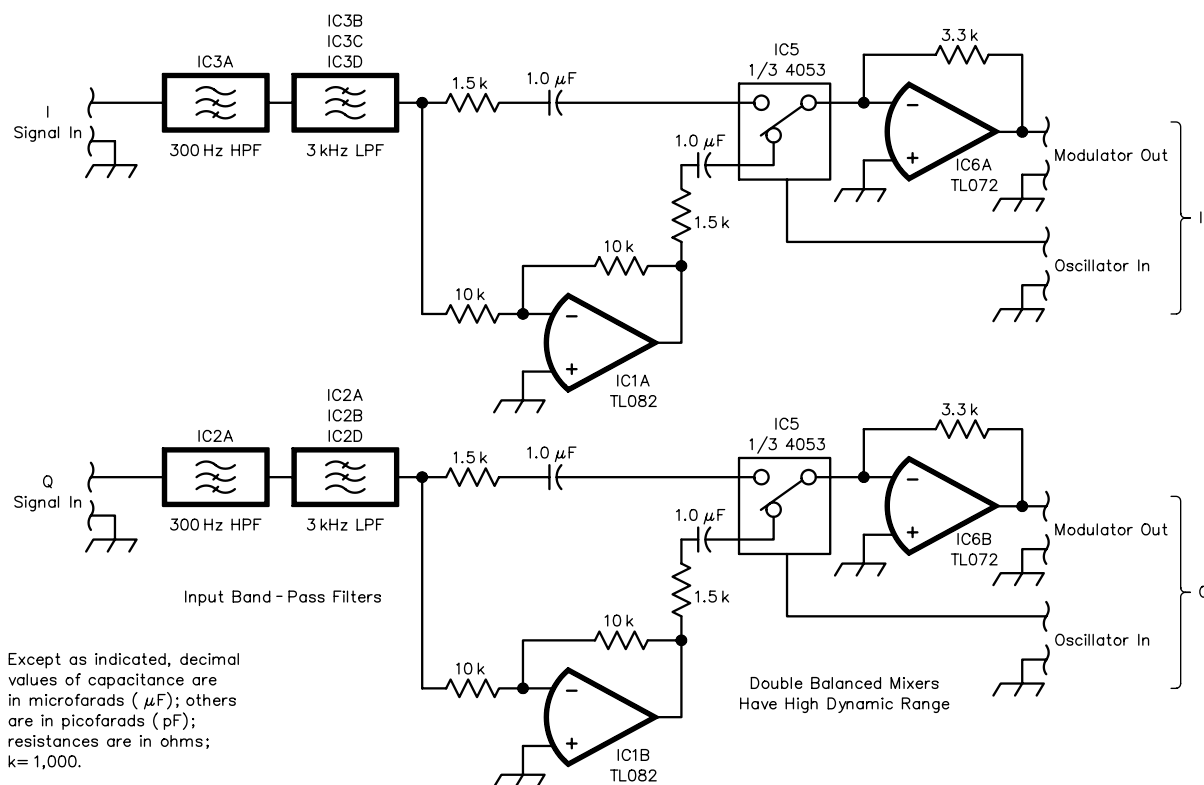


Fig 9—Variable-bandwidth filter section block diagram. Some part designations differ from ARRL style in order to comply with the author's materials.

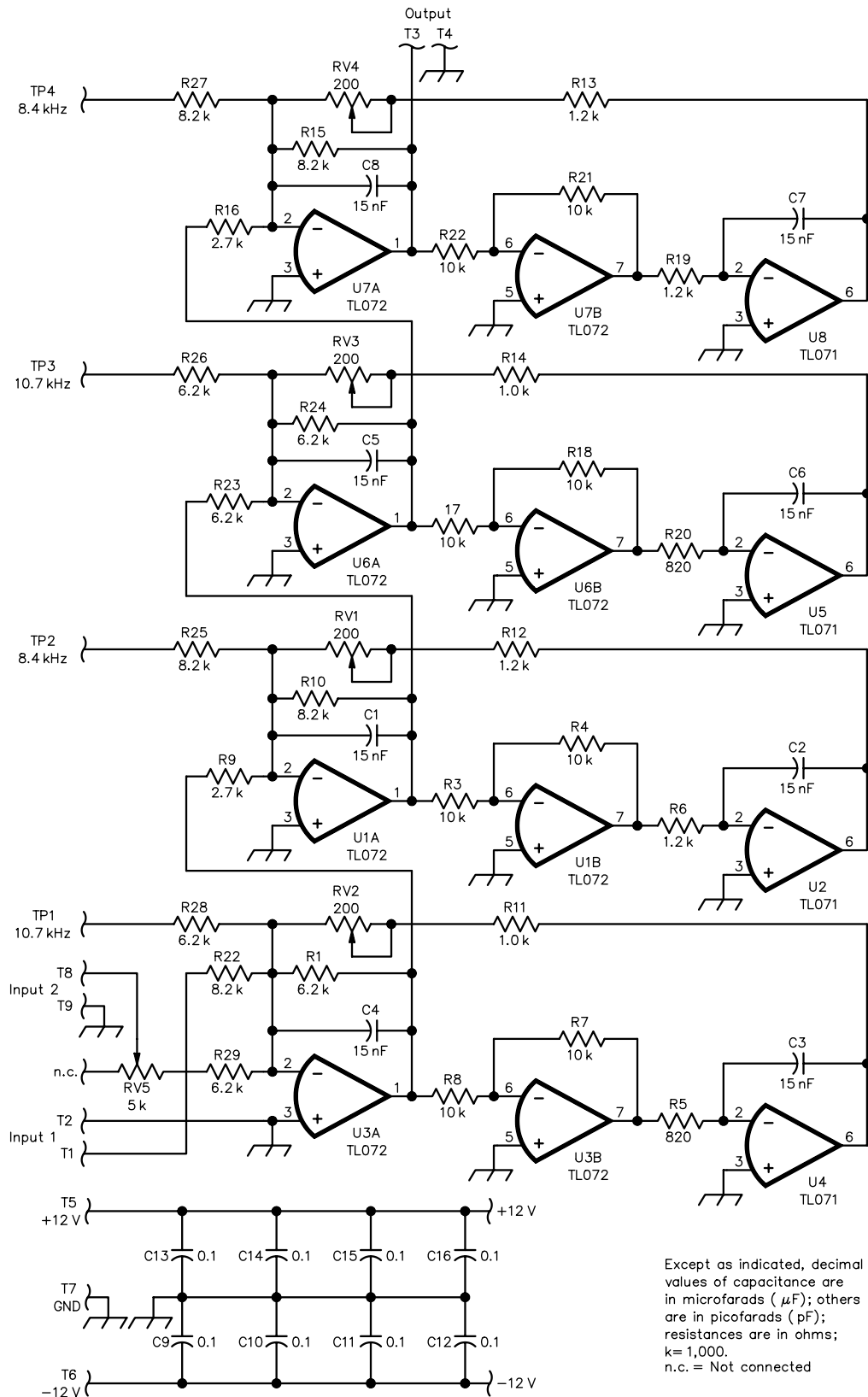
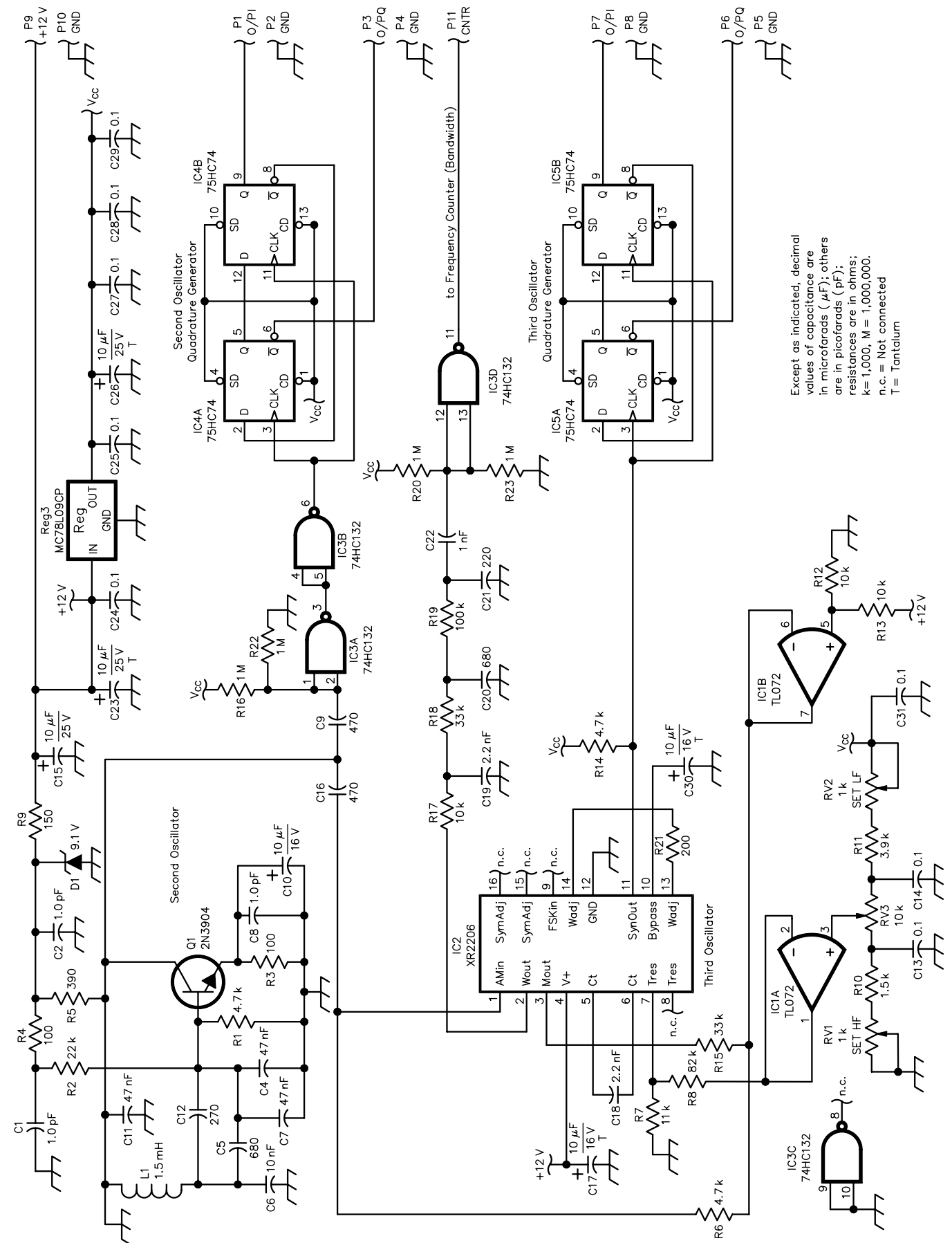


Fig 10—10-kHz BPF schematic. Some part designations differ from ARRL style in order to comply with the author's materials.



Except as indicated, decimal values of capacitance are in microfarads (μF); others are in picofarads (pF); resistances are in ohms; k=1,000, M=1,000,000. n.c.= Not connected T= Tantalum

Fig 13—Second and third oscillators. Some part designations differ from ARRL style in order to comply with the author's materials.

time and performance is superb. The frequency range can be set with the aid of a frequency counter.

The VFO phase-shifter prototype uses a tiny sub-board for the 90° phase-shift network. This can be mounted in the same box as the VFO and connected. You can check for output from this network using a diode probe and multimeter, or an oscilloscope. The output level from the phase-shift network on the prototype is 1.1 V (P-P).

Preliminary Receiver Setup

Once the front end, VFO, first audio phase-shift network and AGC/audio boards have been built and tested, they should be wired together to form a basic phasing receiver as shown in Fig 16. Set the audio phase-shift board to receive upper sideband as shown in Fig 2. Switch on and tune the radio to a convenient weak signal and set up for a tone of about 1 kHz. To check that all is well, adjust the receiver VFO across both sides of the signal. You should notice that the received signal on one side of the carrier will be stronger than that on the other. If this is correct, then the stronger side is the one in which an increase in the signal source frequency causes an increase in the received audio frequency. This is the upper sideband. If the other sideband is predominant, then reverse the VFO phase-shifter connections. If there is no difference between sideband levels, there could be too much signal input and the AGC could be kicking in. Now that you have USB the louder of the two signals, tune to the LSB side and null it out with trimpot RV1 on the audio phase-shift board.

Adjusting the Brick-Wall Filter Section

Once the basic receiver is working satisfactorily, remove the ACG/audio power-amplifier board and connect the second mixers and second local

oscillators as shown in Fig 2. Set the frequency of the second local-oscillator output to 7.80 kHz by adjusting the slug of L1. Measure at P1 on the oscillator PCB. If you have a 'scope, check that the outputs at P1 and P3 are square waves, 90° apart.

Now adjust the frequency of the first local oscillator to 3599 kHz and the signal generator to 3600.0 kHz, at a level of around -40 dBm. Check for a 1-kHz signal at the two inputs of the second mixers. The level was 225 mV (P-P) on the prototype.

Second Mixers

Now measure the outputs of the second mixers at T11 and T13 on the second mixer PCB. Each should consist of a composite RF envelope of about 2 V (P-P). These signals are double-sideband signals, phased relative to each other such that when summed at the input of the 10-kHz band-pass filter, the upper sideband is enhanced and the lower sideband canceled.

10-kHz Band-Pass Filter

Connect the 10-kHz Band-Pass Filter board as shown in Fig 2. Disconnect the signal generator from the front end and set up an audio generator to 10.70 kHz and 1 V (P-P). Connect it to TP1 on the 10-kHz Band-Pass Filter board. Place the scope probe on the filter output T3. Adjust RV2 for a peak reading on the scope. Now place the audio generator signal on TP3 and adjust RV3 for a peak reading. Now adjust the audio generator frequency to 8.4 kHz, connect it to TP2 and adjust RV1 for a peak reading. Place the audio signal generator on TP4

and adjust RV4 for a peak reading.

Now adjust the audio generator frequency to 9.48 kHz and measure the output level at T3—it should be about 1 V (P-P). The filter should peak at 10.4 kHz and 8.6 kHz, with a reading of about 1.4 V (P-P). If all is well, this completes the tuning of the filter. If further testing is desired, the prototype had the characteristics shown in Table 1.

The purpose of RV5 is to minimize the level of the unwanted sideband from the second mixers. The unwanted sideband is attenuated greatly by the 10-kHz filter and is difficult to detect at the filter output. In my opinion, the second mixer need not have been a quadrature affair; only one mixer could have been used, allowing the 10-kHz filter to be the selective element here. However, I used a selective voltmeter (spectrum analyzer) connected to pin 1 of U3 of Fig 8 to tune out the unwanted sideband. A noise and distortion meter may work well here, too. To do this adjustment, the test signal must be fed in via the receive antenna. Note, however, that the improvement in receiver performance is negligible and thus RV5 can be left in the center position.

Third Mixers and Polyphase Network

The receiver wiring can now be completed as shown in Fig 2. First, set the tuning range of the third local oscillator as follows. Set the bandwidth control RV3 to the minimum-bandwidth position (counterclockwise with wiper at maximum voltage). Adjust trimpot RV2 for the third local-oscillator

Table 1—10-kHz Filter Response

3-dB points	8.2 kHz and 10.9 kHz
6-dB points	8.0 kHz and 11.1 kHz
20-dB points	7.4 kHz and 12.0 kHz
60-dB points	4.9 kHz and 18.6 kHz
3-dB bandwidth	2.7 kHz
Noise relative to 12 V (P-P) output	-102 dB
Lower-freq. peak	8.6 kHz
Upper-freq. peak	10.4 kHz

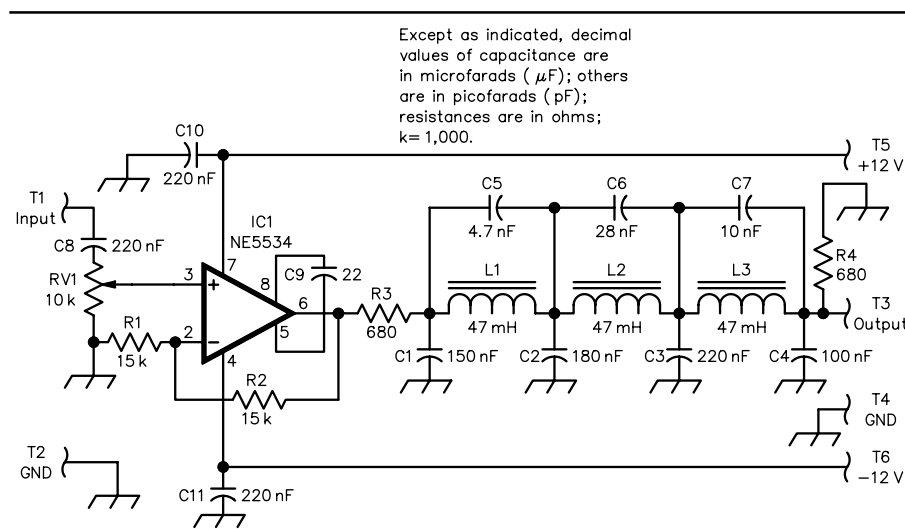


Fig 14—2.4-kHz elliptical low-pass filter. Some part designations differ from ARRL style in order to comply with the author's materials.

output frequency of 8.2 kHz, measured at P6 or P7 on this PCB. Set RV3 to the maximum-bandwidth position and adjust trimpot RV1 for 11.0 kHz at P6 or P7. Repeat the above steps until the two extreme frequencies are correct.

Connect the audio test oscillator to TP1 on the 10-kHz Band-Pass Filter. Set the frequency to 9.50 kHz at 1 V (P-P). Set the third local-oscillator frequency to 10.5 kHz with front-panel bandwidth control RV3. You should now hear a strong signal of 1 kHz in the speaker or headphones. Now change the frequency of the audio test oscillator to 11.5 kHz. Again, you should hear a 1-kHz tone, most likely weaker this time. Adjust RV1 on the last polyphase board to null out this tone. You should be able to cancel it almost completely.

You will likely hear a low-level tone, which is equal to the frequency difference between the second and third local oscillators. Don't be concerned about it at this point, as it is an easy matter to cancel this tone in the last adjustment.

Final Adjustment

If building the receiver exactly as shown, the trimpot on the 2.4-kHz elliptical low-pass filter can be set for maximum gain. Set the RF test signal generator to -40 dBm and tune the receiver such that an approximately 1-kHz tone is heard in the headphones or speaker. Check that the output of the 2.4-kHz low-pass filter board is about 200 mV (P-P).

AGC/Audio Board

The only control on this PCB, RV1, is for compression onset. For this application, the wiper of RV1 should sit at 9.1 V. This makes the receiver start AGC action at an input signal level of -80 dBm, which seems fine judging by off-air signals. This board can be built from scratch, or you can buy it from the author.⁶

To test this PCB, adjust the RF test signal generator to -100 dBm and note the output level with a scope, or even just your ears. Adjust the level of the signal generator to -90 dBm and notice that the output level can be seen to rise by 10 dB (three times the output voltage). Now bring the level of the signal generator up to -80 dBm. Note the signal level and progressively raise the generator level to -30 dBm. You should not be able to hear any differ-

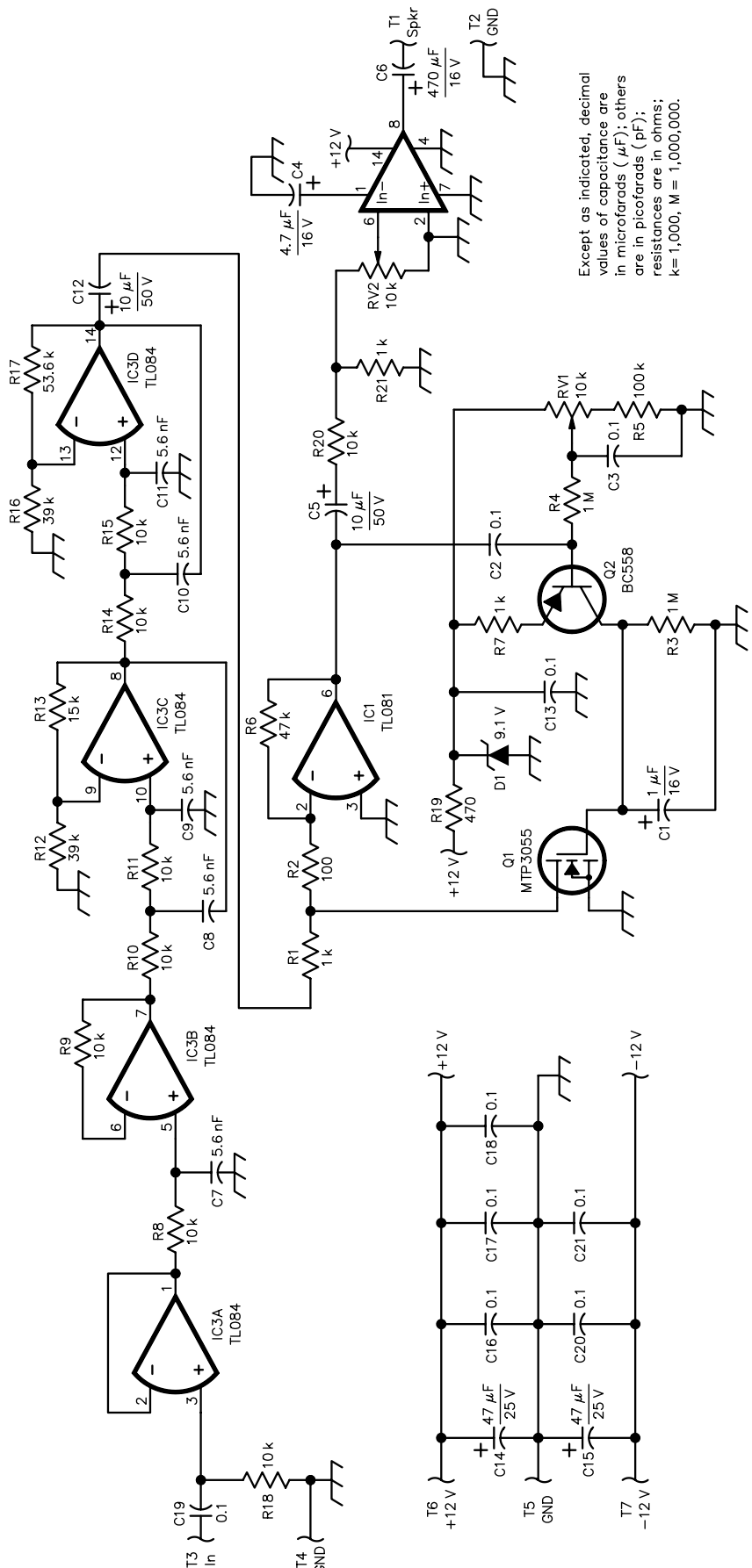


Fig 15—AGC/audio power-amplifier board. Some part designations differ from ARRL style in order to comply with the author's materials.

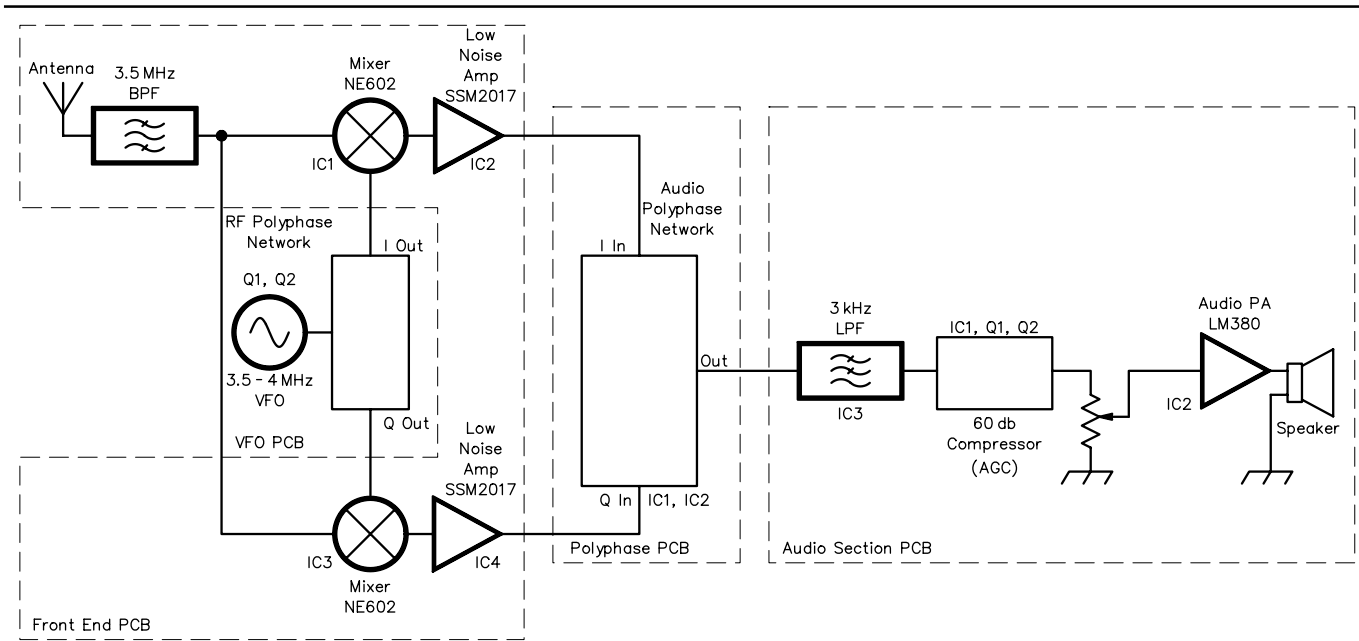


Fig 16—Preliminary receiver set-up configuration.

ence in signal loudness. You may see about 1 to 2 dB difference on the scope.

There is only one more thing to do: Adjust the bandwidth control such that you can hear a tone without any input signal to the receiver. A useful decrease in the level of this tone can easily be obtained by feeding some of the second local-oscillator signal into the input of the 10-kHz band-pass filter at TP1. The amount required for cancellation is exceedingly small and may even depend on exact layout. What I did in the prototype was to connect a 7-pF trimmer capacitor in series with a 2.2-pF ceramic cap between one of the two second local-oscillator outputs and TP1 on the 10-kHz filter PCB. These components were simply strung in mid air. Just experiment a bit for best results. On the prototype, this was achieved on the first attempt.

Conclusion

This work has been published with the hopes that more people might take up the challenge of this very different method of filtering, and that it may find new applications. Please note that it is still experimental. Improvements can be made. So good luck if you want to try out this system. I will be happy to answer queries sent to me.

Notes

¹Signetics, *Linear Data Book*, NE602.

²ARRL publications are available from your local ARRL dealer or directly from the ARRL. Mail orders to Pub Sales Dept, ARRL, 225 Main St, Newington, CT 06111-1494. You can call us toll-free at 888-277-5289; fax your order to 860-594-0303; or send e-mail to pubsales@arrl.org. Check out the full ARRL publications line on the World Wide Web at <http://www.arrl.org/catalog>.

³The front-end's unwanted sideband rejection performance may be improved by replacing the VFO phase-shift network with one similar to that used on the second and third oscillators. If this is done, the performance of the brick-wall filter will also improve, as the unwanted sideband signal from the front end appears as unwanted stop-band filter response. This is quite tricky to explain, and the best way to look at it is by first-hand experience. The VFO will also need to have a new tuning range, from 14 to 16 MHz.

⁴The polyphase audio phase-shift networks have a rising response outside the intended frequency range on both ends of about 3 dB per octave. That is, above 8 kHz and below 300 Hz. This was not fully accounted for in the prototype. It caused a hump in the frequency response of the brick-wall filter below 300 Hz. Were I to do another design, I would add an extra pole of high- and low-pass filtering on the polyphase boards. Even as it is, however, the circuit is well worth the effort of construction.

⁵The 2.4-kHz elliptical filter courtesy of VK6BER.

⁶The PCB is available from VK6KRG for \$20 Australian, postpaid. A comprehensive assembly manual is included.

⁷You can download parts placement diagrams for this receiver from the ARRL

<http://www.arrl.org/files/qex>. Look for the file Bedf0999.ZIP.

Rod Green, VK6KRG, has been interested in things scientific since early childhood. It's in his blood: His grandfather built radios in the early 1900s. Rod's technical training began in 1968, when he specialized in radio with the Australian Post Master Generals Department. In the PMG, he worked mostly at TV transmitter sites for 20 years. Wherever Rod was stationed, he designed accessory gear for the installation.

He received his first amateur license around 1976. That was a technical class license.

Beginning in 1988, Rod spent 10 years doing RF design with a local company that produces 90% of Australian radio-studio equipment. In 1998, he joined Barrett Communications as their Senior R and D design technician (their chief RF designer). Barrett makes 100-W HF transceivers and related equipment. At work, he must design to order, but Rod enjoys the challenge of designing "something different" at home. He has chosen to develop equipment based on the phasing method of RF processing. He often teams up with Richard, VK6BRO, in a combined effort.

Rod holds no degrees other than his technician's certificate from long ago. Nonetheless, he has great experience that permits his employment in the field of RF design. □□

Parabolic Dish Feeds— Phase and Phase Center

An earlier article evaluated feed performance with respect to antenna gain, but how does the feed style and location affect phase? As usual, Paul Wade has the answer.

By Paul Wade, W1GHZ

The antenna computer analysis that I have seen has only considered the amplitude of the radiated pattern. Last year¹ in *QEX*, I wrote about analysis of parabolic dish feeds, using the amplitude pattern for analysis. While I was doing the analysis, a nagging voice in my head kept saying, “What about the phase?”

While measurement of the phase pattern of an antenna is extremely difficult, calculation of an antenna pattern with both amplitude and phase is much easier. With today’s fast personal computers, it is possible to

calculate the radiation pattern of most common feed antennas, including both amplitude and phase data.

The personal computer is also valuable in helping us to understand the radiation-pattern data, by transforming it into a graphical format so that we may visually comprehend the result. These plots make it possible to quickly see not only the radiation pattern of a feed antenna, but also how a dish will perform with the feed. The results of these calculations and plots show that most of the feed antennas in common use have good phase performance.

Another result is that the phase center of each feed may be calculated, so that the feed may be accurately located with its phase center at the focus of a parabolic dish, an essential

ingredient for good dish performance.

Phase

For a parabolic dish antenna to perform well,² the feed must provide good illumination to the reflector, as shown in [Fig 1](#). The illumination energy leaving the feed must not only have good amplitude characteristics, but also must all have the same phase. Energy that is out of phase can subtract from the total radiated power, so that the effect is worse than energy that is simply lost, such as spillover that misses the reflector.

[Fig 2](#) illustrates phase cancellation. [Figs 2A, B and C](#) illustrate two in-phase signals adding, two out-of-phase signals canceling and partial cancellation when two signals are partially out of phase. [Fig 2D](#) shows the

¹Notes appear on [page 34](#).

■ Illumination loss
■ Spillover loss

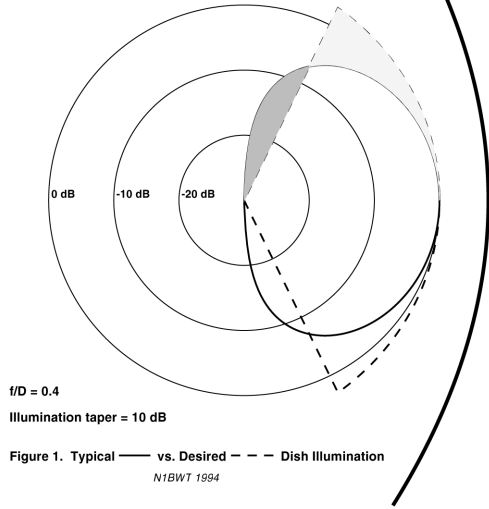
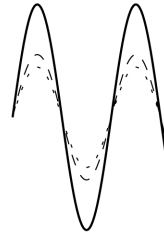
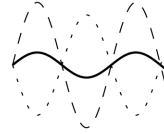


Figure 1. Typical — vs. Desired - - - Dish Illumination
N1BWT 1994

Figure 1



(a) In phase - addition

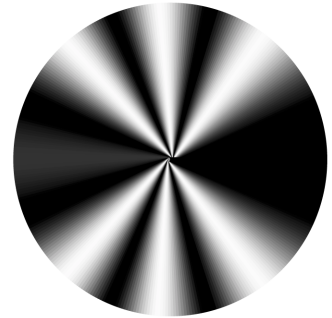


(b) Out of phase - cancellation



(c) 120 degree phase difference

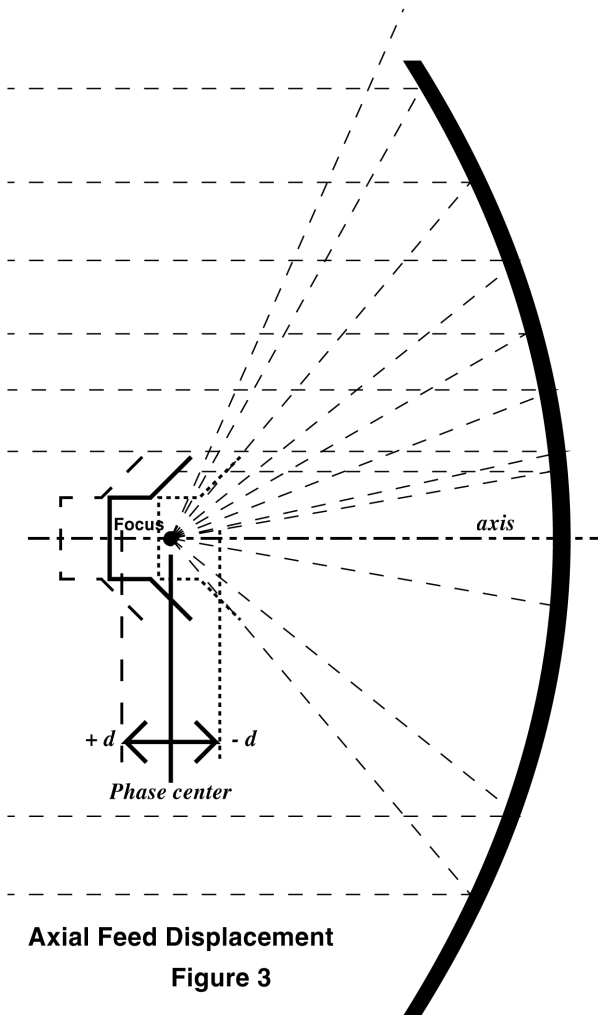
(d) Point source - single phase center



(e) Two sources - interference pattern

Figure 2. Phase and Phase Center
N1BWT 1994

Figure 2

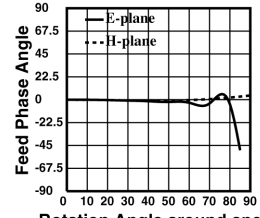
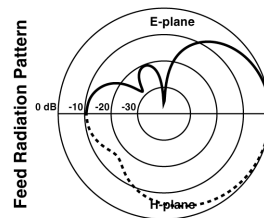


Axial Feed Displacement

Figure 3

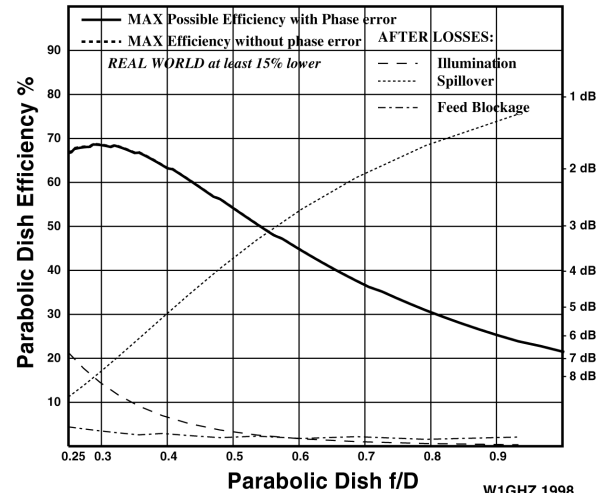
RSGB dipole-splashplate feed, by NEC2

Figure 4



Dish diameter = 10λ . Feed diameter = 1λ .

Rotation Angle around specified Phase Center = 0.11λ behind dipole



W1GHZ 1998

uniform amplitude around a single-source antenna, while 2E shows the interference pattern created by two sources. The lighter areas are directions where there is little radiated energy because of phase cancellation. A feed whose radiation does not all have the same phase will appear to have multiple sources, which may produce an interference pattern when illuminating a dish, thus reducing the effective radiation illuminating the dish.

It is possible to measure the phase of an antenna pattern as well as the amplitude, perhaps by using an automatic network analyzer. Since only the relative phase is important, it might even be possible to make the measurement manually using phase cancellation techniques—it would definitely be tedious. However, it is extremely difficult to make the phase measurement accurately. Dyson³ suggests making the measurement several times around different centers of rotation, attempting to bracket the phase center.

Calculation of an antenna pattern with both amplitude and phase is much easier. While measurement of the phase pattern of an antenna is extremely difficult, it is impossible to calculate an antenna pattern without using phase; the electromagnetic field is described using complex vectors, which have both magnitude and phase. Once we have calculated the phase data, why not extract it and make use of it? An antenna radiation pattern may be calculated using a personal computer with a fast Pentium (or even faster Alpha) microprocessor in a few minutes. A few years ago, it would have taken longer even on a supercomputer, and at a prohibitive cost.

I have used two techniques to calculate antenna patterns. The first, for wire-like antennas and simple horns, uses the *NEC2* program,⁴ which uses the method of moments to calculate radiation patterns. The original Fortran program has phase information available in the output, unlike some of the derivative versions with *Windows* interfaces. For more-complex antennas like horns and dishes, I used Physical Optics (PO) routines from Milligan and Diaz.⁵ A description by Rusch⁶: “Physical optics, whereby the free-space dyadic Green’s function is integrated over the geometrical-optics current distribution, is commonly used to analyze high-frequency reflectors, particularly, focusing reflectors.”

Of course, a computer model of an antenna is only an approximation of a real antenna, achieved by segmenting

the antenna into a number of small pieces for purposes of calculation. Calculated patterns may be compared with published results and measurements, which have their own inaccuracies. What we find, for a reasonably detailed model, is that the calculated forward patterns, out to about 90° rotation from the axis, are fairly accurate in amplitude and phase. The back half of the patterns (from 90° to 180°) are less accurate, particularly for the Physical Optics technique, which finds spurious side lobes at about ±150° and a null at 180°. However, it is only the forward half of the feed pattern that illuminates a dish, even a very deep dish, with $f/D = 0.25$, has an illumination angle of 180°, or ±90°, from the axis. The back half of the pattern is just spillover that does not contribute to useful radiation.

Thus the amplitude and phase of the spillover at any particular angle does not matter; only the total amount of power lost is needed for an efficiency calculation. If the forward half of the pattern is accurate, then, by conservation of energy, the total power in the back half of the pattern is known, so we can also calculate efficiency with reasonable accuracy.

Phase Center

For all of the energy illuminating a parabolic reflector to have the same phase, the energy must emanate from a single point at the focus of the reflector. Since all real antennas have physical size, radiation from a single point is impossible. Over a limited arc, however, the radiation from most antennas has a spherical wavefront, so that the radiation appears to emanate from the center of a sphere, the apparent phase center of the antenna.

A feed antenna should have a spherical wavefront over the full illumination angle, so that the whole reflector is illuminated from a single phase center. When this phase center is at the focus of the parabola, then all of the energy radiated in the main beam of the dish is in phase and efficiency is maximized. Taking a rule of thumb from optics, we can estimate that a feed antenna whose phase changes less than $\lambda/16$ over the illumination angle will provide good performance and high efficiency.

If the phase center of the feed is not at the focus of the parabola, then additional phase error will be present. We will examine the error in more detail later. Thus, it is important to locate the phase center accurately. When the phase pattern of a feed is calculated or

measured, it is near some arbitrary reference point such as a horn’s center of aperture. The phase data is a series of data points, each consisting of a phase angle ϕ and an associated pattern rotation angle θ . The phase center is probably on a line through the center of the feed; unless we were very lucky and chose a reference point at the phase center, the measured phase ϕ will vary with rotation angle θ . If we don’t choose a reference point at the phase center, we must calculate⁷ the axial distance, d , from the reference point to the apparent phase center using:

$$d = \frac{\Delta\phi \cdot \lambda}{2\pi(1 - \cos\theta)} \quad (\text{Eq 1})$$

where $\Delta\phi$ is the change in phase from the on-axis phase, and d is the displacement of the phase center toward the source, as illustrated in Fig 3. If d is positive, then the phase center is closer to the dish (or the test-range source if we are only measuring a feed); a negative d is farther away from the dish (or source). For example, if the phase-reference point is at the aperture of a horn and d is negative, then the phase center is inside the horn.

A good first approximation when finding the phase center is to calculate d for the rotation angle θ , where the amplitude is –10 dB, or for the desired illumination half-angle. Later we will see how to place phase center to deliver best efficiency.

Once we have determined the distance d to the phase center, we must adjust all the phase data so the new reference point for the feed-antenna pattern is the phase center. We do this by turning the above equation around to calculate a new $\Delta\phi$ for each rotation angle θ :

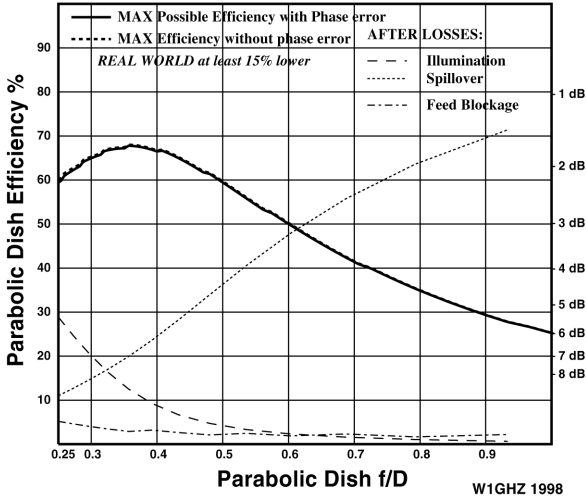
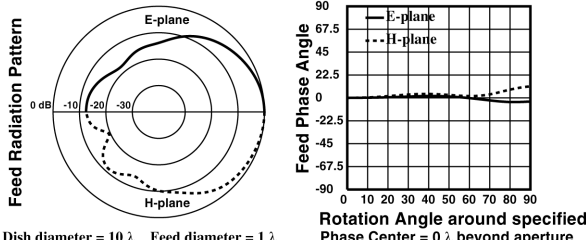
$$\Delta\phi = \frac{2\pi(1 - \cos\theta) \cdot d}{\lambda} \quad (\text{Eq 2})$$

then adjusting the original phase angle ϕ by adding $\Delta\phi$. We can also verify this phase-center calculation by adjusting the reference point in the NEC model and showing that the resulting phase pattern is the same as the one adjusted by the above calculations.

To illustrate the effect of feed phase on dish performance, I modified my *FEEDPATT* program (see Reference 1) to calculate and plot dish efficiency, including the effects of phase, as well as for amplitude only. Fig 4 is our first example of an output plot from the modified program, called *PHASEPAT*.⁸ The original amplitude-only efficiency is shown as a dashed line, so that the effect of phase error is readily

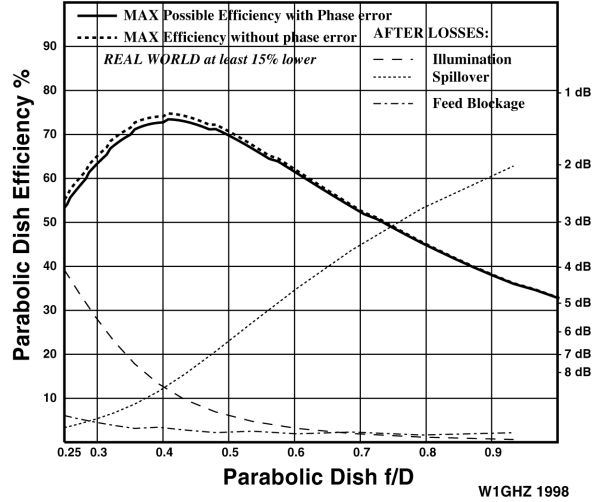
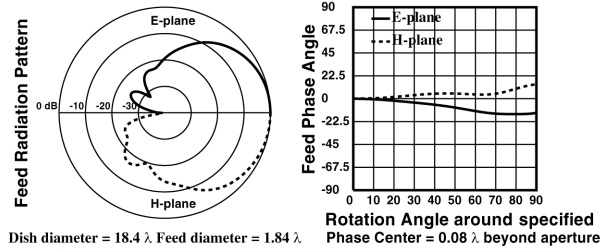
Coffee can feed 0.76λ diameter, by NEC2

Figure 5



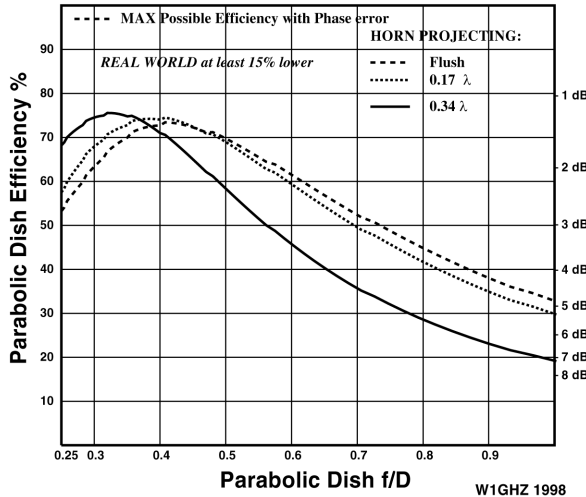
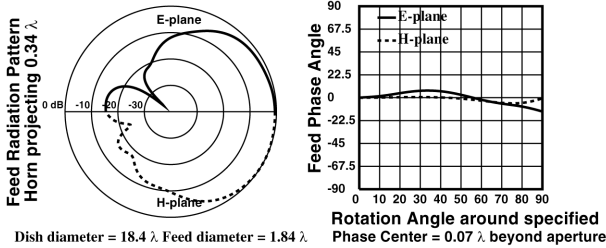
VE4MA 1296 feed, horn flush with choke ring, by NEC2

Figure 6



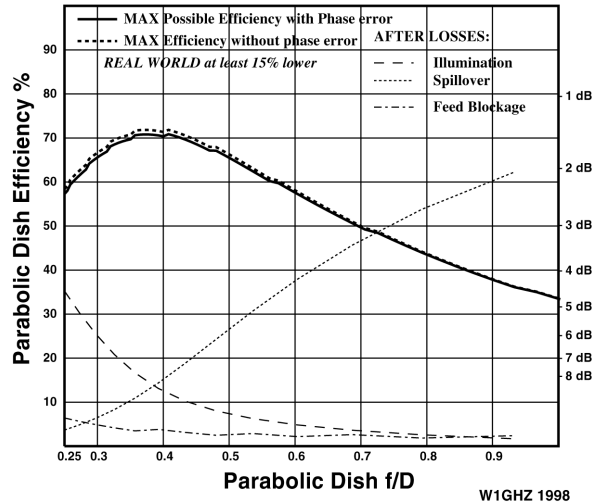
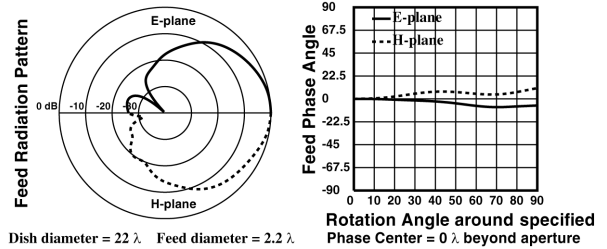
VE4MA 1296 feed - adjusting for f/D, by NEC2

Figure 7



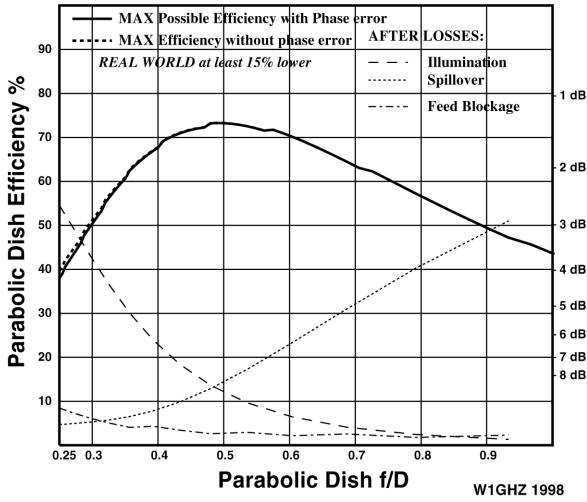
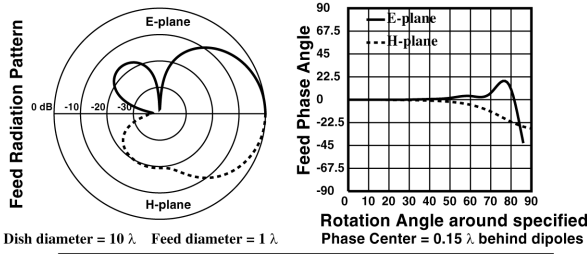
Chaparral style feed, 0.76λ dia horn projecting 0.26λ , by NEC2

Figure 8



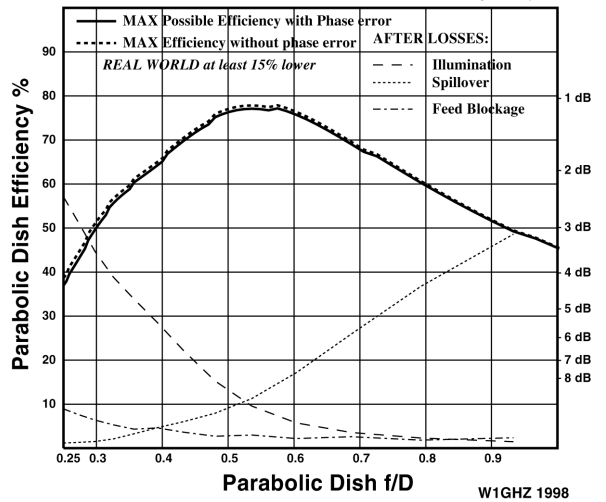
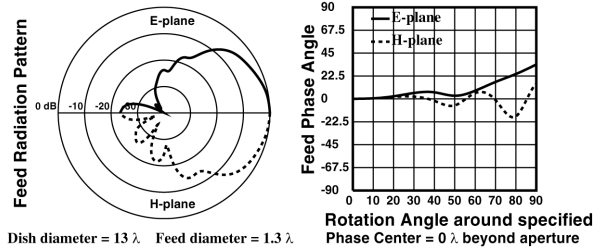
EIA dual-dipole reference antenna as feed, by NEC2

Figure 9



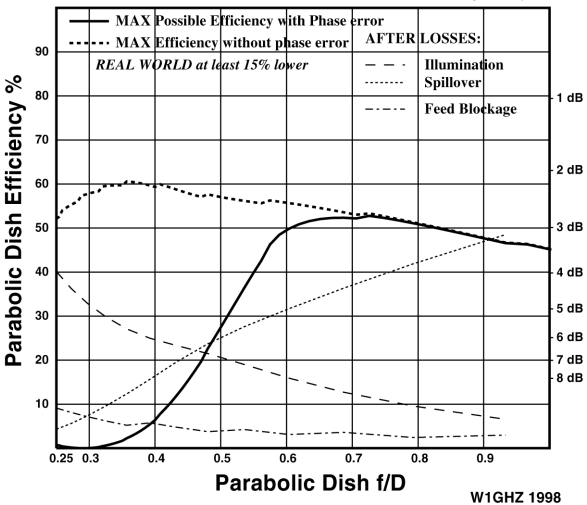
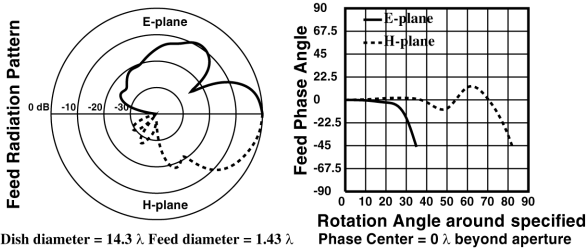
W2IMU dual-mode feedhorn, by NEC2

Figure 10



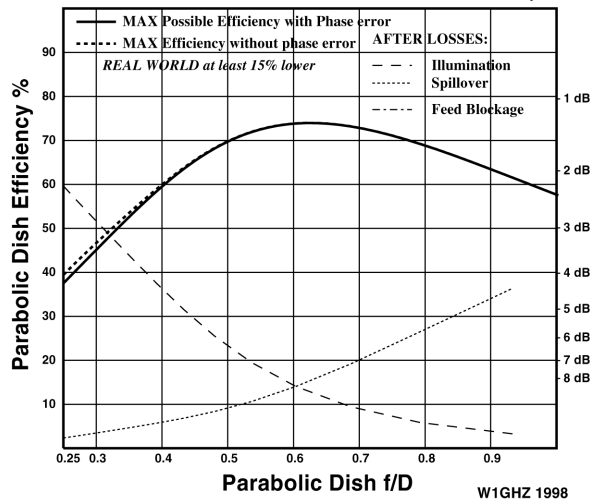
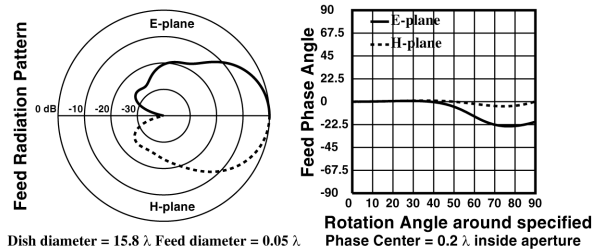
W2IMU feed - bad imitation, by NEC2

Figure 11



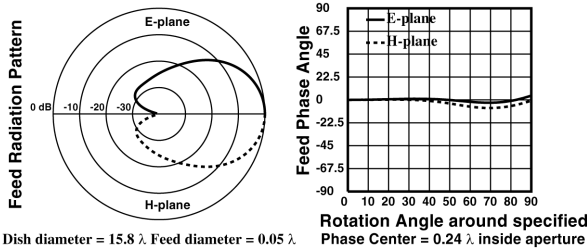
WR-90 horn for DSS offset dish at 10.368 GHz, by P.O.

Figure 12



RCA DSS corrugated horn at 10.368 GHz, by P.O.

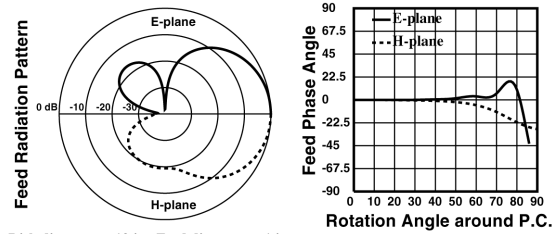
Figure 13



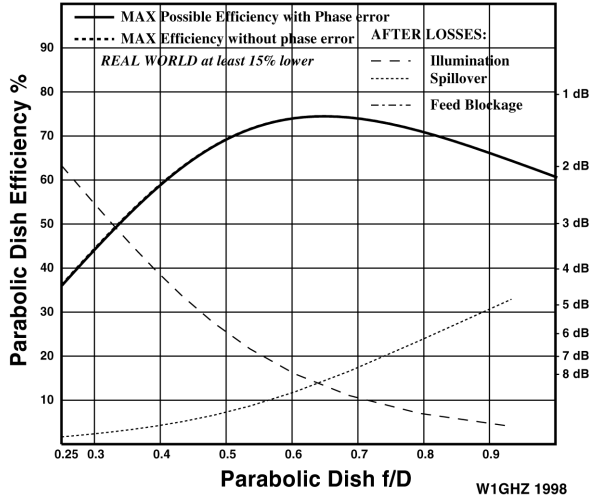
Dish diameter = 15.8λ Feed diameter = 0.05λ

EIA feed with axial feed displacement in 0.25λ steps

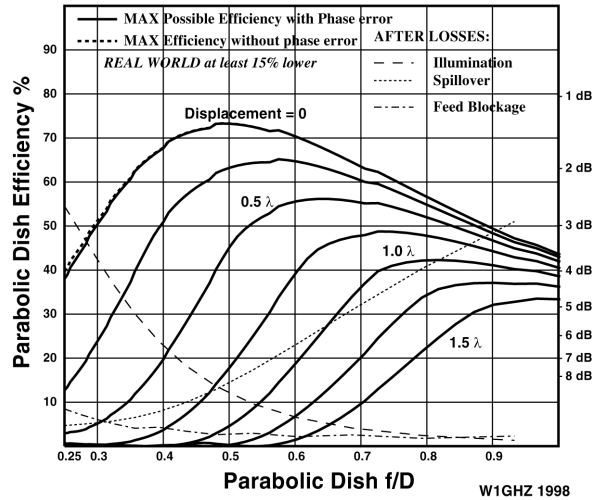
Figure 14



Dish diameter = 10λ Feed diameter = 1λ



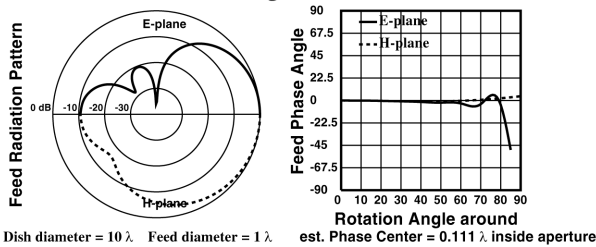
W1GHZ 1998



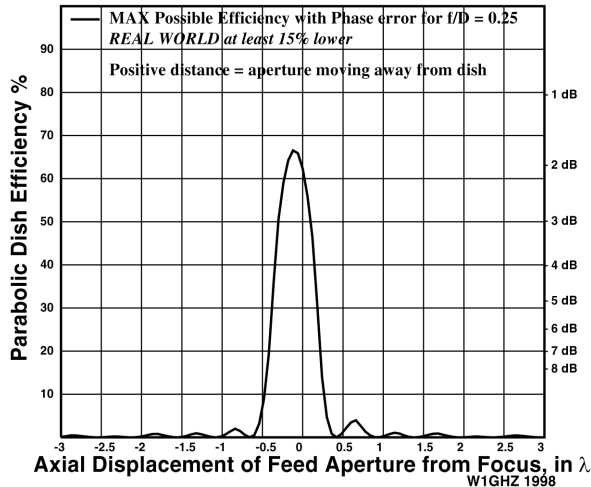
W1GHZ 1998

RSGB dipole-splashplate feed, by NEC2

Figure 15



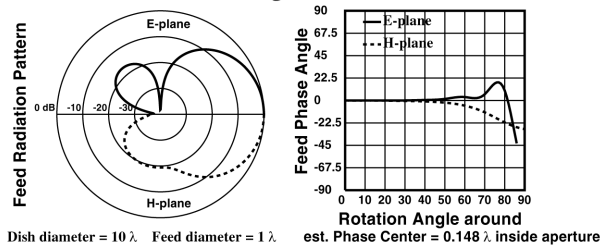
Dish diameter = 10λ Feed diameter = 1λ est. Phase Center = 0.111λ inside aperture



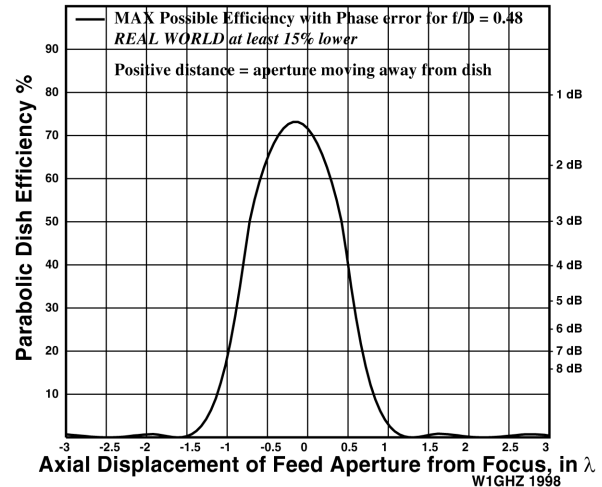
W1GHZ 1998

EIA dual-dipole feed, by NEC2

Figure 16



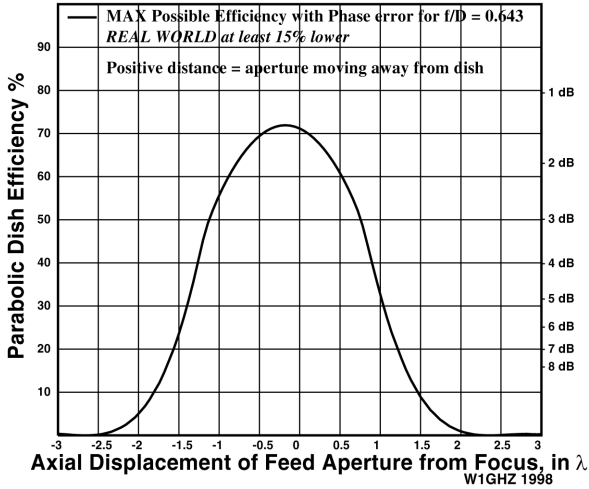
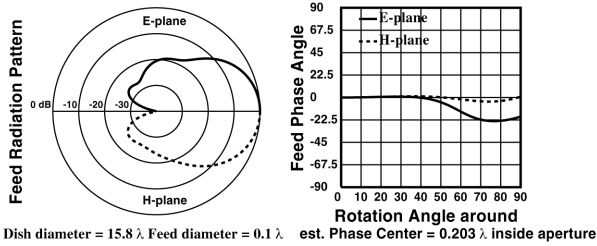
Dish diameter = 10λ Feed diameter = 1λ est. Phase Center = 0.148λ inside aperture



W1GHZ 1998

WR-90 horn for DSS offset dish at 10.368 GHz, by P.O.

Figure 17

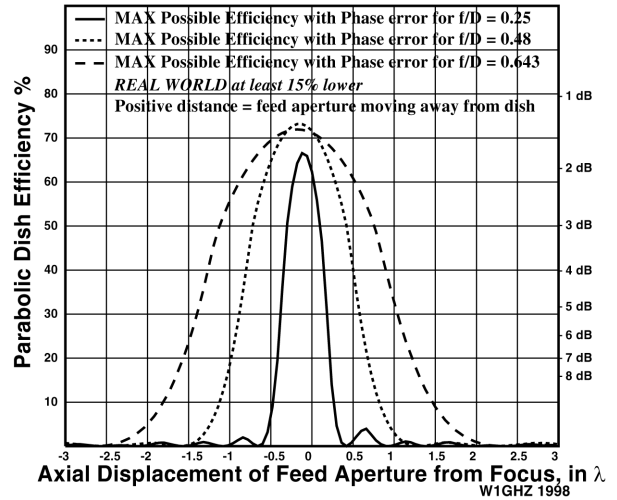


Focal Point Sensitivity of Real Feeds
 Figure 18

$f/D = 0.25$: RSGB dipole-splasher feed, by NEC2

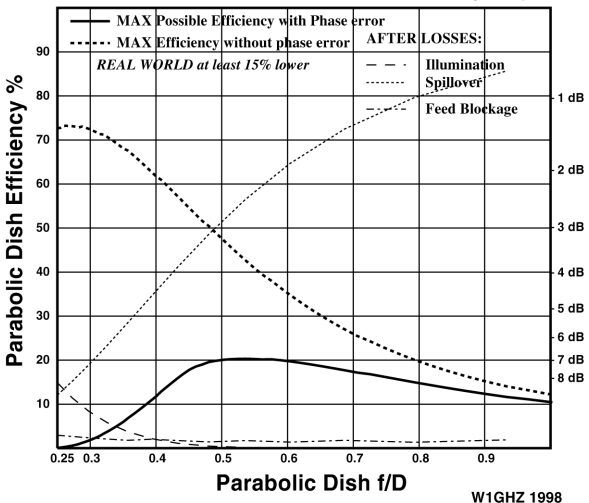
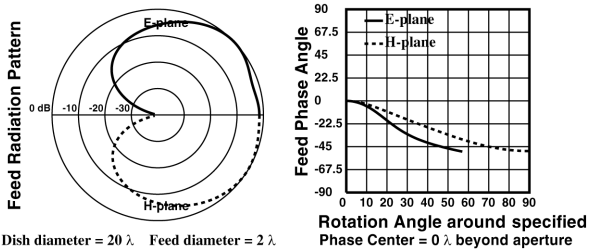
$f/D = 0.48$: EIA dual-dipole feed, by NEC2

$f/D = 0.64$: WR-90 horn for DSS offset dish at 10.368 GHz, by P.O.



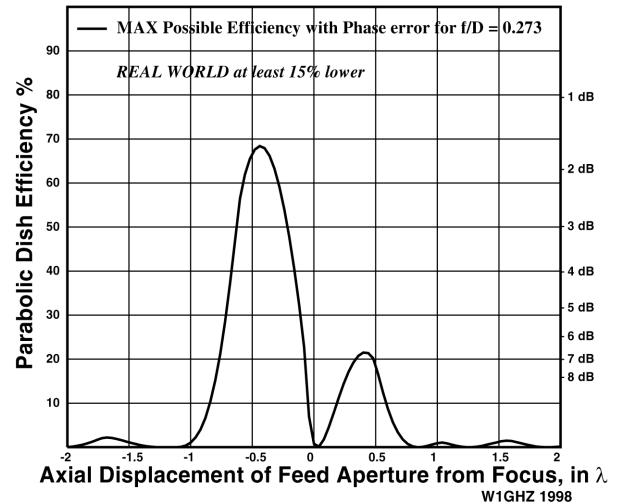
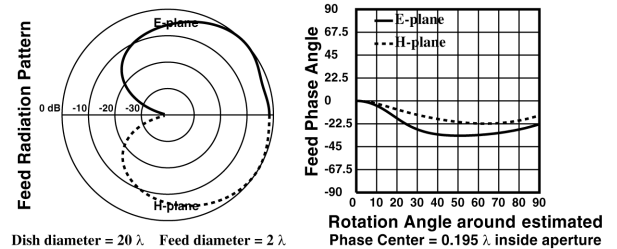
WR-90 small horn with cardioid pattern, by P.O.

Figure 19



WR-90 small horn with cardioid pattern, by P.O.

Figure 20



apparent. The output now also includes a phase plot for the feed in the upper-right part of each figure, in addition to the more common amplitude-radiation pattern for the feed at the upper-left. I used the modified program, *PHASEPAT*, to make plots for the feed patterns I was able to calculate. The modified program may be downloaded from <http://www.qsl.net/n1bwt/phasepat.zip>.

Real antennas have a number of other small losses that can add up to a significant loss of efficiency. My empirical estimate is that careful work can keep the loss to about 15%. Thus, each plot includes the statement, "REAL WORLD at least 15% lower."

Phase Performance of Feed Antennas

Most of the feeds we commonly use are popular because experience has shown that they work well. Thus, it is not surprising that most of them also have good phase performance—the phase of the radiation is nearly constant as the feed is rotated around its phase center. Let's look at a few examples of common feeds, both good and bad.

Dipole

A simple example is a dipole with a "splash plate" reflector spaced 0.3λ . Fig 4 plots the efficiency based on patterns calculated by *NEC2* from dimensions in the *RSGB Microwave Handbook*.⁹ The phase plot in the upper right of Fig 4 shows that the feed phase is quite uniform over a wide illumination angle, and efficiency is reasonably good for deep dishes, with f/D around 0.25 to 0.3. The calculated phase center is 0.11λ behind the dipole, not far from the recommended starting point of half-way between dipole and reflector.

Coffee can

Another simple feed is the "coffee can" feed,^{10,11} an open cylindrical waveguide. One common size has a diameter of 0.76λ ; Fig 5 is a plot of the pattern calculated by *NEC2*. The phase is uniform, with a phase center at the center of the aperture (the open end of the can). Efficiency is fairly good for f/D around 0.35 to 0.4. On an actual dish, the efficiency would probably be about 50%.

VE4MA

The VE4MA feed horn¹² is a popular feed for many microwave bands. It adds a choke ring to the coffee can feed to improve the front-to-back ratio. The

1296-MHz version is shown in Fig 6 with the choke ring flush with the horn end. The feed pattern calculated by *NEC2* has reasonably uniform phase over the forward half of the pattern-illumination angle, and provides improved efficiency for an f/D around 0.42 compared to a plain coffee-can feed. The choke ring may be moved to fine-tune the feed pattern over a small f/D range. Fig 7 shows the feed pattern with the choke ring moved back so that the horn projects by 0.34λ . The efficiency plot in Fig 7 shows that best f/D is around 0.3 to 0.35 for this case. The efficiency curve from Fig 6 is included for comparison, as well as one for an intermediate horn projection of 0.17λ , illustrating how adjusting the choke ring affects the optimum f/D for the feed. The phase center is close to the center of the aperture and moves slightly in the same direction as the choke ring is moved.

Chaparral

The Chaparral-style feed,¹³ found on many TVRO systems, adds additional choke rings to further improve the efficiency and provide performance over a wider bandwidth. Fig 8 shows the pattern calculated by *NEC2* with the choke rings flush with the end of the horn. The f/D for best efficiency is around 0.42, with quite uniform phase over this illumination angle, and the phase center is at the center of the aperture. The phase starts to vary rapidly at very wide illumination angles, and some deterioration of the calculated efficiency is evident for small f/D s. Like the VE4MA feed, the choke-ring position may be moved to fine-tune the pattern over a small range of f/D , but the pattern is less sensitive to position.

EIA Dual-Dipole

The EIA reference antenna,¹⁴ a dual dipole over a ground plane, is a popular feed at UHF frequencies. The feed pattern calculated by *NEC2*, shown in Fig 9, has some interesting features. The phase is fairly constant over about $\pm 50^\circ$, then starts to change, with a wild variation around an E-plane null at 90° . However, since the f/D for best efficiency is around 0.5, the phase variation is outside the desired illumination angle of 106° , or $\pm 53^\circ$, and misses the reflector. The phase center is about 0.15λ behind the dipoles.

W2IMU

For shallower dishes, the W2IMU dual-mode feed¹⁵ is a popular choice. The feed pattern in Fig 10, calculated

by *NEC2*, has uniform phase over the narrower illumination angle suitable for a shallow dish. Therefore, the calculated efficiency for an f/D around 0.5 to 0.6 is excellent. The phase center is at the center of the aperture.

Not all antennas have good phase performance, however. The W2IMU dual-mode feed has two critical dimensions,¹⁶ so that the two modes arrive at the aperture out of phase to achieve cancellation of currents in the rim of the horn. Any current in the rim will add side lobes and affect the clean pattern shown in Fig 10. As an example, I took an off-the-shelf plumbing adapter. At first glance, it looks like a dual-mode feed for 10 GHz. A typical ham practice would be to try it and see if it is close enough. Unfortunately, the dimensions aren't right, and the calculated pattern, shown in Fig 11, is rather ugly. If we were to consider amplitude only, as we did in the past, the calculated efficiency would be mediocre, but the poor phase performance results in very low efficiency.

Rectangular horn

Offset dishes, like the DSS dish, require narrower illumination angles. I use a small rectangular horn¹⁷ for a feed. Fig 12 shows the pattern calculated using Physical Optics, with excellent phase uniformity and efficiency for an f/D around 0.6. The phase center is about 0.2λ inside the aperture. While Fig 12 only shows the E-plane and H-plane patterns, the 45° planes also have excellent patterns. I was very lucky in designing this horn.

Corrugated horn

The RCA DSS system uses a corrugated conical horn to feed the offset dish. The corrugations, if deeper than $\lambda/4$, prevent current from flowing in the walls of the horn, so that side lobes are reduced. Fortunately, the corrugations are deep enough to work at 10 GHz. The pattern for this horn at 10.368 GHz, calculated by Physical Optics, is shown in Fig 13. The phase center is about 0.24λ inside the aperture. The pattern looks cleaner than the pattern for my rectangular horn, but the efficiency is only 1 or 2% higher. The advantage is that the corrugated horn probably works well over a wider bandwidth. W1RIL uses a modified RCA feed horn on his offset dish and provided the dimensions needed for pattern calculation.

Multiband feeds

Multiband feeds present another

problem: The phase center usually has a different location at each frequency. Complex structures with poor symmetry such as log-periodic arrays are particularly bad. Therefore, we need to calculate radiation patterns and phase centers for each frequency of interest, and choose some compromise for positioning the feed with respect to the focal point of the dish. I suggest that the highest frequency is the most critical one for phase-center location.

Axial-Displacement Error

When the phase center of a feed is not at the focus, but at some other distance from the reflector, the resulting phase error causes a loss in efficiency that is referred to as axial-displacement error. In a previous article (see [Reference 2](#)), I showed curves for axial-displacement error based on uniform illumination, since it was a much simpler calculation. Now that we can calculate feed patterns and phase centers, we can also calculate the axial phase error for actual feeds.

In the same way that we adjust the phase pattern to the desired phase center, we may adjust it to some other point along the axis, where the new phase pattern is identical to that at the focus of the dish. Then we can plot the resulting efficiency curve. [Fig 14](#) shows a family of efficiency curves for axial displacement in 0.25λ steps toward the dish, using an EIA dual-dipole feed as an example. Clearly, the peak efficiency decreases with axial feed displacement from the focus and decreases faster at smaller f/D s. Displacement in the other direction, away from the dish, produces a similar family of efficiency curves.

If we plot peak efficiency *versus* axial displacement, we can clearly see the sensitivity of efficiency to axial displacement. [Fig 15](#) shows this relationship for the dipole-splash-plate feed; zero displacement on this plot is with the dipole at the focus. However, best efficiency does not occur at zero displacement, but with the dipole displaced toward the reflector by 0.11λ . This position is obviously the best phase center for this feed and f/D , so we can conclude that the best phase center is 0.11λ behind the dipole. This is the technique used to find all the phase centers previously cited.

Similar plots of peak efficiency *versus* axial displacement are shown in [Fig 16](#) for the EIA dual-dipole feed and [Fig 17](#) for the rectangular-horn feed for the DSS dish. When we plot the curves for the three feeds on the same

graph in [Fig 18](#), it is quickly apparent that deep dishes, with small f/D s, are much more sensitive to axial-displacement error.

It might be informative to evaluate this sensitivity. Returning to [Eq 2](#), which we used to find the phase center, we can see that the phase error for a given axial displacement d is a function of the rotation angle. Therefore, the error increases as the illumination angle of the dish becomes larger. A larger illumination angle is more sensitive to phase error in the feed.

Since most offset-fed reflectors need a small illumination angle, equivalent to a large f/D , the phase error resulting from a given feed displacement equals that for a dish with a large f/D . Thus, the efficiency of an offset dish has a low sensitivity to axial feed-displacement errors. The combination of this low sensitivity with the other advantage of offset dishes, elimination of feed blockage, makes the offset dish highly attractive.

Before doing the analysis of phase-center sensitivity, I had thought that the sensitivity to axial-displacement error would be related to the f/D of the full parabola. Since the DSS offset-fed dish is a section of a full parabola with a small f/D of about 0.3, I had concluded that the offset dish would be sensitive to axial-displacement error (see [Reference 16](#)). Now that it is clear that the axial-displacement error is caused by the phase error resulting from feed displacement and is a function of illumination angle, we can see that the offset dish is insensitive to feed-positioning errors.

An important point to note in [Fig 18](#) is that the feed axial displacement is in wavelengths, regardless of dish size. A $1\text{-}\lambda$ error in feed placement will result in the same efficiency reduction whether the dish is one foot or 50 feet in diameter. For multiband feeds, the error is larger at higher frequencies, since each millimeter is a larger part of wavelength. Thus, the feed placement should be chosen to favor the phase center at the highest frequency.

For the three feeds illustrated in [Fig 18](#), an intuitive location for the phase center would be at the aperture of the horn, or the plane of the dipole. Calculating the actual location of the phase center provides some improvement, but these feeds would work pretty well using the intuitive location. Some feeds are not so forgiving, however. While looking through W8JK's famous book, *Antennas*,¹⁸ I noticed that some of the rectangular-horn patterns have cardioid

shapes, which might provide increased illumination at the edge of a dish like the desired illumination pattern of [Fig 1](#). After calculating a few trial patterns for small horns, I arrived at a set of dimensions that seemed promising and used an early version of PHASEPAT—without phase-center correction—to analyze its performance as a feed. The resulting dish efficiency, shown in [Fig 19](#), was abysmal. A plot of axial-displacement error, [Fig 20](#), shows why: The phase center is about 0.4λ inside the horn, with a large axial-displacement error at the aperture. The efficiency without correcting for phase center is very low. An efficiency plot for the best phase center, [Fig 21](#), shows dramatic improvement, but the best calculated efficiency is around 66% for a small f/D around 0.25. The efficiency on a real dish would likely be around 50%, which isn't bad for a very deep dish. I have not actually tried this feed, however.

Dish Patterns with Axial-Displacement Error

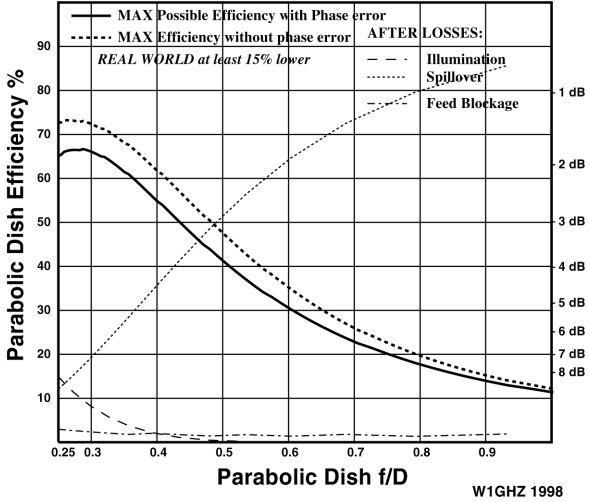
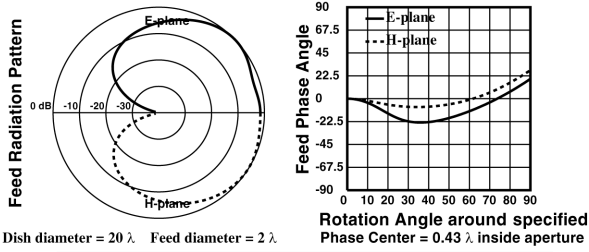
When I first discussed axial-displacement error, one of the first questions that arose was: "Where does the power go when the gain is reduced?" The best way to answer this is by calculating sample patterns for a dish with various feed displacements, using Physical Optics. For this example, we will use a simple feed horn, 1.2λ in diameter (any larger diameter could support additional waveguide modes). The feed radiation pattern and predicted dish efficiency, about 72% for an $f/D = 0.5$, is shown in [Fig 22](#). Experience suggests that efficiency on a real dish would be perhaps 15% lower than predicted. [Fig 23](#) shows the calculated pattern for a $0.5 f/D$ dish, 20λ in diameter, when illuminated by this horn with the horn phase center at the focus of the dish. Calculated gain—neglecting feed blockage—is about 34.4 dBi, for an efficiency of about 70%, very close to our prediction. The 3-dB beamwidth is about 5° .

The axial-displacement error for this feed is shown in [Fig 24](#), so that we may choose some other interesting locations for closer examination. With an axial displacement of 0.5λ , gain is reduced by less than 1 dB, but a $1\text{-}\lambda$ displacement produces a huge reduction, so an intermediate point of $3/4 \lambda$ might be interesting. There is an apparent null at about 1.5λ displacement and very poor performance with further displacement.

To examine the effect of axial feed displacement at the points chosen

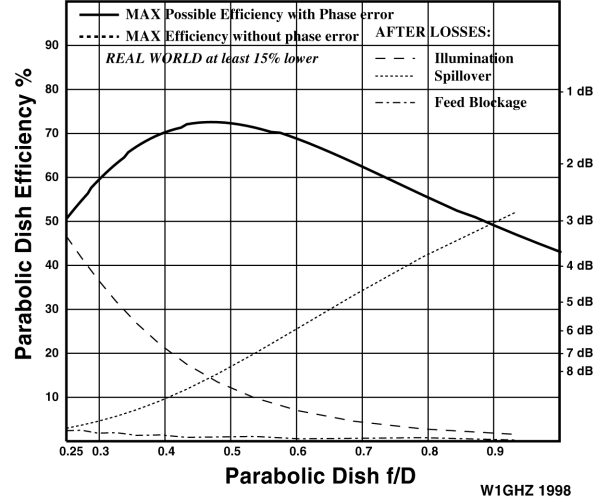
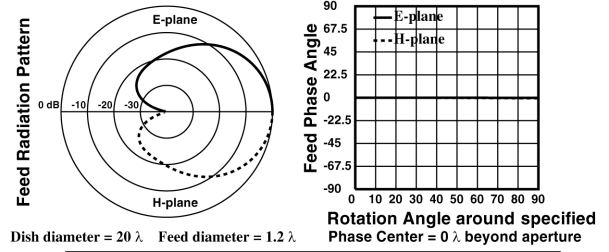
WR-90 small horn with cardioid pattern, PC at focus, by P.O.

Figure 21



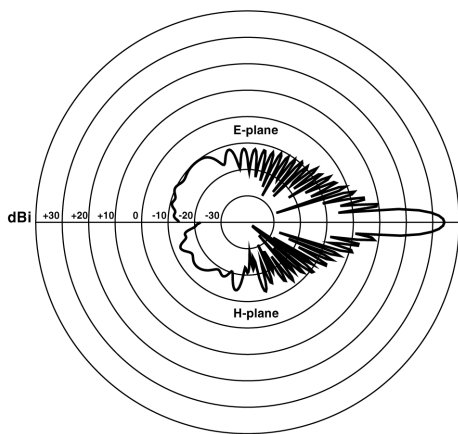
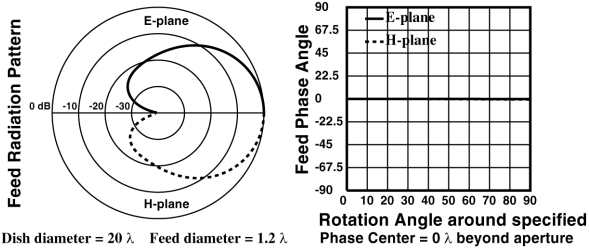
Test horn for dish examples, 1.2λ diameter, by P.O.

Figure 22



Test dish with feed at focus, by P.O.

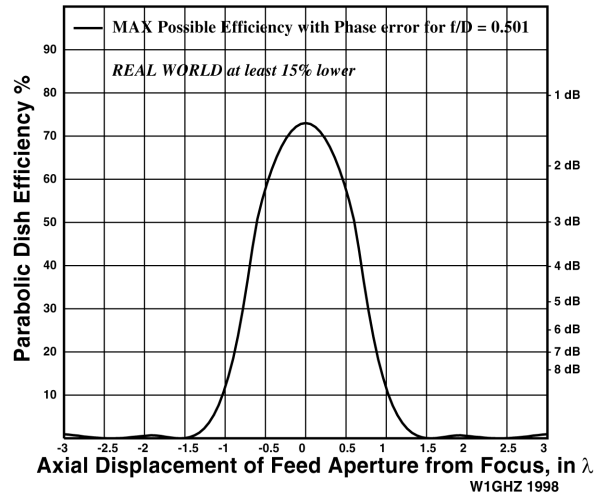
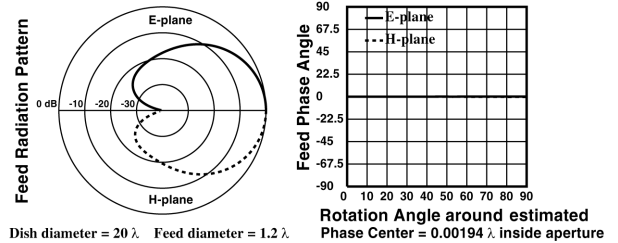
Figure 23



W1GHZ 1998

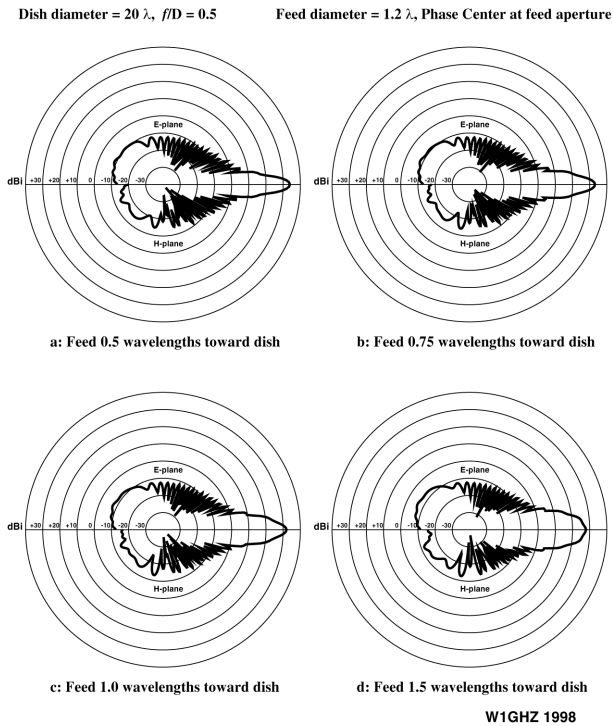
Test horn for dish examples, 1.2λ diameter, by P.O.

Figure 24



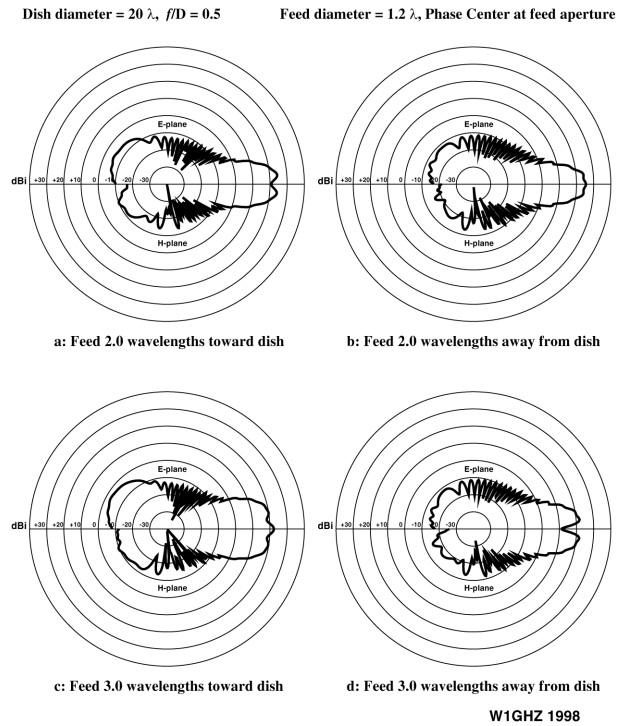
Dish patterns with feed displaced axially from focus, by P.O.

Figure 25



Dish patterns with feed displaced axially from focus, by P.O.

Figure 26



above, we calculate dish radiation patterns at these displacements as the feed is moved axially toward the reflector. Fig 25 shows the patterns at the chosen displacements. In Fig 25A, at 0.5λ of axial displacement, gain has dropped by about 0.5 dB. As the feed is moved farther toward the dish, gain decreases. The reduction is 1.3 dB at 0.75λ in Fig 25B, 2.5 dB at 1λ in Fig 25C and 6.6 dB at 1.5λ displacement in Fig 25D. Feed displacement in the other direction, away from the reflector, produces similar results. The dish patterns show gain and efficiency decreasing with axial displacement. The lost energy goes into a broadening of the near side lobes. The 3-dB beamwidth of the main beam remains constant at about 5° for displacements less than about 1λ .

Larger axial-feed displacements are even worse. Fig 26 shows the dish radiation patterns for displacements of 2 and 3λ in each direction. All the larger displacements result in large gain reductions—more than 10 dB—and ugly patterns. The patterns in Figs 26A and 26D have a dip on the bore sight. Try to visualize a donut-shaped main lobe, with a hole in the middle. It would be difficult to peak a signal with this antenna pattern.

Readers astute enough to calculate efficiencies may have noticed that the

efficiency found in the radiation patterns does not drop off quite so quickly as shown in Fig 24 with axial displacement, probably because of the different approximations used. Since the main value of axial displacement plots is to accurately locate the best phase center for a feed, I'm not concerned about small errors in the undesirable regions.

The radiation pattern of a dish is quite sharp, and it can be difficult to find signals if the direction is not accurately known. I have heard of hams who deliberately moved the feed inward to defocus the dish, as a sort of zoom control. Since we found that the 3-dB beamwidth does not change for small axial displacements, this strategy obviously does not work. The beamwidth does become broader at large displacements, but the resulting gain is much lower and the pattern is dirty, so it would still be difficult to locate and peak weak signals. I think that being able to aim a dish accurately would be more effective in locating weak signals. For the very sharp beamwidths available at the higher microwave bands, scheduling or liaison on lower frequencies is often necessary.

Summary

The ability to calculate antenna patterns with both amplitude and phase

allows us to more accurately estimate performance of various parabolic-dish feeds. It also provides the ability to calculate phase centers of the feeds and see the effects of axial-displacement errors. Graphical presentation enables us to visualize the data and use them to optimize the performance of our dishes.

As we concluded previously (see References 1 and 2), optimum dish performance is realized by matching the feed to the f/D of the dish and aligning the phase center of the feed at the focus of the parabola. Computer analysis is useful in both choosing the best feed and calculating its phase center.

Acknowledgements

The NEC models for many of the feed horns were derived from models for the VE4MA and W2IMU feeds provided to me by Peter Beyer, PA3AEF. The NEC2 program was compiled to run under *linux* on an Alpha PC by Matt Reilly, KB1VC.

References

- 1P. Wade, N1BWT, "Parabolic Dish Feeds, Performance Analysis," *QEX*, Jan 1998, pp 9-33.
- 2P. Wade, N1BWT, "Practical Microwave Antennas, Part 2," *The ARRL UHF/Microwave Projects Manual*, Vol 2, pp 1-9 to 1-19. ARRL publications are available from your

local ARRL dealer or directly from the ARRL. Mail orders to Pub Sales Dept, ARRL, 225 Main St, Newington, CT 06111-1494. You can call us toll-free at tel 888-277-5289; fax your order to 860-594-0303; or send e-mail to pubsales@arrl.org. Check out the full ARRL publications line on the World Wide Web at <http://www.arrl.org/catalog>.

- ³J. D. Dyson, "Phase Centres," in *The Handbook of Antenna Design*; A. W. Rudge, K. Milne, A. D. Olver and P. Knight, Editors, (London: Peter Perigrinus, Ltd, 1986), p 657.
- ⁴G. J. Burke and A. J. Poggio, *Numerical Electromagnetic Code (NEC)—Method of Moments*, Lawrence Livermore Laboratory, 1981.
- ⁵L. Diaz and T. Milligan, *Antenna Engineering Using Physical Optics*, (Boston: Artech House, 1996).
- ⁶W. V. T. Rusch, "A Comparison of Geometrical and Integral Fields From High Frequency Reflectors," *Proceedings of the*

IEEE, November 1974, pp 1603-1604.

- ⁷G. A. Evans, *Antenna Measurement Techniques*, (Boston: Artech House, 1990), p 82.
- ⁸The figures have been printed in a small format to conserve space. All necessary detail is shown, but some readers may want to see more. Therefore, the figures are available on the QEX download site. You can download this package from the ARRL Web <http://www.arrl.org/files/qex/>. Look for 9909WADE.ZIP.
- ⁹M. W. Dixon, G3PFR, *Microwave Handbook*, Vol 3, RSGB, 1992, p 14.25.
- ¹⁰D. Vilardi, WA2VTR, "Simple and Efficient Feed for Parabolic Antennas," *QST*, March 1973, pp 43-44.
- ¹¹J. Harrison, W5ZN, "Horns for the Holidays," *Proceedings of Microwave Update '97* (Newington: ARRL, 1997), pp 147-149.
- ¹²B. W. Malowanchuk, VE4MA, "Selection of an Optimum Dish Feed," *Proceedings of the 23rd Conference of the Central States VHF Society* (Newington: ARRL, 1989),

pp 35-43.

- ¹³R. Wohlleben, H. Mattes, O. Lochner, "Simple Small Primary Feed for Large Opening Angles and High Aperture Efficiency," *Electronics Letters*, 21 Sep 1972, pp 181-183 [reprinted in A. W. Love, *Electromagnetic Horn Antennas* (New Jersey: IEEE, 1976), pp 181-183.]
- ¹⁴D. Turrin, W2IMU, "Antenna Performance Measurements," *QST*, Nov 1974, pp 35-41.
- ¹⁵D. Turrin, W2IMU, "A Paraboloidal Reflector Antenna for 1296 mc/s," *Crawford Hill Technical Report #5*, 1971.
- ¹⁶R. C. Johnson, *Antenna Engineering Handbook* (New York: McGraw-Hill, 1993), pp 15-23 to 15-25.
- ¹⁷P. Wade, N1BWT, "More on Parabolic Dish Antennas," *The ARRL UHF/Microwave Projects Manual*, Vol 2 (Newington: ARRL, 1997), pp 1-30 to 1-38.
- ¹⁸J. D. Kraus, W8JK, *Antennas* (New York: McGraw-Hill, 1950), p 376.



Join the effort in developing Spread Spectrum Communications for the amateur radio service. Join TAPR and become part of the largest packet radio group in the world. TAPR is a non-profit amateur radio organization that develops new communications technology, provides useful/affordable kits, and promotes the advancement of the amateur art through publications, meetings, and standards. Membership includes a subscription to the *TAPR Packet Status Register* quarterly newsletter, which provides up-to-date news and user/technical information. Annual membership US/Canada/Mexico \$20, and outside North America \$25.



TAPR CD-ROM

Over 600 Megs of Data in ISO 9660 format. TAPR Software Library: 40 megs of software on BBSs, Satellites, Switches, TNCs, Terminals, TCP/IP, and more! 150Megs of APRS Software and Maps. RealAudio Files. Quicktime Movies. Mail Archives from TAPR's SIGs, and much, much more!

Wireless Digital Communications: Design and Theory

Finally a book covering a broad spectrum of wireless digital subjects in one place, written by Tom McDermott, N5EG. Topics include: DSP-based modem filters, forward-error-correcting codes, carrier transmission types, data codes, data slicers, clock recovery, matched filters, carrier recovery, propagation channel models, and much more! Includes a disk!



Tucson Amateur Packet Radio

8987-309 E. Tanque Verde Rd #337 • Tucson, Arizona • 85749-9399
Office: (940) 383-0000 • Fax: (940) 566-2544 • Internet: tapr@tapr.org www.tapr.org
Non-Profit Research and Development Corporation

Basics of Digital-Receiver Design

Advances in data-converter and radio technology have greatly simplified the design of complex receivers. Come learn the basic techniques and calculations to design radios and estimate performance.

By Brad Brannon, N4RGI

[Reprinted with permission from EDN Magazine (November 5, 1998). Copyright Cahners Business Information, A Division of Reed Elsevier Inc.]

Many advances in design and architecture are now allowing rapid changes in the field of radio. These changes allow reduction of size, cost and complexity; they improve manufacturing by using digital components to replace unreliable and inaccurate analog components. For this to happen, many advances in semiconductor design and fabrication were required; these have come to fruition over the last few years. Some of these advances include better integrated mixers and LNAs; improved SAW filters; lower-cost, high-performance ADCs and programmable digital tuners and filters. This article summarizes the design issues related to these

devices and their implementation in complete radio systems.

What is a Radio?

Traditionally, a radio has been considered to be the box that connects to the antenna and everything behind that; however, many system designs are segmented into two separate subsystems: the radio and the digital processor. With this segmentation, the purpose of the radio is to down convert and filter the desired signal, then digitize the information. The purpose of the digital processor is to take the digitized data and extract the desired information.

An important point to understand is that a digital receiver is not the same thing as digital radio (modulation). In fact, a digital receiver will do an excellent job of receiving any analog signal such as AM or FM. Digital receivers can be used to receive any type of modulation including any analog or digital modulation standards. Furthermore, since the core of a digital radio is a digi-

tal signal processor (DSP), this allows many aspects of the entire receiver to be controlled through software. These DSPs can be reprogrammed with upgrades or new features based on customer segmentation, all using the same hardware. However, this is a complete discussion in itself and not the focus of this article.

The focus of this article is the radio, how to design for performance and predict the results. The following topics will be discussed:

- Available Noise Power
- Cascaded Noise Figure
- Noise Figure and ADCs
- Conversion Gain and Sensitivity
- ADC Spurious Signals and Dither
- Third-Order Intercept Point (IP3)
- ADC Clock Jitter
- Phase Noise
- IP3 in the RF section

Single-Carrier versus Multi-Carrier

There are two basic types of radios under discussion. The first is called a

1714 Hobbs Rd
Greensboro, NC 27410
brad.brannon@analog.com

single-carrier (Fig 1) and the second a multi-carrier receiver (Fig 2). Their names imply the obvious; however, their functions may not be fully clear. The single-carrier receiver is a traditional radio receiver deriving selectivity in the analog filters of the IF stages. The multi-carrier receiver processes all signals within the band with a single RF/IF analog strip, deriving selectivity from the digital filters that follow the analog-to-digital converter. The benefit of such a receiver is that in applications with multiple receivers tuned to different frequencies within the same band, it can achieve smaller system designs and reduced cost because of eliminated redundant circuits. A typical application is a cellular/wireless local-loop base station. Another application might be surveillance receivers that typically use scanners to monitor multiple frequencies. This application allows simultaneous monitoring of many frequencies without the need for sequential scanning.

Benefits of Implementing a Digital Radio Receiver

Before a detailed discussion of designing a digital radio receiver, some of the technical benefits need to be exposed. These include oversampling,

processing gain, undersampling, frequency planning and spur placement. Many of these provide technical advantages not otherwise achievable with a traditional radio receiver design.

Oversampling and Process Gain

The Nyquist criterion compactly determines the sample rate required for any given signal. Many times, the Nyquist rate is quoted as twice that of the highest frequency component. This implies that for an IF sampling application at 70 MHz, a sample rate of 140 MSPS would be required. If our signal only occupies 5 MHz around 70 MHz, then sampling at 140 MSPS is overkill. Instead, Nyquist requires that the signal be sampled at twice the

signal *bandwidth*. Therefore, if our signal bandwidth is 5 MHz, then sampling at 10 MHz is adequate. Anything beyond this is called oversampling. Oversampling is a very important function because it allows for an effective gain in received SNR in the digital domain.

In contrast to oversampling, is undersampling. Undersampling is the act of sampling at a frequency much less than half the actual signal frequency (see the [section](#) below). Therefore, it is possible to oversample and undersample simultaneously, since one is defined with respect to bandwidth and the other by the frequencies of interest.

In any digitization process, faster

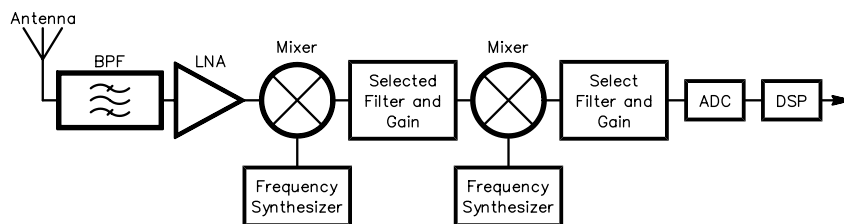


Fig 1—Typical single-carrier receiver.

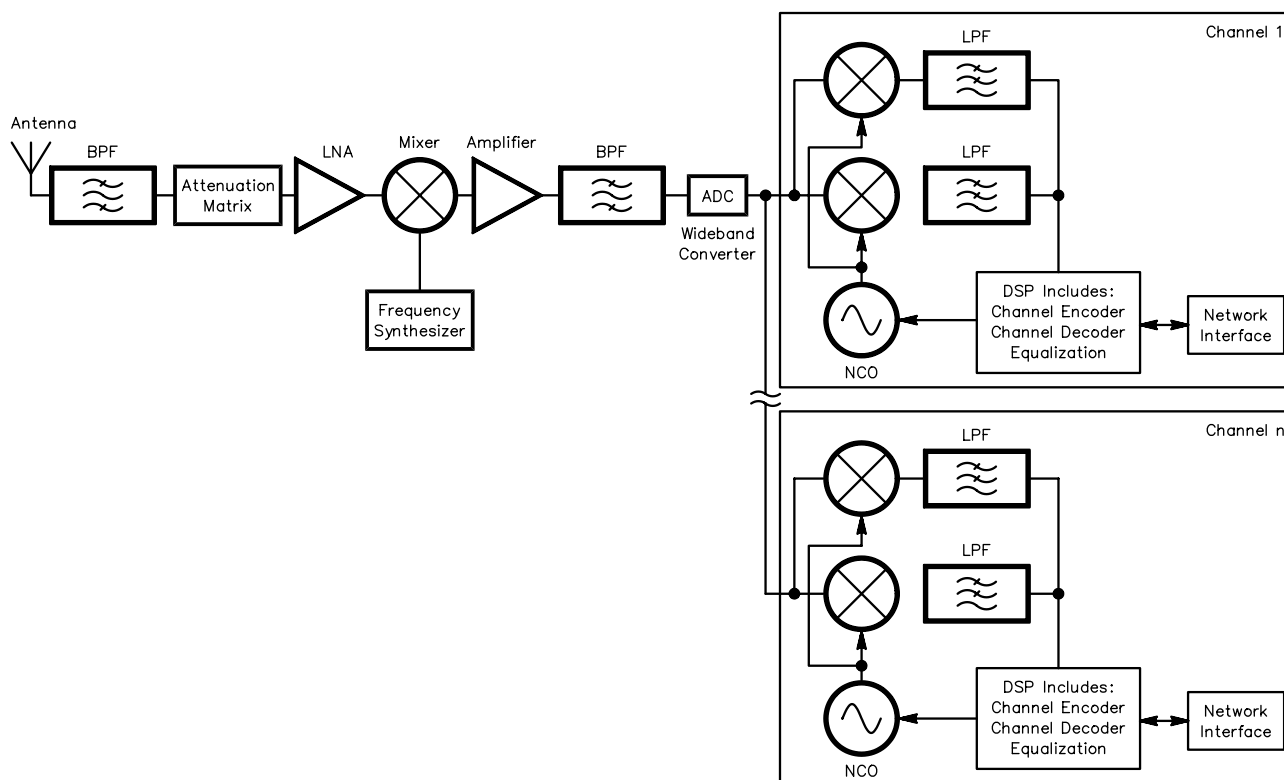


Fig 2—Typical multi-carrier receiver.

sampling lowers the noise floor because noise is spread out over more frequencies. This has benefits if the ADC is followed by a digital filter. The noise floor follows the equation:

$$\text{Noise Floor} = 6.02B + 1.8 + 10 \log \left(\frac{F_s}{2} \right) \quad (\text{Eq 1})$$

This equation represents the level of the quantization noise within the converter and shows the relationship between noise and the sample rate, F_s . Therefore, each time the sample rate is doubled, the effective noise floor improves by 3 dB!

Digital filtering has the effect of removing all unwanted noise and spurious signals, leaving only the desired signal, as shown in the figures below. The SNR of the ADC may be greatly improved as shown in Figs 3 and 4. In fact, the SNR can be improved by:

$$\text{Process Gain} = 10 \log \left(\frac{f_{\text{SampleRate}}}{2BW_{\text{Signal}}} \right) \quad (\text{Eq 2})$$

As shown, the greater the ratio of sample rate to signal bandwidth, the higher the process gain. In fact, gains as high as 30 dB are achievable.

Undersampling and Frequency Translation

As stated earlier, undersampling is the act of sampling at a frequency much less than the half the actual signal frequency. For example, a 70-MHz signal sampled at 13 MSPS is undersampled.

Undersampling is important because it can serve a function very similar to mixing. When a signal is undersampled, the frequencies are aliased into baseband or the first Nyquist zone as if they were in the baseband originally. For example, when our 70-MHz signal is sampled at 13 MSPS it would appear at 5 MHz. This can be mathematically described by:

$$f_{\text{Signal}} \text{ MOD } f_{\text{SampleRate}} \quad (\text{Eq 3})$$

This quantity provides the resulting frequency in the first and second Nyquist zones. Since the ADC aliases all information to the first Nyquist zone, results generated by this term must be checked to see if they are above $f_{\text{SampleRate}} / 2$. If they are, then the frequency must be folded back into the first Nyquist zone by subtracting the result from $f_{\text{SampleRate}}$.

The table below shows how signals can be aliased into baseband and their spectral orientation. Although the process of sampling (aliasing) is different than mixing (multiplication), the

results are quite similar, but periodic about the sample rate. Another phenomenon is that of spectral reversal. As in mixers, certain products become reversed in the sampling process such as upper and lower sidebands. Table 1 also shows which cases cause spectral reversal.

Frequency Planning and Spur Placement

One of the biggest challenges in radio architecture is that of IF placement. This problem is compounded by the tendency of drive amplifiers and

ADCs to generate unwanted harmonics that show up in the digital spectrum of the data conversion, appearing as false signals. Careful selection of sample rates and IFs can place these spurs at locations that render them harmless when used with digital tuners and filters—like the AD6620—that can select the signal of interest and reject all others. All of this is good, because by carefully selecting input frequency range and sample rate, the drive-amplifier and ADC harmonics can actually be placed out of band. Oversampling only simplifies matters

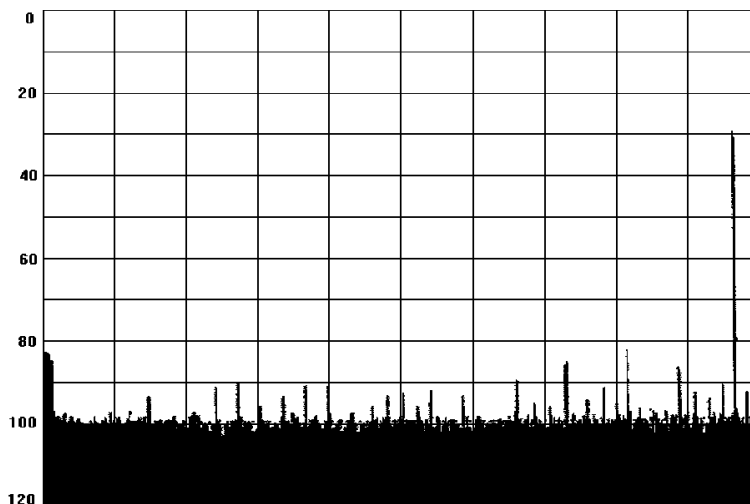


Fig 3—Typical ADC spectrum before digital filtering.

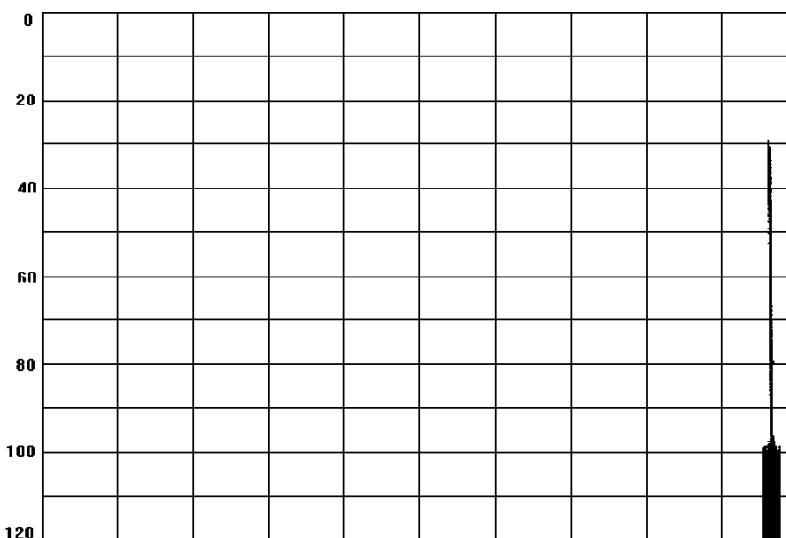


Fig 4—Typical ADC spectrum after digital filtering.

by providing more spectrum in which the harmonics may harmlessly fall.

For example, if the second and third harmonics are determined to be especially strong, by carefully selecting where the analog signal falls with respect to the sample rate, these second and third harmonics can be placed out of band. For the case of an encode rate equal to 40.96 MSPS and a signal bandwidth of 5.12 MHz, placing the IF between 5.12 and 10.24 MHz places the second and third harmonics out of band as shown in Fig 5. Although this example is very simple, it can be tailored to suit many differed applications.

As can be seen, the second and third harmonics fall away from the band of interest and cause no interference to the fundamental components. Note that the seconds and thirds do overlap with one another and the thirds alias around $F_s/2$. In tabular form, this looks as shown in Table 2.

Another example of frequency planning can be found in undersampling. (Refer to Fig 6.) If the analog input signal range is from dc to $F_s/2$, then the amplifier and filter combination must perform to the specification required. However, if the signal is placed in the third Nyquist zone (F_s to $3F_s/2$), the amplifier is no longer required to meet the harmonic performance required by the system specifications, since all harmonics would fall outside the passband filter. For example, the passband filter would range from F_s to $3F_s/2$. The second harmonic would span from $2F_s$ to $3F_s$, well outside the passband filter's range. The burden then has been passed off to the filter design, provided that the ADC meets the basic specifications at the frequency of interest. In many applications, this is a worthwhile tradeoff, since many complex filters can easily be realized using SAW and LCR techniques alike at these relatively high IFs. Although harmonic performance of the drive amplifier is relaxed by this technique, intermodulation performance cannot be sacrificed.

Using this technique to place harmonics outside the Nyquist zone of interest allows them to be easily filtered

as shown. If the ADC still generates harmonics of its own, however, the technique previously discussed can be used to carefully select sample rate and analog frequency so that harmonics fall into unused sections of bandwidth and are digitally filtered.

Receiver Performance Expectations

With these thoughts in mind, how can the performance of a radio be determined and what tradeoffs can be made? Many techniques from traditional radio design can be used, as seen below.

Throughout the discussion, there are some differences between a multi-channel and single-channel radio. These will be pointed out. Keep in mind that this discussion is not complete and many areas are left untouched. For additional reading on this subject, consult one of the references at the end of this article. Additionally, this discussion only covers the data delivered to the DSP. Many receivers use proprietary schemes to further enhance performance through additional noise rejection and heterodyne elimination.

Table 1 — Frequency Translation and Aliasing

<i>Input Signal</i>	<i>Freq Range</i>	<i>Freq Shift</i>	<i>Spectral Sense</i>
1st Nyquist Zone	DC - $F_s/2$	Input	Normal
2nd Nyquist Zone	$F_s/2 - F_s$	F_s -Input	Reversed
3rd Nyquist Zone	$F_s - 3F_s/2$	Input - F_s	Normal
4th Nyquist Zone	$3F_s/2 - 2F_s$	$2F_s$ - Input	Reversed
5th Nyquist Zone	$2F_s - 5F_s/2$	Input - $2F_s$	Normal

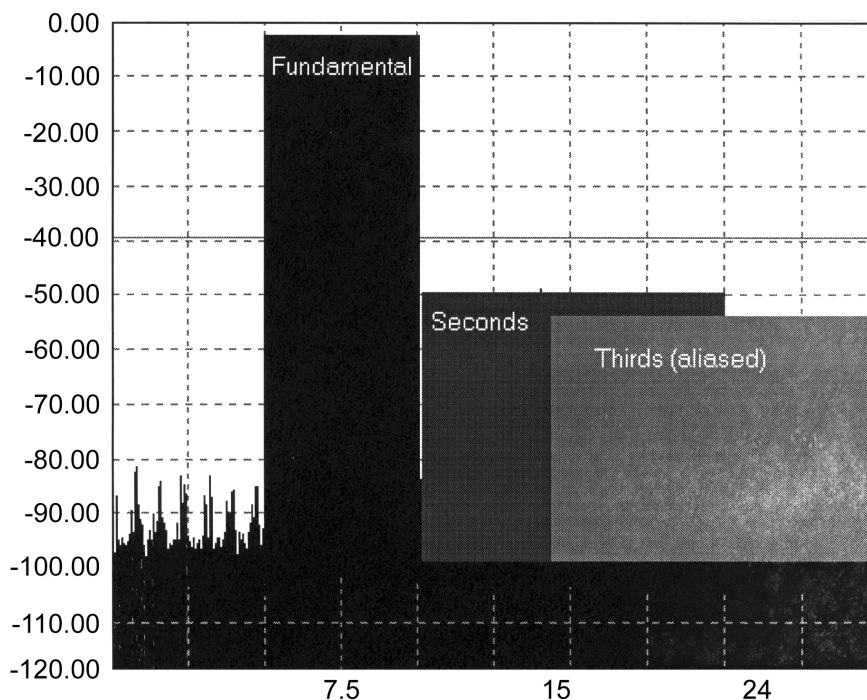


Fig 5—Placing harmonics out of band.

Table 2—Placing Harmonics Out of Band

<i>Encode Rate</i>	40.96 MSPS
Fundamental	5.12-10.24 MHz
Second Harmonic	10.24-20.48 MHz
Third Harmonic	15.36-30.72 MHz

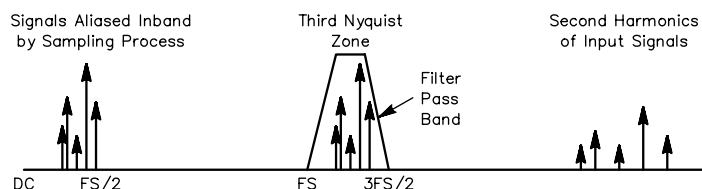


Fig 6—IF sampling.

For the discussion that follows, the generic receiver design is shown in Fig 7. Considerations begin with the antenna and end with the digital tuner/filter at the end. Beyond this point is the digital processor, which is outside the scope of this article.

Analysis starts with several assumptions. First, it is assumed that the receiver is noise-limited. That is, that no in-band spurs exist that would otherwise limit performance. It is reasonable to assume that LO and IF choices can be made such that this is true. Additionally, it will be shown later that spurs generated within the ADC are generally not a problem, as they can often be eliminated with the application of dither or through judicious use of oversampling and signal placement. In some instances these may not be realistic assumptions, but they do provide a starting point with which performance limits can be benchmarked.

The second assumption is that the bandwidth of the receiver front end is our Nyquist bandwidth (or less). Although our actual allocated bandwidth may be only 5 MHz, using the Nyquist bandwidth will simplify computations along the way. Therefore, a sample rate of 65 MSPS would give a Nyquist bandwidth of 32.5 MHz.

Available Noise Power

To start the analysis, the noise at the antenna port must be considered. Since a properly matched antenna is resistive, the following equation can be used to determine the noise voltage across the matched input terminals:

$$V_n^2 = 4kTRB \quad (\text{Eq 4})$$

where:

k is Boltzmann's constant (1.38-23 J/K)

T is temperature, in Kelvins

R is resistance, in ohms

B is bandwidth, in hertz

Available power from the source—in this case, the antenna—is thus:

$$P_a = \frac{V_n^2}{4R} \quad (\text{Eq 5})$$

which simplifies when the previous equation is substituted to:

$$P_a = kTB \quad (\text{Eq 6})$$

Thus, in reality, the available noise power from the source in this case is independent of impedance for non-zero and finite resistance values.

This is important because it is the reference point with which our receiver will be compared. It is often stated—when dealing with noise figure of a stage—that it exhibits “x” dB

above “kT” noise. This is the source of that expression.

With each progressive stage through the receiver, this noise is degraded by the noise figure of the stage, as discussed below. Finally, when the channel is tuned and filtered, much of the noise is removed, leaving only that which lies within the channel of interest.

Cascaded Noise Figure

Noise figure is a figure of merit used to describe how much noise is added to a signal in the receive chain of a radio. Usually, it is specified in decibels, although in the computation of noise figure, the numerical ratio (non-log) is used. The non-log is called *noise factor* and is usually denoted as F . It is defined as:

$$F = \frac{SNR_{Out}}{SNR_{In}} \quad (\text{Eq 7})$$

Once noise figures are assigned to each of the stages in a radio, they can be used to determine the cascaded performance. The total noise factor, referenced to the input port, can be computed as:

$$F_{Total} = F_1 + \frac{F_2^{-1}}{G_1} + \frac{F_3^{-1}}{G_1 G_2} + \frac{F_4^{-1}}{G_1 G_2 G_3} + \dots \quad (\text{Eq 8})$$

The F s above are the noise factors for each of the serial stages, while the G s are the gains of the stages. Neither the noise factor nor the gains are in log form at this point. When this equation is applied, it reflects all component noise to the antenna port. Thus, the available noise from the previous section can be degraded directly using the noise figure:

$$P_{Total} = P_a + NF + G \quad (\text{Eq 9})$$

For example, if the available noise is -100 dBm, the computed noise figure is 10 dB and conversion gain is 20 dB, the total equivalent noise at the output is -70 dBm.

There are several points to consider when applying these equations. First, for passive components, assume that their noise figure is equal to their loss. Second, series connected passive components can be summed before the equation is applied. For example if two low-pass filters are in series, each with an insertion loss of 3 dB, they may be combined, and the loss of the single element assumed to be 6 dB. Finally, mixers often have no noise figure assigned to them by the manufacturer. If no noise figure is specified, use the insertion loss.

Noise Figures and ADCs

Although a noise figure could be assigned to the ADC, it is often easier to work the ADC in a different manner. ADCs are voltage devices, whereas noise figure is really a noise power issue. Therefore, it is often easier to work the analog sections to the ADC in terms of noise figure, then convert to voltage at the ADC. Then work the ADC's noise into an input-referenced voltage. Finally, the noise from the analog and ADC can be summed at the ADC input to find the total effective noise.

For this application, an ADC such as the AD9042 or AD6640 12-bit device has been selected. These products can sample up to 65 MSPS, a rate suitable for entire-band AMPS digitization and capable of the GSM 5 × reference clock rate. This is more than adequate for AMPS (Advanced Mobile Phone Service), GSM (Global Standard for Mobile) and CDMA (Code-Division Multiple-Access) applications. From the data sheet, the typical SNR is 68 dB. Therefore, the next step is to figure the noise degradation within the receiver caused by the ADC noise. Again, the simplest method is to convert both the SNR and receiver noise into RMS volts, then sum them for the total RMS noise [since noise powers add— E_d]. If an ADC has a 2-V P-P input range:

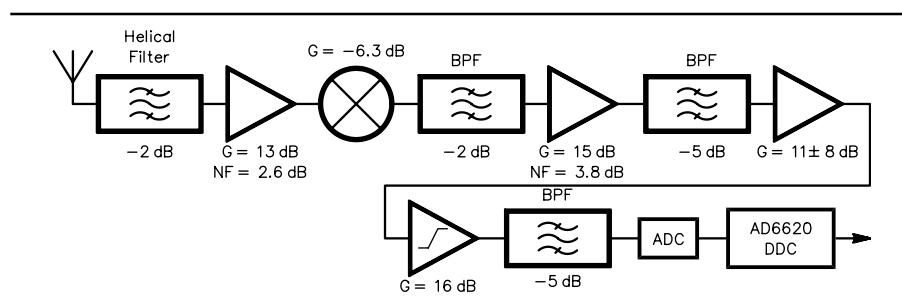


Fig 7—Generic digital-receiver design.

$$V_{\text{Noise}}^2 = \left(0.707 \cdot 10^{-\frac{\text{SNR}}{20}} \right)^2 \quad (\text{Eq 10})$$

$$= 79.22 \cdot 10^{-9} \text{ V}^2$$

This voltage represents all noises within the ADC, thermal and quantization. The full-scale range of the ADC is 0.707-V RMS.

With the ADC equivalent input noise computed, the next computation is the noise generated by the receiver itself. Since we are assuming that the receiver bandwidth is the Nyquist bandwidth, a sample rate of 65 MSPS produces a bandwidth of 32.5 MHz. From the available-noise-power equations, noise power from the analog front end is $134.55 \times 10^{-15} \text{ W}$ or -98.7 dBm . This noise is present at the antenna; it must be multiplied by the conversion gain and degraded by the noise figure. If conversion gain is 25 dB and the noise figure is 5 dB, then the noise presented to the ADC input network is:

$$-98.7 \text{ dBm} + 25 \text{ dB} + 5 \text{ dB} = -68.7 \text{ dBm} \quad (\text{Eq 11})$$

into 50Ω ($134.9 \times 10^{-12} \text{ W}$). Since the ADC has an input impedance of about 1000Ω , we must either match the standard $50\text{-}\Omega$ IF impedance to this, or pad the ADC impedance. A reasonable compromise is to pad the range down to 200Ω with a parallel resistor and then use a 1:4 transformer to match the rest. The transformer also serves to convert the unbalanced input to the balanced signal required for the ADC as well as provide some voltage gain. Since there is a 1:4 impedance step up, there is also a voltage gain of two in the process.

$$V^2 = P \cdot R \quad (\text{Eq 12})$$

From this equation, our voltage, squared, into 50Ω is 6.745×10^{-9} , or into 200Ω , 26.98×10^{-9} .

Now that we know the noise from the ADC and the RF front end, the total noise in the system can be computed by the square root of the sum of the squares. The total voltage is thus $325.9 \mu\text{V}$. This is the total noise present in the ADC, due to both receiver noise and ADC noise, including quantization noise.

Conversion Gain and Sensitivity

How does this noise voltage contribute to the overall performance of the ADC? Assume that only one RF signal is present in the receiver bandwidth. The signal to noise ratio would then be:

$$20 \log \left(\frac{\text{Sig}}{\text{Noise}} \right) = 20 \log \left(\frac{0.707}{325.9 \cdot 10^{-6}} \right) = 66.7 \quad (\text{Eq 13})$$

Since this is an oversampling application and the actual signal bandwidth is much less than the sample rate, noise will be greatly reduced once digitally filtered. Since the front-end bandwidth is the same as our ADC bandwidth, both ADC noise and RF/IF noise will improve at the same rate. Since many communications standards support narrow channel bandwidths, we'll assume a 30-kHz channel. Therefore, we achieve 30.3 dB from process gain, and our original

SNR of 66.7 dB is now 97.0 dB. Remember that SNR increased because excess noise was filtered; that is the source of process gain.

If this is a multi-carrier radio, the ADC dynamic range must be shared with other RF carriers. For example, if there are eight carriers of equal power as shown in Fig 8, each signal should be no larger than 1/8th (-18 dBc) the total range if peak-to-peak signals are considered. However, since the signals are not normally in

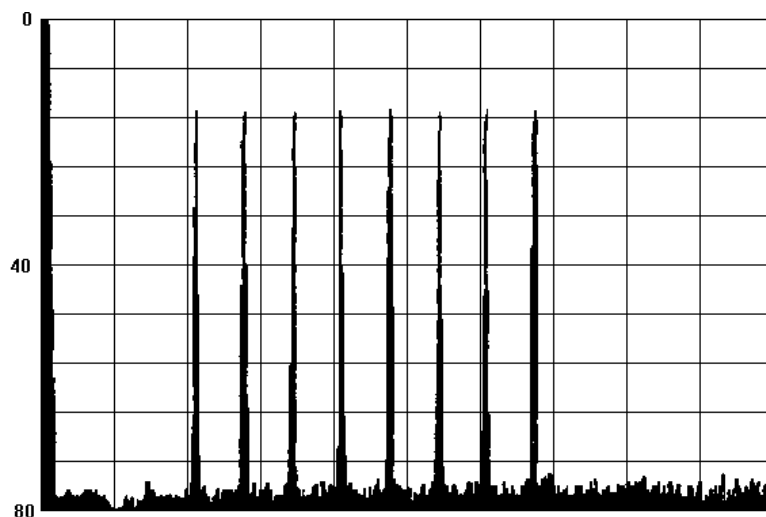


Fig 8—Eight equal-power carriers.

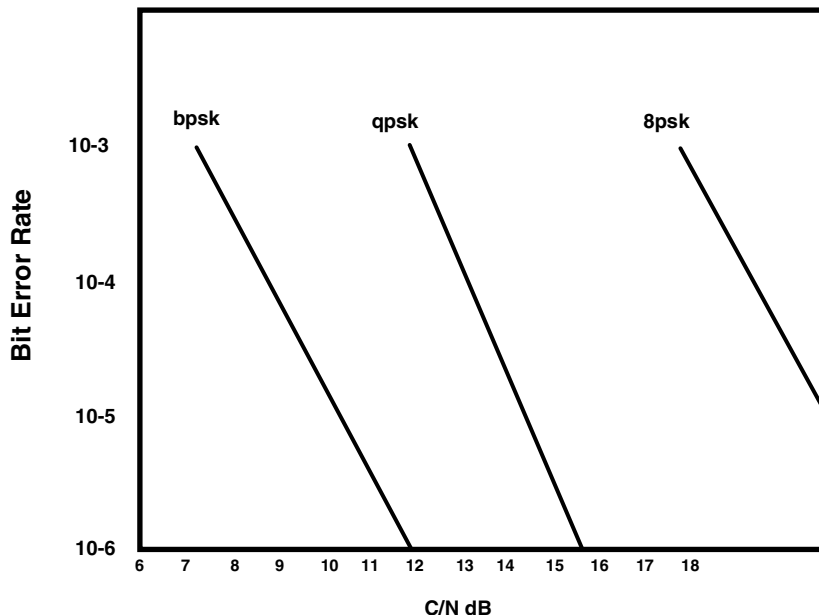


Fig 9—Bit Error Rate versus SNR.

phase with one another in a receiver (because handsets are not phase locked), the signals will rarely align—if ever. Therefore, less than 18 dB of dynamic range is required. Since in reality, only no more than two signals will align at any one time and because they are modulated signals, only 3 dB (5 to 6 dB for a conservative design) will be reserved for headroom. If signals do align and cause the converter to clip, it will occur for only a small fraction of a second before the overdrive condition is cleared. For a single-carrier radio, no headroom is required.

Depending on the modulation scheme, a minimum CNR (carrier-to-noise ratio) is required for adequate demodulation. If the scheme is digital, then the bit-error rate (BER) must be considered as shown in Fig 9. Assuming a minimum CNR of 10 dB is required, our input signal level cannot be so small that the remaining SNR is less than 10 dB. Thus, our signal level may fall 87.0 dB from its present level. Since the ADC has a full-scale range of +4 dBm (200 Ω), the signal level at the ADC input is then -83.0 dBFS. If there were 25 dB of gain in the RF/IF path, then receiver sensitivity at the antenna would be -83.0 minus 25 dB or -108.0 dBm. If more sensitivity is required, then more gain can be added in the RF/IF stages. Noise is not independent of gain, however, a gain increase may also have an adverse effect on noise performance, from additional gain stages.

ADC Spurious Signals and Dither

A noise-limited example does not adequately demonstrate the true limitations in a receiver. Other limitations such as SFDR are more restrictive than SNR and noise. Assume that the ADC has an SFDR specification of -80 dBFS or -76 dBm (full scale = +4 dBm). Also, assume that a tolerable carrier-to-interferer ratio (CIR, different from CNR) is 18 dB. This means that the minimum signal level is -62 dBFS (-80 plus 18) or -58 dBm. At the antenna, this is -83 dBm (-58 minus 25). Therefore, as can be seen, SFDR (single or multitone) would limit receiver performance long before the actual noise limitation is reached.

However, a technique known as *dither* can greatly improve SFDR. As shown in Analog Devices Application Note AN-410, the addition of out-of-band noise can improve SFDR well into the noise floor. Although the amount of dither is converter-specific,

the technique applies to all ADCs as long as static differential nonlinearity (DNL) is the performance limitation and not ac problems such as slew rate. In the AD9042 documented in the application note, the amount of noise added is only -32.5 dBm or 21 codes RMS. As shown in Figs 10 and 11, the plots both before and after dither provide insight into the potential for improvement. In simple terms, dither works by randomizing the coherent spurious signals generated within the ADC. Since the energy of the spurs

must be conserved, dither simply causes them to appear as additional noise in the floor of the converter. This can be observed in the “before” and “after” plots of dither as a slight increase in the average noise floor of the converter. Thus, the tradeoff made through use of out-of-band dither is that literally all internally generated spurious signals can be removed. However, there is a slight hit in the overall SNR of the converter. In practical terms this amounts to much less than 1 dB of sensitivity loss compared

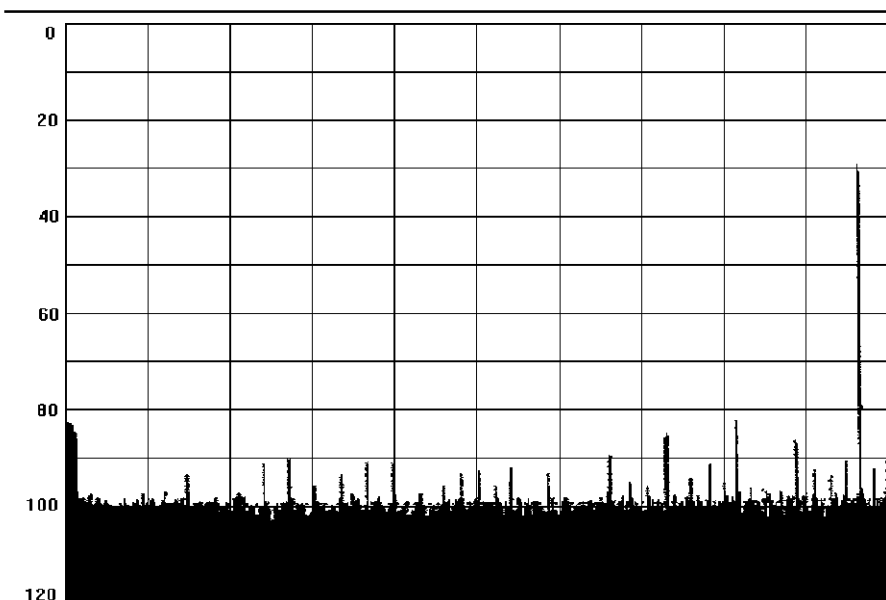


Fig 10—ADC without dither.

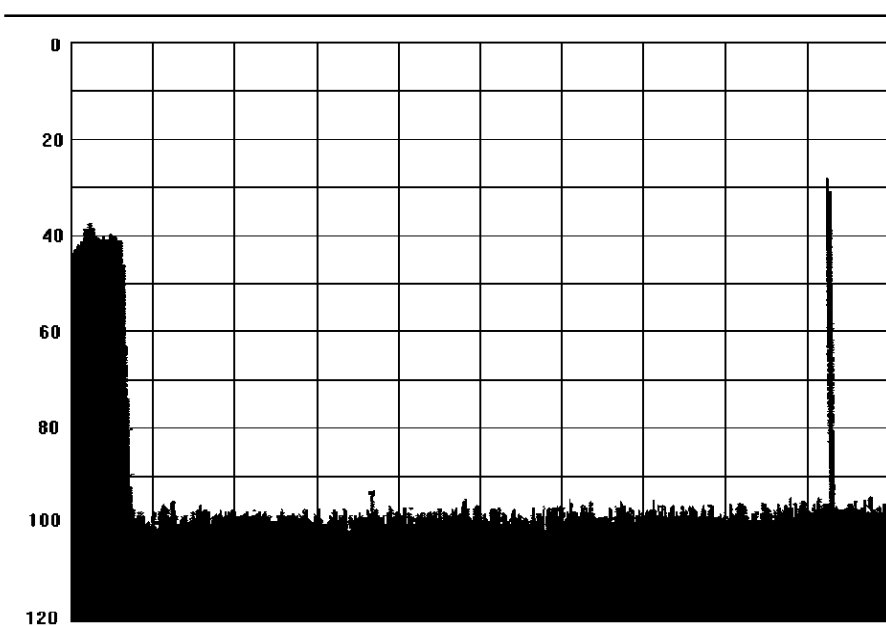


Fig 11—ADC with dither.

to the noise-limited example, which is much better than the SFDR-limited example shown earlier.

Let's consider two additional important points about dither before the topic is closed. First, in a multi-carrier receiver, we cannot expect any of the channels to be correlated. Often, the multiple signals will serve as self-dither for the receiver channel. This is sometimes true, but when signal strengths are weak, additional dither may be needed.

Second, the noise contributed from the analog front end alone is insufficient to dither the ADC. From the example above, -32.5 dBm of dither was added to yield an optimum improvement in SFDR. In comparison, the analog front end only provides -68 dBm of noise power, far from what is needed to provide optimum performance.

Third-Order Intercept Point

Besides converter SFDR, the RF section contributes to the spurious performance of the receiver. These spurs are unaffected by techniques such as dither and must be addressed to prevent disruption of receiver performance. Third-order intercept is an important measure, as the signal levels within the receiver chain increase throughout the receiver.

In order to understand what level of performance is required of wide-band RF components, we will review the GSM specification, perhaps the most demanding of receiver applications.

A GSM receiver must be able to recover a signal with a power level between -13 dBm and -104 dBm. Assume also that the full-scale input of the ADC is 0 dBm, and losses through the receiver filters and mixers are 12 dB. In addition, since multiple signals are to be processed simultaneously, an AGC should not be employed. This would reduce RF sensitivity and cause the weaker signals to be dropped. Working with this information, RF/IF gain is calculated to be 25 dB ($0 = -13 - 6 - 6 + X$).

The 25-dB gain required is distributed as shown in Fig 12. Although a complete system would have additional

components, this will serve the discussion. From this, with a full-scale GSM signal at -13 dBm, ADC input will be 0 dBm. However, with a minimal GSM signal of -104 dBm, the signal at the ADC would be -91 dBm. From this point, the discussion above can be used to determine the suitability of the ADC by noise and spurious performance.

With these signals and the system gains required, the amplifier and mixer specifications can now be examined when driven by the full-scale signal of -13 dBm. Solving for the third-order products in terms of signal full-scale:

$$IP_{in} = \frac{3}{2} \left(Sig - \frac{3OP}{3} \right) \quad (\text{Eq 14})$$

where *Sig* is the full-scale input level of the stage, in dBm, and *3OP* is the required third-order product level.

Assuming that overall spurious performance must be greater than 100 dB (the requirements for AMPS and CDMA), the above equation shows that you need an input amplifier (LNA) with a third-order input, *IP3*, greater than +37 dBm. At the mixer, the signal's level increases by the 10 dB gain, and the new signal level is -3 dBm. However, specifying mixers at their output reduces this level by at least 6 dB for a new signal level of -9 dBm. Therefore at the mixer, you need an *IP3* greater than +41 dBm. At the final gain stage, the signal is attenuated to -9 dBm. For the IF amplifier, you need an *IP3* greater than +41 dBm.

ADC Clock Jitter

One dynamic specification that is vital to good radio performance is ADC clock jitter. Although low jitter is important for excellent baseband performance, its effect is magnified when sampling higher frequency signals (higher slew rate) such as is found in undersampling applications. The overall effect of a poor jitter specification is a reduction in SNR as input frequencies increase. The terms aperture jitter and aperture uncertainty are frequently interchanged in text. In this application, they have the same meaning. Aperture uncertainty is the

sample-to-sample variation in the encode process. Aperture uncertainty has three residual effects. The first is an increase in system noise. The second is an uncertainty in the actual phase of the sampled signal itself. Third is inter-symbol interference. Aperture uncertainty of less than 1 ps is required when IF sampling in order to achieve required noise performance. In terms of phase accuracy and inter-symbol interference, the effects of aperture uncertainty are small. In a worst case scenario of 1 ps RMS at a 250-MHz IF, the phase error is 0.09° RMS. This is quite acceptable even for a demanding specification such as GSM. Therefore, the focus of this analysis will be on noise contribution due to aperture uncertainty.

In a sine wave, the maximum slew rate is at the zero crossing. At this point, the slew rate is defined by the first derivative of the sine function evaluated at $t = 0$:

$$v(t) = A \sin(2\pi ft) \quad (\text{Eq 15})$$

$$\frac{dv(t)}{dt} = A(2\pi f) \cos(2\pi ft) \quad (\text{Eq 16})$$

At $t = 0$, Eq 16 simplifies to:

$$\frac{dv(t)}{dt} = A(2\pi f) \quad (\text{Eq 17})$$

The units of slew rate are volts per second (V/s), representing how fast the signal slews through a zero crossing of the input signal. In a sampling system,

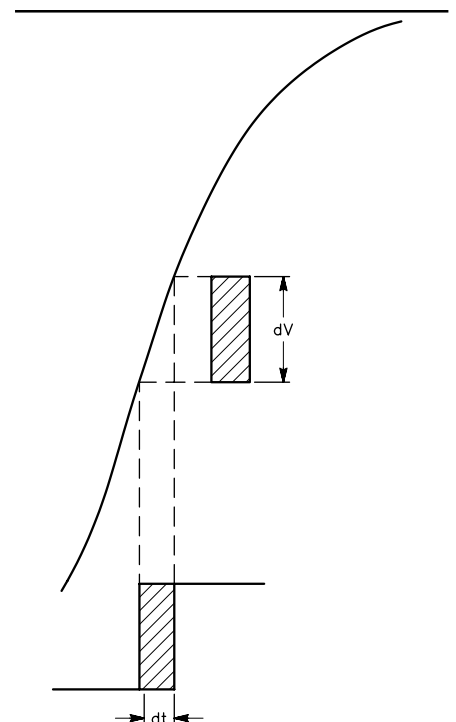


Fig 13—Input slew rate.

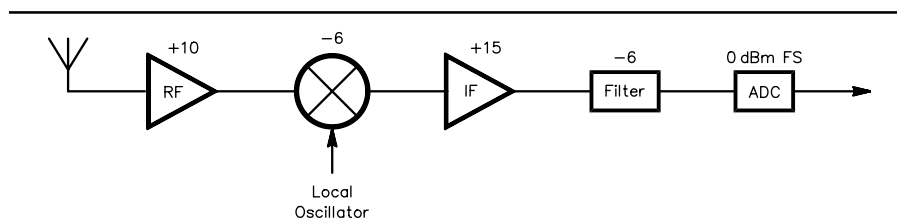


Fig 12—Receiver gain distribution for *IP3* calculation.

a reference clock is used to sample the input signal. If the sample clock has aperture uncertainty, then an error voltage is generated (see Fig 13). This error voltage can be determined by multiplying the input slew rate by the jitter:

$$v_{Error} = (Slewrate)(t_{Jitter}) \quad (\text{Eq 18})$$

By analyzing the units, it can be seen that this yields units of volts. Usually, aperture uncertainty is expressed in seconds RMS; therefore, the error voltage would be in volts RMS. Additional analysis of this equation shows that as analog input frequency increases, the RMS error voltage also increases in direct proportion to the aperture uncertainty.

In IF sampling converters, clock purity is of extreme importance. As with the mixing process, the input signal is multiplied by a local oscillator, or in this case, a sampling clock. Since multiplication in time is convolution in the frequency domain, the spectrum of the sample clock is convoluted with the spectrum of the input signal. Since aperture uncertainty is wide-band noise on the clock, it shows up as wide-band noise in the sampled spectrum as well. In addition, since an ADC is a sampling system, the spectrum is periodic and repeated around the sample rate. This wide-band noise therefore degrades the noise-floor performance of the ADC. The theoretical SNR for an ADC as limited by aperture uncertainty is determined by the following equation:

$$SNR = -20 \log(2\pi F_{Analog} t_{jRMS}) \quad (\text{Eq 19})$$

If this equation is evaluated for an analog input of 201 MHz and 0.7 ps RMS jitter, the theoretical SNR is limited to 61 dB. Note that this is the same requirement demanded of any other mixer stage. Therefore, systems that require very-high dynamic range and very-high analog input frequencies also require a very low jitter encode source. When using standard TTL/CMOS clock-oscillator modules, 0.7 ps RMS has been verified for both the ADC and oscillator. Better numbers can be achieved with low-noise modules.

When considering system performance overall, a more generalized equation may be used. This equation builds on the previous equation, but includes the effects of thermal noise and DNL:

$$SNR = -20 \log \left[\left(2\pi F_{analog} t_{jRMS} \right)^2 + \left(\frac{1+\epsilon}{2^N} \right)^2 + \left(\frac{v_{Noise_{RMS}}}{2^N} \right)^2 \right]^{\frac{1}{2}} \quad (\text{Eq 20})$$

where:

F_{Analog} = analog IF

t_{jRMS} = aperture uncertainty

ϵ = average DNL of converter (approximately 0.4 bits)

$v_{Noise_{RMS}}$ = thermal noise in bits

N = number of bits

Although this is a simple equation, it provides much insight into the noise performance that can be expected from a data converter. For more details on aperture jitter, see Analog Devices AN-501.

Phase Noise

Although synthesizer phase noise is similar to jitter on the encode clock, it has slightly different effects on the receiver. In the end, however, the effects are very similar. The primary difference between jitter and phase noise is that jitter is a wide-band problem with uniform density around the sample clock frequencies. Phase noise exhibits non-uniform distribution around a local oscillator and usually weakens as the measurement frequency moves away from that of the oscillator. As with jitter, less phase noise is better.

Since the local oscillator is mixed with incoming signals, noise on the LO effects the desired signal. The frequency-domain process of the mixer is convolution; the time-domain process of the mixer is multiplication. Because of mixing, phase noise from the LO moves energy from adjacent (and active) channels into the desired channel as an increased noise floor. This is called reciprocal mixing. To determine the amount of noise in an unused channel when an alternate channel is occupied by a full-power signal, the following analysis is offered.

Again, since GSM is a difficult specification, this will serve as an example. In this case, the following equation is valid:

$$Noise = \int_{-0.1}^{0.1} x(f) \times p(f) df \quad (\text{Eq 21})$$

where $Noise$ is the noise (in the desire channel) caused by phase noise, $x(f)$ is the phase noise expressed in non-log format, and $p(f)$ is the spectral-density function of the GSMK function. For this example, assume that the GSM signal power is -13 dBm. Also, assume that the LO has a phase noise that is constant across frequency (most often, the phase noise reduces with carrier offset). When this integration is performed over the channel bandwidth, a simple equation falls out. Since $x(f)$ was assumed to be constant (PN – phase noise) and the integrated power of a full-scale GSM channel is -13 dBm, the equation simplifies to:

$$Noise = (PN)(Signal_{Adjacent})$$

or in log form,

$$= PN_{\log} + Signal_{\log} \quad (\text{Eq 22})$$

$$= PN + (-13 \text{ dBm})$$

and:

$$PN_{Required} = Noise - (-13 \text{ dBm}) \quad (\text{Eq 23})$$

since the goal is to require that phase noise be lower than thermal noise. Assuming that noise at the mixer is the same as at the antenna, -121 dBm (noise in 200 kHz at the antenna $-P_a = kTB$) can be used. Thus, the phase noise from the LO must be lower than -108 dBm with an offset of 200 kHz.

References

1. C. Olmstead and M. Petrowski, *Digital IF Processing*, TBD, September 1994, pp 30-40.
2. R. Groshong and S. Ruscak, "Undersampling Techniques Simplify Digital Radio," *Electronic Design*, May 23, 1991, pp 67-78.
3. T. Gratzek and F. Murden, "Optimize ADCs For Enhanced Signal Processing," *Microwaves & RF* reprint.
4. B. Brannon, "Using Wide Dynamic Range Converters for Wide Band Radios," *RF Design*, May 1995, pp 50-65.
5. B. Brannon, *Overcoming Converter Non-linearities with Dither*, AN-410, Analog Devices.
6. F. Harris, *Exact FM Detection of Complex Time Series*, Electrical and Computer Engineering Department, San Diego State University, San Diego, California 92182.
7. AD9042 Datasheet, Analog Devices.
8. AD6620 Datasheet, Analog Devices.
9. AD6640 Datasheet, Analog Devices.
10. W. Hayward, *Introduction To Radio Frequency Design* (Newington, Connecticut: ARRL, 1994, #4920). ARRL publications are available from your local ARRL dealer or directly from the ARRL. Mail orders to Pub Sales Dept, ARRL, 225 Main St, Newington, CT 06111-1494. You can call us toll-free at tel 888-277-5289; fax your order to 860-594-0303; or send e-mail to pubsales@arrl.org. Check out the full ARRL publications line on the World Wide Web at <http://www.arrl.org/catalog>.
11. Krauss, Bostian and Raab, *Solid-State Radio Engineering* (New York: John Wiley & Sons, 1980).
12. W. Kester, *High Speed Design Seminar*, Analog Devices, 1990.
13. B. Brannon, *Aperture Uncertainty and ADC System Performance*, AN-501, Analog Devices. □□

Narrow-Band Doppler Spectrum Techniques for Propagation Study

*The ionosphere is the lifeblood of HF communication.
Use this technique to view and understand the
invisible medium that transports our signals.*

By Peter Martinez, G3PLX

A November 1997 *RadCom* article I wrote¹ described the use of extremely narrow-band DSP techniques to receive the very-weak signals on the VLF amateur bands. This was done by using a very narrow-span spectrum analyzer to view a small section of the band on a real-time computer display that showed frequency as the Y-axis, time as the X-axis and signal-level as brightness. The result was a receiving system that was capable of receiving signals

¹P. Martinez, G3PLX, "Extreme Narrowband Reception," *RadCom*, Nov 1997, pp 45-48.

High Blakeband Farm
Underbarrow, Kendal,
Cumbria, LA8 8HP
England

buried far below the audible noise level by virtue of its extremely narrow effective bandwidth.

Some readers of that article may have asked the question: What happens if we use this technique on the higher bands? The propagation medium on the higher bands is not as stable as it is on VLF. Instead of seeing a thin, straight line on the screen from a transmitted carrier, the signal spreads out over an appreciable band of frequencies. The ionosphere, which reflects HF radio waves, is constantly in motion, causing the path length to vary. As with moving low-orbit Oscar satellites, a changing path length causes a change in the received frequency known as the Doppler shift. While a moving satellite on VHF can give a Doppler shift of several kilo-

hertz, the moving ionosphere at HF only gives a Doppler shifts of about 1 Hz. This is much more than the 25-mHz (that's *millihertz!*) bandwidths we were using on VLF and would make communication at these narrow bandwidths impossible on HF.

In this article, I would like to introduce the idea of using these narrow-band techniques, not to communicate on HF, but to study the ionosphere itself. The narrow-band spectrum analyzer can be used to create *dopplergrams* of typical HF signals. These can be an effective way of showing many of the features of the ionosphere that have previously only been made visible with equipment that is well beyond the reach of the average amateur.

To begin, let us consider perhaps the

best-known example of the Doppler effect, familiar to radio amateurs and television viewers alike, which is that of aircraft flutter. If we suppose that the height of the aircraft is small compared to the other distances, then we can make a two-dimensional model of the reflected path.

Fig 1 shows such a model and what happens when the signal from T is reflected from a moving aircraft at point A and received at R. As the aircraft moves closer to the line joining T to R, the path gets shorter, giving rise to a positive Doppler shift, which decreases as it moves away from the line between T and R. If we also have a direct path between T and R, the presence of two signals of different frequencies at the same time gives rise to a beat-note. Its usually subaudible frequency shows as the well-known flutter fading effect.

The elliptical rings drawn on Fig 1 are lines of constant path-length from T to R via any point on the ellipse. We can imagine that these were drawn by fastening each end of a length of string to T and R, starting with the string one wavelength longer than the distance TR. Drawing the string tight with a pencil at point A, we can then trace out the innermost ellipse. The second ellipse is drawn with two wavelengths of extra string and so on. An aircraft flying tangential to any ellipse will have zero Doppler shift, and the Doppler shift (in hertz) on an aircraft flying in any other direction, is numerically equal to the number of wavelength rings that it crosses per second.

From this we can see that an aircraft approaching from some distance will appear first with an almost-constant positive HF Doppler shift, which will drop, pass through zero as the aircraft either crosses between the transmitter and the receiver or its flightpath becomes tangential to an ellipse, then become negative as it flies away. The Doppler shift is proportional to the RF frequency, and with typical jumbo jets a shift as high as 250 Hz is possible on a 144 MHz signal. The narrow-band spectrum analyzer technique described in November 1997 *RadCom* can be easily used to display these Doppler-shifted signals, even on much lower frequencies than 144 MHz.

Fig 2 shows a dopplergram taken on a BBC World Service AM transmitter on 15.485 MHz at Penrith, Cumbria, about 40 km north of my home, at about 4 o'clock in the afternoon. This signal is at the limit of surface-wave propagation but well inside the skip

zone. Listening in USB mode with the carrier tuned to give a 1000-Hz tone, it shows signs of aircraft flutter from time to time. The horizontal center-line of the dopplergram represents the carrier-frequency where the direct signal is visible. The top and bottom of the dopplergram are respectively 25 Hz above and below the carrier frequency. The marks along the bottom edge represent ten-minute intervals.

The striking feature of Fig 2 is the very large number of aircraft Doppler

trails visible, far more than can be detected by ear. The narrow-band analyzer is doing a far better job of separating out the faint closely spaced signals than can the human ear. To get some idea how far away some of these aircraft are, we can note that the area swept out between an aircraft trace and the center-line over a given time interval is numerically equal to the number of wavelength ellipses crossed by the aircraft in that time. For example, we could estimate this

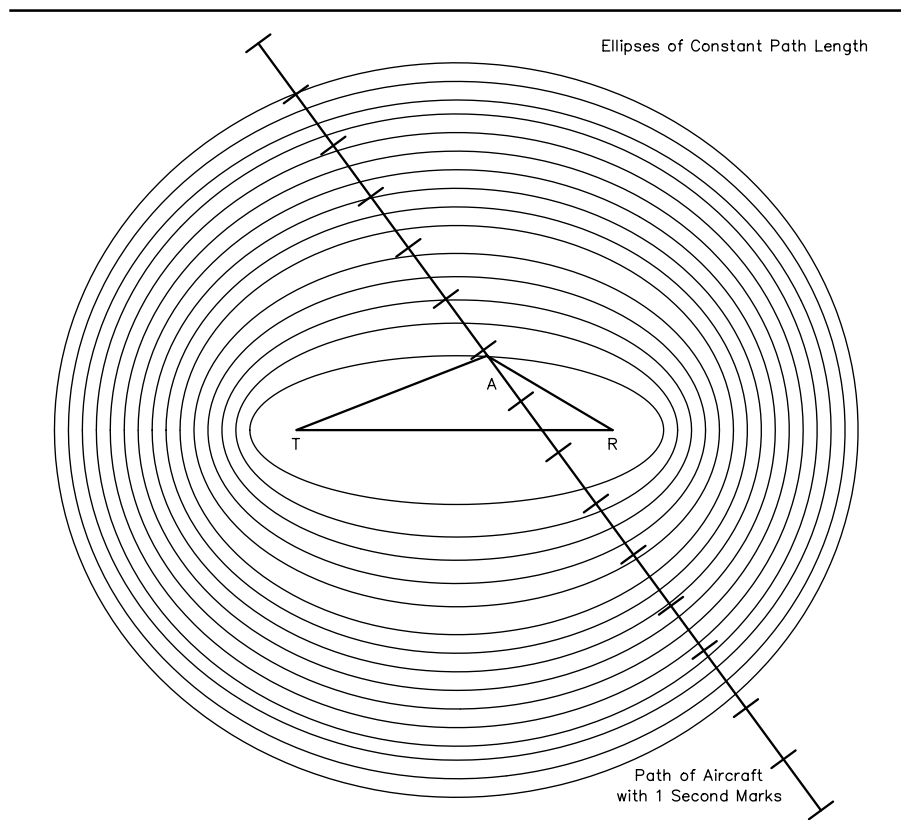


Fig 1—Ellipses of constant path length from T to R.

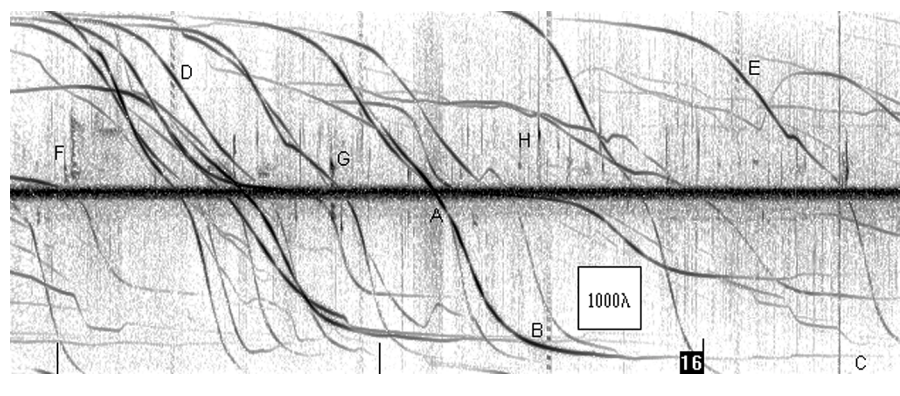


Fig 2—The Doppler trails from numerous

area by counting the number of 1-Hz by 1-second squares in the area swept out on the dopplergram. Since we know that the aircraft is at its closest when the trace crosses the center-line of the dopplergram, an estimate of the triangular area between the point where the trace crosses the center-line and that of the faintest detectable signal will give us a figure for the most-distant path length minus the closest. We can then say that the most-distant path-length is certainly longer than this figure. Since the path is from the transmitter to the aircraft and back to the receiver, we can thus get a lower limit for the distance to the aircraft by halving this path-length. The square area marked 1000λ in Fig 2 represents a distance of 1000λ , that is a path-length of 19.3 km at this frequency. Using this method, the aircraft that crossed the centerline at point A and produced the trail to B and was just detectable at point C in Fig 2 was at least 150 km away at point C.

Some of the traces in Fig 2 do not follow smooth curves, and these can be attributed to aircraft that are changing speed or direction. Some traces run along the centerline for some time, and these result from aircraft that are flying along the line between transmitter and receiver. It is interesting to speculate on the possibility of using several receivers spaced out around a single broadcast transmitter and combining all the Doppler signals to give an almost completely "passive" radar picture of the aircraft activity in the area. The sensitivity is actually limited in Fig 2, not by receiver background noise but by close-in sideband noise in the BBC transmitter resulting from low-level second-order distortion in the modulated signal.

There are other strange marks (as at F, G and H in Fig 2) and numerous short vertical streaks (both above and below the centerline) that can be explained. They take us into the main uses of dopplergrams for propagation study. To explain these, we need to look much higher in the sky than the aircraft. It helps to find a signal coming from much farther away, so that aircraft reflections are below the horizon and not visible. Fig 3 shows just such a trace, from a French AM broadcast transmitter on 21.580 MHz at about 1000 km distance, recorded at about 10:00 UTC in April. There is no surface wave but this station is still within the skip zone so there is no skywave; the stripe across the center of the trace is probably a scatter sig-

nal. Again the vertical scale is 50 Hz top-to-bottom, but the horizontal time base is twice as fast as that of Fig 2, and the marks along the bottom now represent one-minute intervals.

The various streaks and squiggles in Fig 3 are in fact meteor-trail reflections. Meteors are small particles of interplanetary debris, typically the size of a grain of sand, which burn up on entering the top of the earth's atmosphere. Occurring at heights between 80 and 120 km, they leave ionized trails rather like vapor trails, which gradually fade away, and radio signals can be reflected from such trails. Unlike an aircraft, which can be considered as a point reflector and scatters RF in all directions, a meteor trail is a line, and gives a strong mirror-like reflection when the trail is at the correct angle to the path.

This is the textbook explanation for meteor-scatter, but it does not yet explain the strange shapes we see on the dopplergram. If a meteor trail were

stationary in the sky, the reflection would be exactly on the same frequency as the transmitter and would appear exactly on the dopplergram centerline. Meteor pings have Doppler shifts because the trails are moving, blown along by high-altitude winds. They give positive or negative Doppler shifts depending on whether the trail is upwind or downwind of the path between the transmitter and the receiver. This accounts for some of the blobs in Fig 3, namely the horizontal streaks at A, B and C.

Nonetheless, several reflections seem to spread out over ranges of Doppler-shifts, with tendencies to have leading "noses" with two or more tails. Once again, we can explore what is happening by reference to a diagram.

Fig 4 is a simplified diagram of a vertical section through the atmosphere at a height of about 100-km where a typical trail is being formed. It shows at (A) a meteor that is falling vertically downward, with the wind

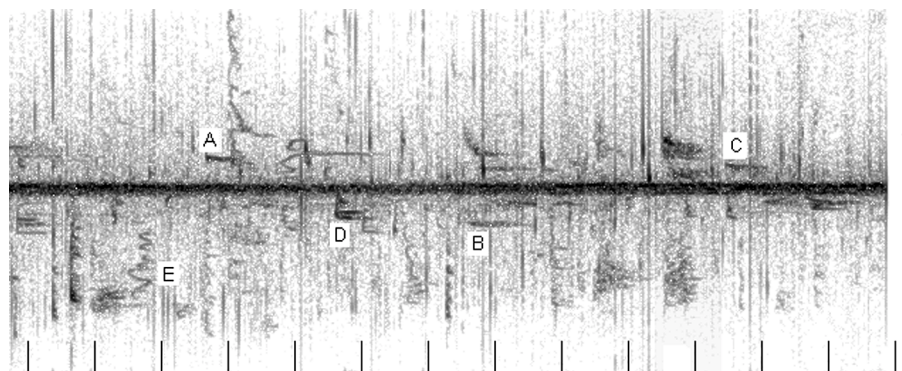


Fig 3—Meteor trails, caused by the burning of interplanetary debris at about the same height as the E layer (80 to 120 km).

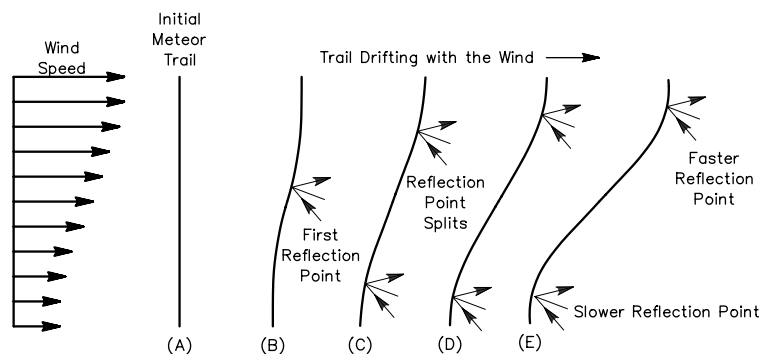


Fig 4—How the initially straight trail from a vertically falling meteor can be blown out of shape by high-altitude winds.

blowing from left to right across the diagram. In general, the wind speed will not be the same at all levels. Let's suppose that the wind is stronger at higher levels, as shown by the arrows, that the transmitter is in front, to the right and below the diagram and the receiver is behind it. Thus, the diagram is a slice across the path that includes the meteor trail.

At the instant when the trail is formed, there is no reflection because the trail is vertical and the transmitter/receiver are on the ground 100 km below and not aligned with the trail. After a few seconds maybe, the wind gradient along the trail may blow it into the shape of Fig 4B, the middle of the trail becomes perpendicular to the transmitter/receiver plane and a signal is reflected. Note that different portions of the reflecting part of the trail move with different speeds. In other words, it rotates so that the reflected signal has a range of simultaneous Doppler shifts, and this gives the Doppler trace its flat "nose." As the trail shape blows farther from the vertical (Fig 4C), the middle of the trail rotates out of line and ceases to reflect, but adjacent sections come into line and reflect. The upper reflecting section travels faster than the lower one, so the nose of the Doppler trace splits into two tails, one higher in frequency than the other, just like trace D in Fig 3.

Fig 4 shows only one possible, simple path geometry. In general, the alignment of the trail and the transmitter/receiver paths will be more complex, and the wind speed may vary with height in more-complex ways. Nonetheless, this example gives the basic idea of how a wind-blown meteor trail can produce convoluted shapes such as the one at E in Fig 3. The dopplergram technique thus gives some real insight into the nature of meteor trails and the physics of the E layer. In particular, the ability to visualize E-layer vertical wind gradients may help in the study of sporadic-E propagation.

There remain a large number of faint vertical streaks on the dopplergram of Fig 3, some of which have blobs at their lower ends or occur at the start of larger squiggles. These can be explained by the Doppler shift of a signal reflected from the expanding tip of the ionized trail as it is actually being formed. The surface of the trail's leading edge will be rounded rather than flat, so the scattered signal will be fainter and not so highly directional. The Doppler shift will be due not only

to the wind speed but will also contain a component from the much higher velocity of the meteor itself. Each meteor ping thus starts with a faint, wide-angle "chirp" from the HF side. Some of these faint chirps are received even though the resulting trail is *never* in the right alignment to produce a real ping, such chirps are probably from meteors that fall quite close to the transmitter or the receiver.

For the next dopplergram (Fig 5), we come right down to the lower HF bands. Fig 5 shows a signal on about 5 MHz, received at my home over a distance of about 80 km. It is actually an unmodulated spare channel of a commercial

multi-channel RTTY signal. During daytime, the ionosphere reflects signals on this frequency from a height of about 300 km, so the reflection point is almost overhead. For this dopplergram, the vertical scale is 3-Hz (top-to-bottom) and the time marks along the horizontal scale are at 10-minute intervals, with the UTC hours also marked. The signal is reflected from the F layer, and it appears to randomly wander about ± 0.5 Hz. This is not caused only by frequency instability in the transmitter or receiver. If this transmitter had been located sufficiently close by for the trace to show the direct (ground wave) signal, the signal would have

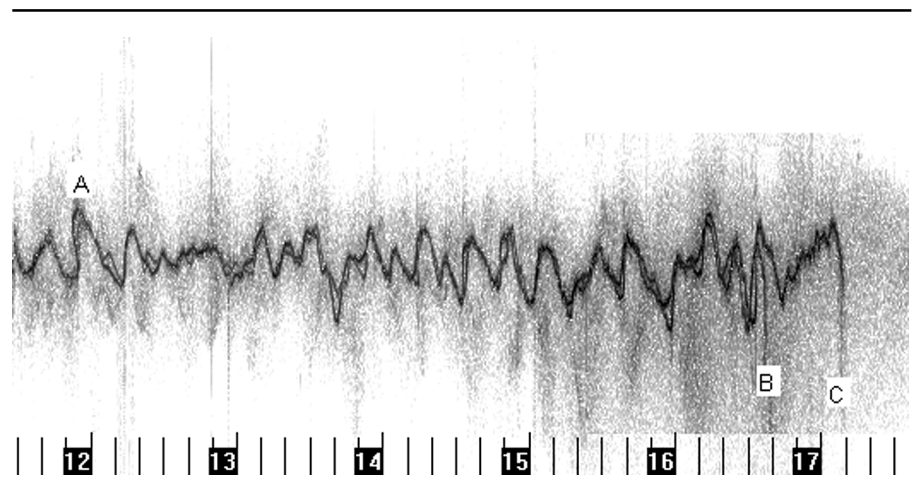


Fig 5—Vertical motion of the F layer leads to Doppler shift, including a "switch-back" effect at point A. Left and right-hand polarized signals from the same transmitter fade out at different times (points B and C).

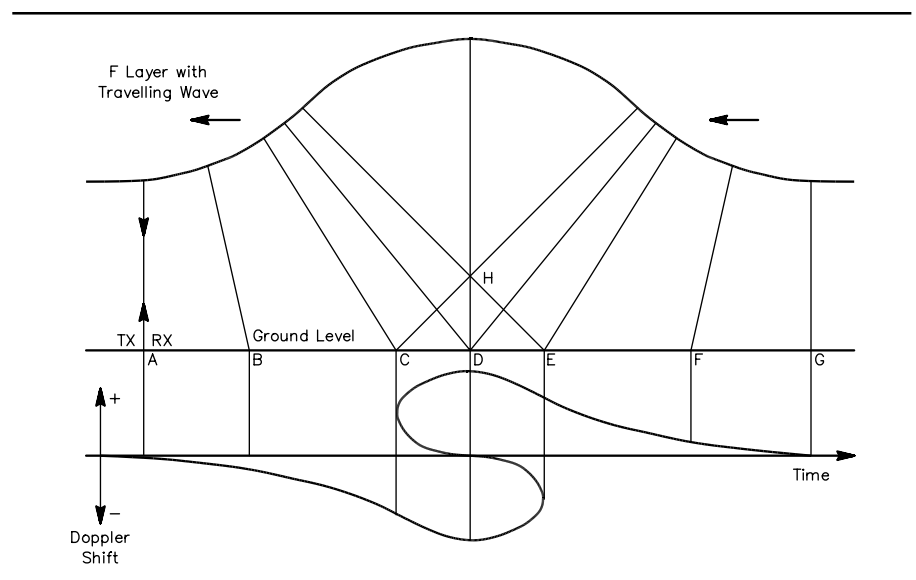


Fig 6—Multiple reflection points across an upward bulge in the F layer, illustrating the "switch-back" effect at point A of Fig 5.

been visible as a straight line across the center of the chart.

The ionosphere is essentially a flat, horizontal reflecting layer, and it can be shown that—unlike the meteor-scatter case—there can be no Doppler-shift due to horizontal motion of a horizontal layer. The observed Doppler shift is actually caused in this case by vertical motion of the F layer. Some of this motion can arise from weather effects in the atmosphere below, but in the same way that waves can propagate long distances across the surface of a pond, such disturbances can propagate horizontally as waves at the height of the F layer. Even quite small disturbances, due to thunderstorms in the atmosphere below, become magnified in size as they expand into the lower densities of the higher altitudes. If we could monitor the Doppler shift at two or more receiving sites, it might be possible to see the direction of these waves' motion. There is another phenomenon, however, that demonstrates the travelling-wave effect very clearly, and incidentally, might also help to convince some readers that this wobbly trace is not just transmitter or receiver frequency drift. At several points in time, the wandering Doppler trace seems to have an almost vertical rising edge. Indeed, at point A of Fig 5 the trace seems to defy the laws of physics and lean *backward* in time. This can certainly not be receiver drift, but we can explain how this strange effect occurs by reference to Fig 6.

Imagine an upward bulge in the F layer moving, like an tidal wave, from right to left across the top of the diagram above a stationary transmitter with the receiver next to it, shown at point A in Fig 6. To make the diagram less cluttered, in fact, Fig 6 shows a stationary wave and a transmitter moving along the line from A to G, which gives the same effect. At point A, before the transmitter gets under the bulge, the path length to the layer is constant and there is no Doppler shift. At B, the layer is starting to move upward and away from the transmitter, producing a low-frequency Doppler shift at the receiver. This effect gets larger at C, but we also just start to get some signal from the opposite side of the bulge, which is moving and rotating downward and toward the transmitter. Therefore, another signal appears, with a "nose" and a positive Doppler shift.

At D, with the transmitter and receiver right under the center of the wave, there are now *three* points of

reflection. At one, reflection is from the upward-moving leading edge of the bulge. At another, it's from the top and a third reflects from the downward-moving trailing edge. At E, we just lose the reflection from the leading edge as it rotates out of line. At F and G, we have only the upward Doppler shift from the trailing edge as the travelling wave passes away.

Only travelling waves that have a sufficiently small radius of curvature will cause this "switch-back" effect. The audible effect is that an otherwise-steady signal develops deep fading for a few minutes as the three Doppler-shifted paths beat with other.

If we carefully look at the rest of Fig 5, we can see many places where there are two traces close together. It's not difficult to imagine that virtually the whole dopplergram actually consists of two traces that weave in and out of each other. If one listens to the audio while watching the dopplergram appear, it is clear that the fading rate is fast when the two traces are widely separated and slow when they are close together.

To explain this double-trace we need to go a bit deeper into the theory of HF propagation than the average Amateur Radio textbook. Such books tell us that electrons in the ionosphere oscillate in sympathy with electromagnetic waves. When a signal with a frequency below the critical frequency is fired vertically upwards, the oscillations slow it to a standstill and return it back along its original path. What these books do not tell us is that the earth's magnetic field has a subtle effect on this process. The physics between the radio wave, ionospheric electrons and magnetic field are complex, but the result is that a right-hand circularly polarized signal propagating through the ionosphere has a slightly different propagation speed than does a left-hand circularly polarized signal. This means that two waves polarized in opposite senses will take two slightly different ray paths through the ionosphere. One of these paths is known as the *ordinary ray* (O) and is independent of the magnetic field. The other is slowed slightly by the magnetic field and is known as the *extra-ordinary ray* (X). The amount of slowing depends on the strength of the component of the earth's magnetic field along the path.

Since a linearly polarized signal can be resolved into two contra-rotating circularly polarized signals, it follows that even linearly polarized signals passing through the ionosphere are

split into two separate ray paths, except for certain special cases at the magnetic poles and the equator. The dopplergram shows where the two rays separate in frequency due to the motion of the ionosphere itself.

For most of the day, the O and X signals stay close to each other, but at sunset, when the ionization level drops below the level needed to cause reflection, the O signal vanishes first. This can be seen at point B (1638 UTC) in Fig 5. As it goes, the reflection point moves rapidly upward as the ionization drops, giving rise to a characteristic LF "chirp." The extra-ordinary ray, boosted by the extra spin that the electrons get from the magnetic field, keeps going until point C (1709 UTC), when it too vanishes with a downward chirp. Interestingly, although this particular signal shows deep fading throughout the day as the O and X rays beat with each other, for the 30-minute period where only the X trace is present, the signal is quite constant in level.

Behind the main trace, there is a fuzzy signal with a greater Doppler shift that does not track that of the main trace. This is probably due to small-scale irregularities in the F layer caused by solar-wind particles trapped along the earth's magnetic field. This fuzzy trace can sometimes get much stronger, swamping the main trace during periods of solar activity. There is an audible rapid flutter on the signal when this occurs. It is interesting to note that there is still a fuzzy background trace after the main signal has faded out at sunset.

Fig 5 shows a near-vertical path in order to demonstrate vertical motion of the F layer. For the next dopplergram, we move to a 400-km path and decrease frequency to 3.5 MHz. This shows the effects of low-angle propagation and introduces the E layer, which does not reflect signals at 5 MHz. Fig 7 uses the same vertical and horizontal scales as Fig 5, but was taken at sunrise over the path from Great Yarmouth, on the East Coast of England, to my home at Kendal in northwest England. The transmitter is a navigational data broadcast on 3572 kHz, which radiates 24 hrs/day and has a nice clean carrier in the center of its digital-PSK modulation.

It is perhaps no surprise that the sunrise in Fig 7 shows the F-layer traces chirping in from the HF side as the reflection point moves, first very rapidly and then more slowly downwards. There are two traces, the extraordinary ray appearing first.

However, like the travelling wave in the F layer, these traces seem to defy the laws of physics and move *earlier in time* after their first appearance. To explain this, we again need to go a bit deeper into ionospheric theory than the average textbook.

The textbooks tell us that if we fire a radio wave obliquely upward at a shallow angle, it will reflect from the ionosphere, but if fired at a steeper angle it will go through the ionosphere and out into space. This simple model assumes that the ionosphere is a thin layer. To explain the sunrise fold-back effect we need to account for the F layer's thickness. The ionization level must vary smoothly from low intensities above and below the layer to a high intensity in the middle. This is like the ionization profile shown in Fig 8A, which shows the ionization level along the horizontal axis and the corresponding height vertically.

Consider what happens to a ray fired at an angle upwards. Suppose that it is only just reflected from a thin ionospheric layer at a height of 300 km and received back on the ground 400 km from the transmitter. A ray at a higher angle will skip out into space, and a ray at a lower angle will reflect back to the ground farther away. The receiver is thus right on the edge of the skip zone. Let's follow the higher ray for a moment. It passes upward through the 300-km level to a greater height, say 400 km. If the ionization at 400 km is high enough (it would have to be higher than at 300 km because of the steeper angle), this ray too could be reflected to our receiver at 400 km distance. Three such rays at different take-off angles are shown in Fig 8B. With the help of some mathematics, we can draw a smooth curve showing the ionization intensity that would be needed to reflect a signal from a thin layer at *any* height down to our receiver 400 km away. This curve is shown in Fig 8C, and it is known as the transmission curve for that distance.

If we now superimpose this curve on top of the actual F-layer ionization profile of Fig 8A, we can predict what will happen if the F layer is thick. That is, if it consists of a stack of thin layers with different ionization intensities. We find that the two curves cross at two places. This means that there will be simultaneous reflection from *two* different heights in our new thick layer. The high path is sometimes called the Pedersen ray; it is nearly always ignored in the average textbook. Now we can begin to understand

the dopplergram: Before sunrise, the ionization intensity is too low, and the ionization profile never crosses the transmission curve. There comes a point, however, where the ionization profile just touches the transmission curve at a tangent. A signal just starts to reflect over a range of heights and with a range of Doppler shifts. This corresponds to the leading "nose" of the dopplergram of Fig 7. As the ionization intensity increases still further, the reflection height splits, just like the splitting of the reflection point on a drifting meteor trail. This gives rise to the separate upper and lower arms of the dopplergram trace. The Pedersen ray eventually vanishes when the skip zone disappears completely, and we can go back to the textbook thin-layer model, at least until sunset.

The amount of fold-back increases

on longer paths where the take-off angle is lower, but at vertical incidence there is no fold-back, and the signal just "chirps" vertically down from the HF side. In Fig 7, it is just possible to see two more faint traces (marked A and B) that show no fold-back. They would therefore seem to be at a higher angle than the main traces. They could perhaps be reflections from a higher layer, but are more likely to be double-hop paths.

There is a similar effect at sunset, effectively a folded-back version of the fade-out shown in Fig 5. The dopplergram of a sunset fold-back event is another way of looking at the phenomenon known as skip fading. Where the heterodyne between the high and low path gives an audible rhythmic fading pattern, which becomes slower and deeper, reaching zero-beat just as the signal

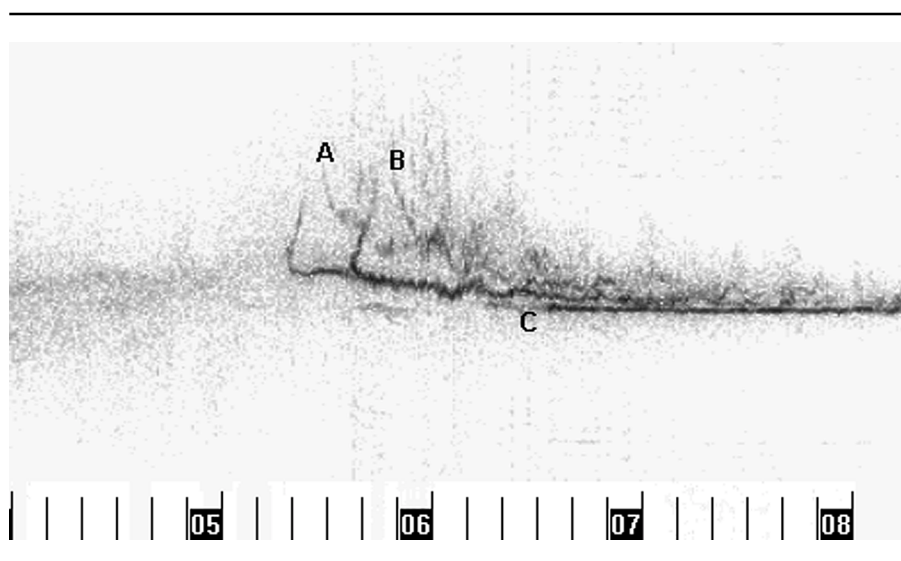


Fig 7—F-layer traces at dawn—showing the "chirp" from the HF side as the reflection height drops—and the onset of the E layer.

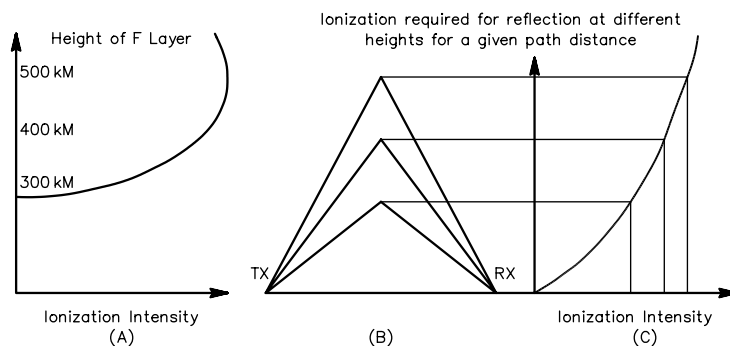


Fig 8—Ionization required for reflection at different heights for a given path distance.

drops out. We can use the same "area swept out" technique that we used to estimate aircraft distances to estimate the height difference between the high and low rays. In other words, we can measure the thickness of the layer.

Finally, at the point marked C in Fig 7, a third trace starts at 0620 UTC. It does not start with the same characteristic chirp from the HF side, and has only a very small Doppler wobble right through the day. This is the E layer, which appears at a height of about 100 km during the daytime and is only ionized enough to reflect 3.5 MHz, so it doesn't show in Fig 5 (5 MHz). Unlike the F layer (the thickness of which explains the fold-back effect), the E layer really is thin. The travelling waves that were visible on the F-layer trace in Fig 5 are hardly visible on the E-layer trace because the vertical wave movement is much smaller in the more-dense E layer lower down. Fig 7 confirms what the textbook tells us, namely that the E layer progressively blankets the F layer, and this gets weaker due to D-layer absorption during the middle of the day.

The dopplergram technique can show many more interesting propagation effects, but space limitations prohibit showing them here. A solar flare shows up as a positive Doppler-shift spike of several hertz on an F-layer trace, with a rise-time of a minute or two and a slower negative recovery. The effects of aurora that are audible as flutter on high frequencies can be clearly be seen on the LF bands. Aircraft reflections and meteor pings can likewise be seen on dopplergrams right down to 3.5 MHz. A local beacon on 28 or 50 MHz will show signs of backscatter on a dopplergram when the band is open for long-distance propagation even though it is well inside the skip-zone. The fascinating subject of sporadic-E propagation has yet to be fully explored with Doppler techniques.

Frequency stabilities better than 1 Hz are needed to produce dopplergrams like those shown in this article. I have achieved this by locking the reference oscillator on my TS-930S transceiver to a standard-frequency broadcast, but even without this high stability, the basic dopplergram shapes can be recognized. Professional ionospheric research is done with high-power pulse transmitters that we radio amateurs

cannot use. Dopplergrams can, however, be produced with a conventional amateur SSB receiver, a readily available low-cost DSP starter kit and an unmodulated carrier, which can often

be provided by an existing broadcast or beacon transmitter in a suitable location. The dopplergram technique could therefore become a very useful tool for amateur propagation study. □□

Without Tears ®

Multimedia Interactive CD-ROM

Get all three CDs for \$1299 +S/H

Receive a free bonus Technical Book while supplies lasts

Call Z Domain Technologies 1-800-967-5034 or 707-591-9620.

Hours: 9 - 5 PST. Or E-mail dsp@zdt.com

Ask for a free demo CD-ROM.

We also have live on-site 3-day seminars: DSP Without Tears, Advanced DSP With a few Tears & Digital-Communications
<http://www.zdt.com/~dsp>

Contract Help Wanted - Antenna and RF Research.

No Walls Inc. is seeking experts in antenna and radio design to work as subcontractors on pending government funded contracts. These contracts pose technical challenges that should be of interest to many readers of this publication. As a contract services provider, you will be free to set your own hours and place of performance.

Please review our web page at **NoWallsInc.com** for details regarding current subcontract opportunities and our corporate structure.

Underground HF Antennas

You've heard tales about "snake" antennas that simply lie on the ground. Let's look at how antennas perform both on and below the earth's surface.

By Grant Bingeman, KM5KG

Editor's note: This analysis ought to be of interest to LF and VLF enthusiasts who are forced to consider antennas in close proximity to ground.

Buried HF antennas are of great interest at clandestine sites that cannot advertise their presence with an elevated antenna, and to underground military and civilian emergency sites that cannot rely on the survival of an above-ground antenna structure. After all, hurricanes and bombs are not very kind to towers. Buried antennas have certain inherent advantages over normally de-

ployed antennas. These buried antennas generally operate within an air space, or they are insulated from direct contact with the earth. We will look at a variety of buried antennas, see how effective they are in bunker-to-air and bunker-to-bunker communication and how well they might protect a receiver from the electromagnetic pulse (EMP) created by a nuclear blast.

Analysis

Unless noted otherwise, we will assume that the receiving antenna is terminated in a high resistive impedance of 10 k Ω . This will not always produce the maximum possible received signal voltage at the antenna terminals, but it will provide a reasonable standard of comparison within

the context of this article. I'll say more about this later.

Our reference transmitting antenna—or source of illumination—will be a $\lambda/2$ horizontal dipole one kilometer above ground, radiating one kilowatt at 14.25 MHz. Unless noted otherwise, the earth throughout this article will have a conductivity of 5 mS/m and a dielectric constant of 13. The self-impedance of the transmitting antenna a kilometer above the ground is 67.7 $-j30.4 \Omega$, determined by *NEC4D* using 19 segments for a 10-meter lossless wire 2 mm in diameter.

Let us begin by determining the induced voltage in a $\lambda/2$ horizontal receiving dipole at various heights above the ground, directly below and parallel to the transmitting antenna (Fig 1). Both of the antennas in this case are

10 meters long and 2 mm in diameter. The transmitting antenna is driven at the center, and the receiving antenna is terminated with a 10-k Ω resistor at its center (Table 1). Note that the signal reflected from the ground is in phase with the direct signal near $\lambda/4$ (5.3 meters) above ground. The electromagnetic wave experiences a 90° phase delay while traveling from the receiving antenna to ground. There is a 180° phase reversal when the wave is reflected from the ground. There is another 90° delay as the reflected wave returns to the receiving dipole. This makes a total delay of 360° or 0°, depending on how you look at it. In other words, the reflected signal ends up in phase back at the terminating resistor. This effect occurs for heights that are an odd multiple of $\lambda/4$, since the round-trip phase delay is another 360° for every additional $\lambda/2$ of height. Minimum signal occurs at $\lambda/2$ above ground, where the reflected signal is out of phase with the direct signal. A standing wave is created by the reflected signal where the voltage minimum appears at 10.5-meter intervals starting 10.5 meters above ground, and the maximum occurs at the same intervals starting 5.3 meters above ground.

The self-impedance referred to in Table 1 is the input impedance of the receiving dipole when the transmitter is replaced by an open circuit. If we think of the receiving dipole as a voltage source driving the receiver load impedance, then the self-impedance gives us an idea of how the signal voltage divides between the antenna and the receiver. If we model this physically as a simple multiport network (Fig 2), some of these relationships become self-evident. I have reduced this to the unbalanced form just to keep things simple.

The self-impedance is measured after placing an open circuit in the center of the opposite dipole. The mutual impedance is simply the negative of the ratio of the open-circuit voltage on the receiving dipole to the input current at the transmitting dipole:

$$Z_{12} = \frac{-V_2}{I_1} \quad (\text{Eq 1})$$

For a dipole spacing of 1 km, the mutual impedance is quite small, and Z_1 is almost equal to Z_{11} . For the specific case of the receiving dipole of Fig 1 located 5 meters above 5 mS/m ground, the following values are obtained:

$$Z_{11} = 67.72 - j30.43 \Omega$$

$$Z_{22} = 75.31 - j15.15 \Omega$$

$$Z_{12} = 0.561 - j0.195 \Omega$$

Maximum power transfer from the transmitter to the receiver occurs when Z_L is equal to the complex conjugate of the self-impedance of the receiving antenna. However, maximum signal voltage occurs when the highest possible load impedance is placed across the receiving dipole. However, since a practical receiver is rarely located exactly at the dipole center, the received signal must be transferred via transmission line to the receiver front end. We want to couple the maximum power into the transmission line. So, in this case we would want to use a 75- Ω transmission line and a series inductance of 15 Ω to tune out the self-reactance of the receiving dipole. Our collected power would be about 48 dB below the transmitted power in this case. See Table 2.

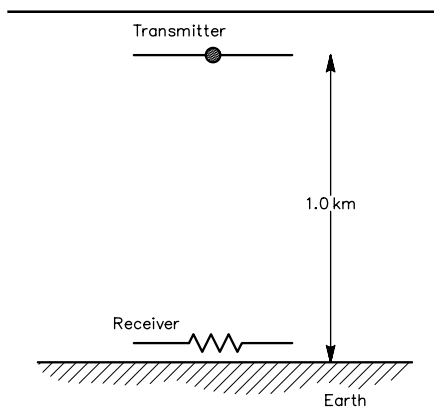


Fig 1—Orientation of transmitting and receiving antennas.

Table 1—Signal Received in a Dipole Close to Ground

n	$n\lambda/4$ (m)	Height (m)	Self-Impedance (Ω)	Induced Voltage (mV RMS)
1	5.3	5	75.3 - j15.2	2270
2	10.5	10	66.7 - j40.4	630
3	15.8	15	66.9 - j23.3	2240
4	21.1	20	69.4 - j35.5	820

Table 2—Signal Received in Various Load Impedances

Z_L (Ω)	V_2 (V)	I_2 (mA)	P_2 (mW)
50 +j0	0.91	18.1	16.6
75 +j0	1.14	15.1	17.2
75.3 +j15.2	1.17	15.2	17.3
10k +j0	2.27	0.23	0.5

Reciprocity

Now let's think about reciprocity for a moment, and transmit from the lower dipole while receiving with the 1-km-high "sky" antenna. Again, one kilowatt is radiated from the lower dipole, and a 10-k Ω resistor is placed in the center of the receiving antenna (Table 3). Obviously, the antenna gain at an elevation angle of 90° above the horizon (straight up) varies considerably depending on the height of the transmitting dipole above ground, as we already saw in Table 1. The gain is maximum for a height near $\lambda/4$, such that the spacing between the dipole and its underground image is a $\lambda/2$ (I assume the reader is familiar with the theory of images).

You may be wondering why the induced voltages are not exactly the same for the reciprocal cases. Note

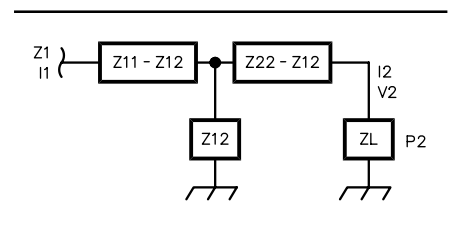


Fig 2—Model of coupled antennas, where: Z_{11} = self-impedance of transmitting dipole. Z_{22} = self-impedance of receiving dipole. Z_{12} = mutual impedance between both dipoles. Z_1 = operating input impedance of transmitting dipole. Z_L = terminating impedance across receiving dipole.

Table 3—Reverse Signal in Sky Antenna

Radiator Height (m)	Induced Voltage (mV RMS) 1 km above ground
5	2150
10	630
15	2250
20	800

that they are the same when the self-impedances of the transmitting and receiving dipoles are equal. Since we have a fixed receiver terminating impedance of 10 k Ω , but a variable self-impedance (Table 1), the voltage division between what we can consider the source impedance and the terminating impedance will naturally vary somewhat. If our terminating impedance were considerably closer to the self-impedance, this effect would be more noticeable. This will vary from one receiver to the next, since receiver input impedances can vary considerably, especially those that have a variable peaking capacitor mounted on their front panel. Some receiver front ends look like a 50- Ω resistor. What is best for a particular receiver and best for communication, maximum power transfer or maximum signal voltage at the RF preamplifier? I think they tend to go hand-in-hand as we saw earlier, but there may be exceptions depending on your exact configuration, especially if the antennas are very close together.

A Buried Dipole

Now let's consider the interesting case of a buried dipole. Assume the wire diameter is still 2 mm, but now we have an air gap extending 10 cm radially around the center of this wire; and surrounding this, of course, we have dirt. As we increase the depth of this dipole below ground, the signal decreases as expected, but it is actually quite useable (Table 4). The signal attenuation is a little more than 2 dB per meter. Note that the self-impedance of the buried dipole is higher than that of a typical $\lambda/2$ dipole, because the wire looks electrically longer when the dielectric constant of the medium surrounding it is greater than one. Even when we have an insulating layer of air surrounding the dipole, the close proximity of the earth clearly influences the dipole's impedance.

The permittivity of earth is quite a bit higher than that of air, so a wavelength is much shorter along a buried wire than it is along a wire suspended in air. A wavelength in air is about $300 / f$ meters, where f is measured in megahertz. A wavelength in dirt or any medium other than free space is $300 / (\eta f)$, where η is a factor based on the dielectric constant (relative permittivity) and conductivity of that medium (see Eq 2). Thus, a wire looks longer in any medium that has a greater permittivity or greater conductivity than air.

Table 4—Signal in Dipole Below 5 mS/m Ground

Depth (m)	Field Intensity (mV/m RMS)	Self-Impedance (Ω)	Induced V (mV RMS)	Attenuation (dB)
1	71	140 + j145	511	2.2
5	26	136 + j150	187	10.9
10	7	137 + j149	52	22.0
15	2	137 + j149	15	32.8
20	0.6	137 + j149	4	44.3

Table 5—Signal in a Dipole Below 1 mS/m Ground

Depth (m)	Field Intensity (mV/m)	Self-Impedance (Ω)	Induced V (mV RMS)	Attenuation (dB)
1	91	154 + j134	614	0.5
5	74	138 + j136	504	2.2
10	59	147 + j149	386	4.5
15	44	149 + j153	298	6.8
20	34	147 + j153	229	9.0

$$\eta = \left[\epsilon_r^2 + 3.23 \times 10^8 \left(\frac{\sigma}{f} \right)^2 \right]^{1/4} \quad (\text{Eq 2})$$

where

ϵ_r = the dielectric constant, usually about 13 for dirt

σ = the conductivity in Siemens/m, typically 0.001 in rock and 0.03 in "good" soil.

Consider the case of average soil having a conductivity of 5 mS/m and a relative permittivity of 13 at 14.2 MHz. Then η becomes the fourth root of $169 + (3.23 \times 10^8) (0.005/14.2)^2$, which works out to be 3.8. This means that what we call the 20-meter band in air looks more like the 5-meter band in average dirt. That is, a $\lambda/2$ dipole at 14.2 MHz is about 10 meters long in air, but only about 2.6 meters long in this particular dirt.

NEC4D predicts that the electric field intensity produced by our 1-km-high sky dipole on the surface of the ground is 93 mV/m RMS. The field intensity one-meter below ground is 71 mV/m. Five meters down, it is 26 mV/m. We know from the induced dipole voltages in Table 3 that the attenuation in our dirt is about 2.2 dB/m, which agrees with the field intensities just described. Note that our attenuation units are decibels per meter (dB/m), *not* decibels relative to a milliwatt (dBm), and *not* decibels relative to a microvolt per meter, $\mu\text{V/m}$ (dB μ).

So if our 14.25-MHz receiving antenna is 10 meters below the surface

of the 5-mS/m earth, we can expect a signal reduction of about 22 dB. This is equivalent to reducing a 1-kW transmitter to 6 W, or a drop in signal strength of more than three S-units. Would this be enough attenuation for the receiver to survive the EMP from a nuclear blast? Perhaps with the aid of some crowbar device, but alone, probably not.

What if our bunker were carved out of solid rock having a conductivity of 1 mS/m? Would you expect the signal intensity to be higher or lower than what we obtained with 5 mS/m earth? Remember that the rock is starting to look like an insulator now, compared to normal dirt (Table 5 tells us that rock is a better "conductor" of RF, compared to dirt). The attenuation through this rock is only 0.5 dB/m, or about four times less than through the soil. At the other extreme, if the earth were a perfect conductor, it would simply short-circuit the dipole, except for the 10-cm insulating layer of air, and the received RF signal would be very weak.

The fact is that solid rock is sometimes a better medium for the internal propagation of RF signals than is plain old dirt (attenuation of 0.5 versus 2.2 dB/m). But don't confuse this characteristic with surface- or ground-wave propagation, which behaves differently. A ground wave propagating on the surface of the earth is attenuated more quickly by low-conductivity earth. So, in the case of ground-wave

Continued on page 56.

Current Sources

Voltage regulators are everywhere, but what happens when you need a source of constant current, such as a battery charger?

By Parker R. Cope, W2GOM/7

Voltage regulators provide a constant output voltage as the input or load changes, but they can be manipulated to provide a regulated current—a current that is independent of the applied voltage or load resistance. IC voltage regulators come in various flavors and sizes from 5 V to 24 V and from milliamps to amps. Of the voltage regulators, the small LM78LXX series is probably the most common. It is in a TO-92 package and can deliver about 0.1 A to the load. Current regulators are not as common as voltage regulators, although Motorola has a line that they call “current diodes.” However, voltage regulators can be connected as current regulators.

Fig 1 shows a voltage regulator. The regulator holds the output voltage V_O across R_L constant. If the common terminal of the regulator floats on some

non-zero voltage, V_O also floats at that voltage. Earlier this year, Sam Ulbing, N4UAU, described how to effectively increase the output voltage by floating the common terminal on a constant voltage.¹

A current regulator holds the output current constant independently of the load. Fig 2 shows a voltage regulator connected to produce a constant current in the load R_L . The voltage regulator holds the voltage across R_L constant. As long as R_L doesn't vary, the current in it is constant. Therefore, when the voltage regulator's common terminal is connected to the load, the current in R_L is independent of R_L . The current in R_L is V_O / R_L .

A voltage regulator has a minimum voltage drop that must be maintained for proper operation. For the LM78L05, the voltage between input and output

must be greater than 2 V. The minimum voltage is somewhat dependent on the current supplied to the load. Of course, the maximum power dissipated in the device and its temperature must be observed.

A current source of a few milliamps can be more economically built with an depletion-mode, N-channel JFET and a resistor, as shown in Fig 3A. The value for R_s can be calculated, but a more realistic approach is to place a pot in the source and adjust it for the desired current.

As an exercise, R_s can be calculated with a simple, but time-consuming, procedure. The values for V_{off} , V_{gs} , and I_{DS} are not usually available and must be established for the particular device you have. V_{off} , and I_{DS} are usually given as maximums and minimums only. The procedure for finding their values is as follows:

1. Apply the operating voltage, short the gate and source and measure I_{DS} .
2. Place a known resistor in the

¹S. Ulbing, N4UAU, “Getting More Voltage Out of a Regulator IC,” QST, Jan 1999, pp 45 and 65.

source (something on the order of 1 kΩ) and measure the voltage across the resistor V_{gs} , then calculate or measure the I_D corresponding to that V_{gs} , $I_D = V_{gs} / R$.

3. Calculate V_{off} .

The drain current in a JFET can be expressed as:

$$I_D = I_{DS} \left(1 - \frac{V_{gs}}{V_{off}} \right)^2 \quad (\text{Eq 1})$$

Rewriting to solve for V_{gs} / V_{off} yields:

$$\frac{V_{gs}}{V_{off}} = 1 - \sqrt{\frac{I_D}{I_{DS}}} \quad (\text{Eq 2})$$

V_{off} can be calculated followed by V_{gs} for any particular I_D .

$$R_s = \left(\frac{V_{off}}{I_D} \right) \left(1 - \sqrt{\frac{I_D}{I_{DS}}} \right) \quad (\text{Eq 3})$$

JFETs should be operated with the drain-to-source voltage above “pinch-off”; that is, operated where drain current is independent of drain-to-source voltage. Pinch-off is approximately V_{off} . The voltage dropped across the current source then should be greater than $V_{off} + V_{gs}$. Again, the maximum power dissipated in the device must be observed.

JFET current sources are limited to a few milliamps, but the current can be

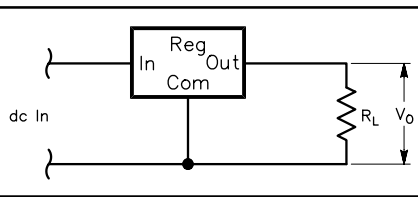


Fig 1—A LM78L05 three-terminal voltage regulator.

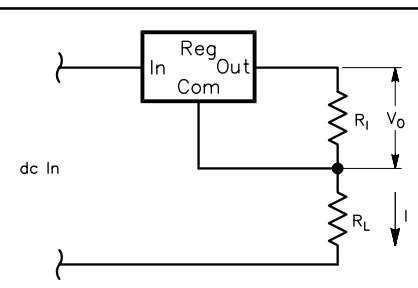


Fig 2—A LM78L05 can be a current regulator.

multiplied by the h_{FE} of a bipolar-junction transistor (BJT). Since the h_{FE} of the transistor isn't well controlled, the base current should be adjusted to produce the required current.

A voltage regulator is a voltage regulator, except when it is a current regu-

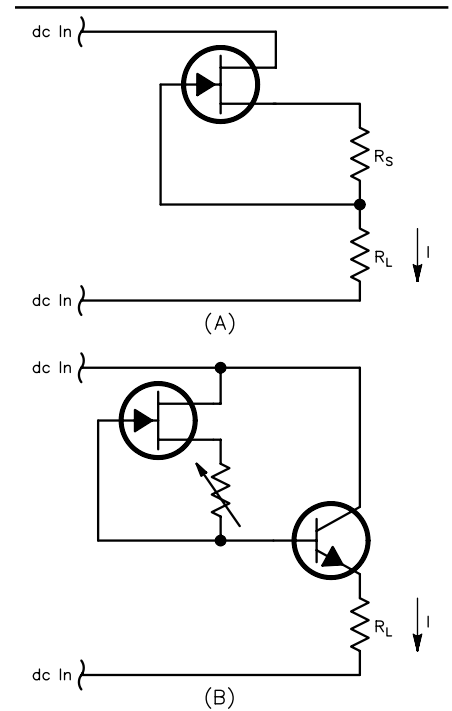


Fig 3—A JFET can be a current regulator.

lator. When you need a current source as opposed to a voltage source, the solution is just a change of reference away.

□□

BINGEMAN, continued from page 54

propagation, higher conductivity earth is more desirable, with the ultimate medium being sea water. For a submarine, however, salt water is the worst possible medium. On the other hand, fresh water would be ideal, since it appears more like an insulator.

Bunker-to-Bunker Communications

Assume we have a second bunker located a kilometer away from the first and a second identical $\lambda/2$ dipole is buried at the same depth, oriented parallel to the first. What is the induced voltage at the receiving end when one kilowatt is radiated from the transmitting end? If we expect an attenuation of 2.2 dB per meter (5 mS/m earth), the answer is: “Not much.” In fact, you would not be able to measure such a small signal (–2200 dB). Even a relatively short path of 100 meters would reduce our signal by 220 dB, which again is a very weak level. Well, what about 50 meters, where we only have 110 dB of attenuation? Assuming an input impedance to the transmitting antenna of $137 + j149 \Omega$, the RF input current is 2.7 A RMS, and the input voltage is about 550 V RMS. The

attenuation factor would be

$$\frac{110}{10^{20}} = 316,000$$

resulting in an induced voltage at the receiving terminals of about 1.7 mV RMS. This is 65 dBμ, or several decibels over S9 on the S-meter, a very respectable signal level. We could expect an induced 1.0 μV signal to exist at a distance of about 80 meters.

Depending on the modulation used and the receiver sensitivity, noise floor and DSP capabilities, I would think that reliable underground HF bunker-to-bunker communication over distances greater than 100 meters (in 5 mS/m earth) is better served by a twisted pair of wires than by radio. If the bunkers are connected by open passages, however, RF can propagate more freely. Since a hole is necessary to pass a pair of wires anyway, you could operate this tunnel as a length of waveguide or simply install an optical transceiver at each end.

Submarine Communications

The interesting thing about ocean water is that its conductivity and dielectric constant are very high compared to dirt. Values of $\sigma = 5 \text{ S/m}$ and

$\epsilon_r = 80$ are typical for sea water. This means that an electromagnetic surface wave propagates very well over the ocean, but very poorly beneath the surface. In both cases, however, attenuation of the field is inversely related to frequency. So lower frequencies yield better signals. That is why the Navy uses 15 kHz VLF to talk to subs.

Summary

We have been reminded that RF propagates best in air, less well in rock, poorly in dirt, and hardly at all in salt water. A submarine, therefore, is naturally EMP resistant. We have seen that maximum received signal power is available when the receiving antenna is terminated in the complex conjugate of its self-impedance. We have also seen that direct bunker-to-bunker underground RF communication is not terribly practical at HF, although it may be attractive at lower frequencies.

Grant Bingeman is Principle Engineer at Continental Electronics in Dallas, Texas. □□

RF

By Zack Lau, W1VT

A Low Loss 50:450-Ω MF/HF Transformer

I got a request from John Devoldere, ON4UN, to develop a low-loss transformer using parts readily available in the USA. It seems that the MN-8-CX cores John uses aren't as readily available as the cores typically available in the United States via mail order. Operators commonly use 50:450-Ω transformers for matching Beverage antennas to 50 Ω. Beverage antennas are popular receiving antennas for low-band DXers with plenty of room.

John got better results by stacking a pair of the MN-8-CX cores than he did with just one. I found similar results with easily obtained FT-37-77 cores. By stacking a pair of cores and using 7 trifilar turns of #28 enameled wire, I obtained good performance from 1.8 to 30 MHz. As shown in [Table 1](#), the return loss was at least 21 dB and the insertion loss was 0.35 dB or better. Two transformers were placed back to back for insertion-loss measurements. The table shows half the measured value.

225 Main St
Newington, CT 06111-1494
zlau@arrl.org

Even better low-frequency performance was obtained by stacking four of these cores and using 6 trifilar turns of #28 enameled wire. I obtained a transformer with excellent performance between 1.8 and 7 MHz. The return loss was at least 26 dB and the insertion loss was 0.25 dB or better across the frequency range. However, the performance at higher frequencies is poor compared to the version with two cores as shown in [Table 2](#).

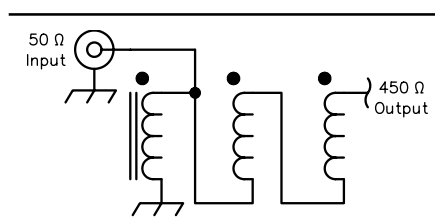


Fig 1—50:450-Ω transformer schematic. See text for core and winding details.

Table 1

A 50:450-Ω transformer using 7 trifilar turns of #28 enameled wire on two stacked FT-37-77 toroids.

<i>F</i> (MHz)	<i>Insertion Loss</i> (dB)	<i>Return Loss</i> (dB)
1.8	0.35	25
3.5	0.33	26
4	0.35	26
7	0.28	27
10	0.25	27
14	0.25	25
18	0.25	25
21	0.25	24
25	0.23	23
28	0.33	22
30	0.30	21

Table 2

A 50:450-Ω transformer using 6 trifilar turns of #28 enameled wire on four stacked FT-37-77 toroidal cores.

<i>F</i> (MHz)	<i>Insertion Loss</i> (dB)	<i>Return Loss</i> (dB)
1.8	0.24	26
3.5	0.23	27
7	0.25	26
10	0.25	24
14	0.27	23
18	0.29	22
21	0.32	21
25	0.34	21
28	0.35	20
30	0.36	19

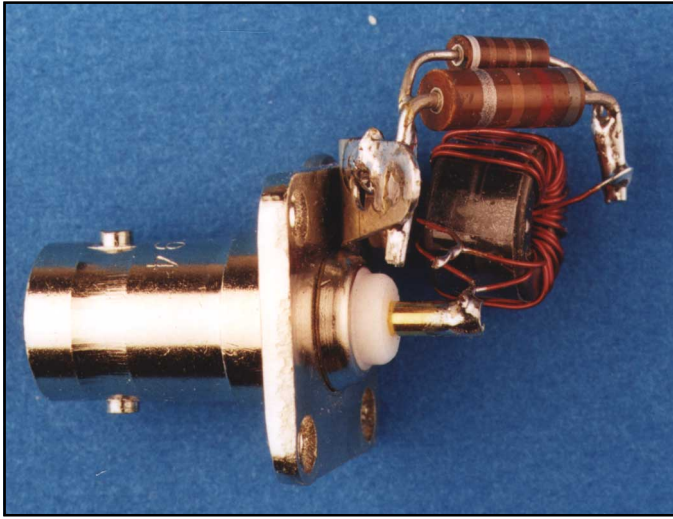


Fig 2—A 50:450-Ω 1.8 through 30-MHz transformer with two stacked cores.

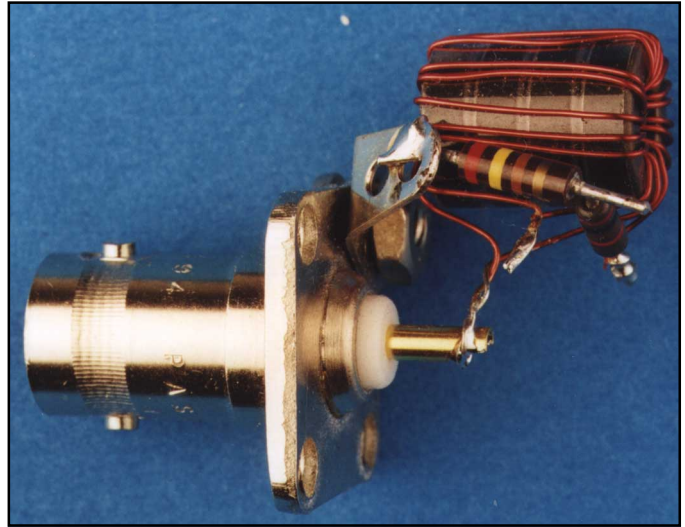


Fig 3—A 50:450-Ω, 1.8 through 7-MHz transformer with four stacked cores.

The return loss was measured using a Mini Circuits Labs ZFDC-20-5 -20 dB directional coupler and a Hewlett Packard HP-141T/8553B/8443A display section/spectrum analyzer/tracking generator. More-accurate measurements were also performed with the Marconi 2041 signal generator and an HP 8563E spectrum analyzer. The load was a selected parallel pair of carbon-composition resistors with a dc resistance of 450 Ω. The insertion loss was measured with a 2041 signal generator and an HP-435B/8481A power meter; though I ended up using the digital HP437B/8482A to get the final numbers for Table 2. The greater precision of the digital display is helpful when measuring small losses.

While manganese-zinc normally isn't the preferred material for low-loss transformers, I think the loss is acceptable in this application. While a nickel-zinc core may offer lower losses, who really enjoys winding lots of trifilar turns on a core? A core with a permeability of 125 requires four times as many turns as a core with a permeability of 2000. A winding with too many turns greatly increases the chances of winding errors. I used strips of K & M self-adhesive laminating sheets to attach the cores together. This tape seems to last longer than ordinary adhesive tapes.

I used the following technique to insure properly wound and connected windings. First, I made six loops/seven turns on the core with #28 enameled wire with *no crossovers*. Next, I put another winding down along side the first, again with no crossovers, and then a third. Next, I made sure there

were six loops of three windings, bunching the turns together to ease the counting problem. There are now two groups of wire ends—each with three wires. I then removed the insulation from the wires out of each group closest together and verified they weren't the same winding with a continuity checker. If they were, I removed insulation from another wire end—which is supposed to be a different wire. Then I soldered them together. Then I removed insulation from two more wires, this time from the center wire and an unused end wire. If they weren't connected together according to the continuity checker, I soldered them together. Otherwise, I removed insulation from another wire, verified it wasn't connected yet, and then soldered them together. You should not be connecting two wires that already have dc continuity.

Similarly, the easiest way to verify the proper 50-Ω tap is to hook up a 450-Ω load to the two single wires and test the two with an antenna analyzer. It should be pretty easy to differentiate between a 4:1 and 1.1:1 SWR. A low-power QRP rig and an SWR meter will also work, although it might be a good idea to use an attenuator to protect the low-power transmitter. Poor loads damage some final amplifiers. Resistive bridge circuits are also useful for measuring SWR while isolating transmitters from poor loads. While heating up resistors is a good sanity check, dumping too much power into carbon-composition resistors will change their values. Metal-oxide resistors are a better choice for abusive testing.

Designing low-loss transformers often involves a bit of trial and error, as deriving good equations from first principles is a stiff challenge for most hams. However, I've found several useful guidelines. For a good low-frequency response, you need enough inductance, typically an inductive reactance of four times the impedance seen by the winding. For a good high-frequency response, you need to keep the winding short. You can often meet both goals with a suitably tiny core, although this often means sacrificing power-handling capability. Similarly, a high-permeability core reduces the number of turns required, but such materials generally have greater loss, reducing the power-handling capability.

Perhaps the area of greatest flexibility is the impedance of the windings. This is easiest to analyze with the bifilar case, which has just two windings. Low losses can be obtained by properly choosing the impedance of the windings. For a 4:1 transformer, the "right" impedance is twice that of the low-impedance side and half that of the high-impedance side.¹ With a 4:1 transformer, this is the same as

$$Z_0 = \sqrt{(Z_{in} \times Z_{out})}$$

the familiar equation for $\lambda/4$ transformers. With high-impedance transformers, such as 50:200 and 50:450-Ω, parallel wires seem to work best. On the other hand, for low-impedance transformers, such as 12.5:50 Ω, better results are obtained with low-impedance windings, such as tightly twisted wires or a coaxial cable.

¹Sevick, Jerry, W2FMI, *Transmission Line Transformers*, p 6-2. □□

Letters to the Editor

A New Look at the Gamma Match (May/June '99)

Dear Ron,

You are quite correct that hams have been in a rut for years on calculating the dimensions for gamma matches, with the result being much more hassle than necessary to adjust the match. The funny thing is that analysis along your lines has been widely published in the professional literature for more than 60 years.

The most important early paper is the classic on shunt-fed verticals by J. F. Morrison and P. H. Smith, "The Shunt-Excited Antenna," *IRE Proceedings*, Vol 25, No. 6, June 1937, pp 673-696. Appendix II gives the impedance relationships. This paper was incorporated in the various editions of Jasik's antenna handbook, and it's still there, in the section on MF antennas.

There is a later paper that takes a similar tack: G. Glinski, "Note on the Impedance Matching of Shunt-Fed, Half-Wave Dipoles," *IRE Proceedings*, June 1945, pp 408-410. There are a number of other papers in the professional literature.

The only reason I know about these papers is that a couple of years back I used shunt feed on a 160-meter vertical and did some research. The gamma match is only one of a variety of possible shunt-fed geometries. In the process of developing the 160-meter vertical, I did some experimenting and quite a bit of modeling with some interesting results:

1. I could get a match for almost any shape: triangles, rectangles, partial-circles etc, with widely varying aspect ratios. The difference between them was primarily in the bandwidth of the match. Geometries with a larger area-to-perimeter ratio appear to have better match bandwidths.

2. Using a lumped-equivalent circuit for the antenna and the match, it can be shown that it forms an inductively coupled, double-tuned circuit. I modeled and "monkeyed" around with the antenna until I got the classic double-hump response, which resulted in less than 2:1 SWR over most of the 160-meter band.

The whole subject of shunt-fed antennas has not been well explained in the ham literature.—73, *Rudy Severns, N6LF, PO Box 589, Cottage Grove, OR 97424; rudys@ordata.com*

Dear Rudy,

Thank you very much indeed for your letter. Although you didn't actually say so, I think that—from the content of your letter overall—you are in general agreement with the model of the gamma match that I propose in the article.

Thank you also for drawing my attention to the earlier work on shunt-fed vertical antennas. I was not aware of this work, which perhaps is not surprising since I have never worked professionally in radio and have never had access to the professional literature. What few reprints of papers from the professional world that I have acquired over the years have been from references that I have seen in amateur periodicals or handbooks. Before writing the article, I made a very careful study of everything I could find on gamma matching; in every case, the Healey-Tolles folded-dipole explanation was all that was offered. I have a copy of *Low-Band DXing* by ON4UN, which has a list of 40 references on the matching of LF antennas, mainly related to verticals. Out of that list, I can't see anything of

relevance to the gamma-match model that I describe. It seems quite amazing to me that such an apparently thorough work as that by ON4UN should have failed to include references to the papers you mention in your letter.

Perhaps we should suggest to Doug that he consider reprinting those articles in *QEX*; I suspect that there are a lot of amateurs out there who would find them very useful. Incidentally, is P. H. Smith the Philip Smith who invented the Smith Chart?

The reason my e-mail address wasn't given is that I have only very recently obtained the facility and didn't have it when I last wrote. Once again, thanks for taking the trouble to write.—73, *Ron Barker, G4JNH, 171 Leicester Rd, New Packington, Ashby de la Zouch, Leics LE6 5TR UK; ron.g4jnh@talk21.com*

Hi Ron,

Yes, I am in agreement with your ideas for gamma-match design. Sorry if I didn't spell that out. And yes, it is the same P. H. Smith of Smith-Chart fame. He did a lot of good work at Bell Labs.

I was very pleased to see your article, as I have felt for some time that the whole subject of shunt matching is very poorly represented in ham literature. After the work I did on 160 meters some time back, I was filled with righteous indignation and good intentions to write something wonderful. Well, that didn't happen!—73, *Rudy*

Hi Doug,

I find the article by Barker very interesting and well conceived if somewhat obscure in the math details. I realize it is not a tutorial on complex algebra! I have been attempting to use his technique to replace the current approaches I have in my *MATCH* program. Currently, I offer both W3PG and WA6IKN methods for calculating the gamma match. Since these two routines never agree, it is obvious that neither is the correct approach.

I have a small problem. In the article, Barker solves the equivalent circuit presented in Figure 4A (p 25) and arrives with the identity Eq 3 (p 26). He further breaks down Eq 3 into a reduced form. A casual inspection of the math will show that if the first part of the right-hand side of Eq 3 remains unchanged, the second part on the second line is in error. In other words, $R_a / 4 + R_a / 4$ do not equal $3R_a / 4$. I must assume that the error lies with publishing the article and not Barker's basic premise. I could revisit the full equivalent circuit and the math, but I thought you might save me the trouble.

When I have adapted Barker's method to computer solution, I will include it in my shareware programs *YAGIMAX* and *MATCH*. Being an ARRL Director does not allow me the time that I would like to write more antenna oriented software, but that situation will end next January 1, when my third and final term expires.—73, *Lew Gordon, K4VX, PO Box 105 Hannibal, MO 63401-0105; k4vx@nemonet.com*

Hi Lew,

You are right! Eq 3 should read:

$$\begin{aligned} \frac{1}{R_{in} + X_r} &= \frac{1}{\frac{R_a}{4} + jX_G} + \frac{1}{\frac{R_a \pm jX_a}{4} - jX_G + \frac{R_a \pm jX_a}{2 \pm 2}} \\ &= \frac{1}{\frac{R_a}{4} + jX_G} + \frac{1}{\frac{3R_a \pm jX_a}{4} - jX_G} \end{aligned} \quad (\text{Eq 3})$$

Thanks for pointing out the error. We'll look forward to hearing from you again.—Ed.

Performance Specifications for Amateur Receivers of the Future (May/June '99)

Doug,

I found DK4SX's article interesting. However, I feel that the relationship that necessarily exists between phase-noise performance and intermodulation performance was not given sufficient prominence. Mentioned as a testing problem, it has actually to be considered in the production of specifications.

In my paper at RF Expo' in 1986, "Phase Noise, Intermodulation, and Dynamic Range in Receivers," I showed that the phase-noise-limited dynamic range and the intermodulation-limited dynamic ranges should be of equal orders of magnitude. This was expanded in the paper I wrote jointly with G4OOA, entitled "System Demands in Personal Radio Services," presented at an IEEE symposium in London in 1996.

Consider a receiver with a 10-dB noise figure, +30-dBm IP_3 , and 3-kHz bandwidth. The noise floor will be at -130 dBm, while two signals at -23 dBm (rounding off decimal parts of decibels) will produce a signal equal to the noise floor. If the phase noise at the offset of the closest signal is -141 dBc/Hz, then there will be noise produced in the IF at the same level as the intermodulation signal. So it can be seen that a high intercept point is of little use without good phase-noise performance. In this point of fact, the use of an antenna attenuator does help the situation, although I would agree with DK4SX that all too often it is there because the designer isn't very good at design!

IMD in crystal filters has been known for many years. Malinowski and Smythe of Motorola described it in a 1973 "Frequency Generation and Control" symposium. Unfortunately, higher-frequency filters suffer more from this than lower-frequency ones. The problem can be overcome by the use of suitable resonant SAW filters: 30-kHz-wide filters are readily available for the IS-136 digital cellular system.

It may be shown that the phase noise performance should be:

$$\frac{2a}{3}(NF - 171 - IP_3) \text{ dBc/Hz}$$

where a is the phase-noise density in dBc/Hz, NF is the noise figure in decibels, and IP_3 is the third-order input IMD intercept point. From the example above, it is obvious that producing the

phase-noise performance required in a high-performance receiver is not a trivial task, and it can be the limiting factor in operation, rather than intermodulation. A good start toward low phase noise is high power in the oscillator with high-Q components—which is perhaps why receivers like the HRO were so good in this respect.

The question of spurious responses is of interest. There are two forms of spurious response in a receiver: internal and external. Internal responses are the "whistles" or "birdies" that are found without an antenna. Particularly troublesome in multiple-conversion receivers are those of the form:

$$\begin{aligned} mf_{LO1} \pm nf_{LO2} &= f_{RF} \\ \text{or...} &= f_{IF1} \\ \text{or...} &= f_{IF2} \end{aligned}$$

or their images, where m and n are integers, f_{LO1} is the first local-oscillator frequency, f_{LO2} is the second local-oscillator frequency, f_{RF} is the signal frequency, and f_{IF1} and f_{IF2} are the first and second intermediate frequencies, respectively (see my article on "Frequency Planning" in the June 1999 edition of *RF design* magazine).

The external spurs, such as image and "half-IF", are controllable; but as DK4SX writes, the use of a DDS synthesizer may well introduce a large number of spurs because of both the truncation process and limitations of DACs. It should be remembered that a 10-bit DAC that is only 6-bit accurate at speed is not as good as an 8-bit DAC that is 7-bit accurate. Especially poor spur performance will be achieved where the effective multiplicand is $2(n + 1)$ or $2(n - 1)$. Such spurs are close in, and can lead to responses that effectively negate the filter skirt selectivity.

Synthesizers are a convenience in amateur equipment. Possibly a simple, single-loop synthesizer with interpolation provided by "pulling" the master crystal might well produce better performance than a multi-loop DDS. Unfortunately, the "simple" approach is frequently able to produce high performance only at high production cost because of set-up time.

It should be noted that acceptable receiver conducted-emission levels are tighter in Europe and Japan (-57 dBm below 1 GHz) than the FCC requirements.

This article may have provoked thought on the subject; I wonder if it will really produce a change in the attitude of manufacturers, though.—

Peter Chadwick, G3RZP, Three Oaks, Braydon Swindon, Wilts SN5 0AD UK; Peter_Chadwick@mitel.com

Hello Doug,

I followed with interest your rag-chew and opinions after *QEX* published the paper about new ham-radio gear specifications. I subscribe to *QEX* and like it very much.

"Birds" may appear across the full RF range, but if they are at MDS level, it will not be a major setback if the radio has very good IMD performance and selectivity. Given the way synthesizers are designed, we have to live with them. My main concern is with reciprocal mixing and IMD products, which become a nuisance when you must listen to signals of S9+30 to 40 dB in contests; or, as now with good propagation, when there are a lot of strong signals on the bands.

Like others, I do not really like to tune or command my radio via PC. It is more convenient to use a knob.

I do not believe that any manufacturer of ham-radio gear will go to a \$100 mixer, a \$6 RF amplifier transistor or FET ($\times 4$ for RF amplifier and post-mixer amplifier), \$2 for a good PIN diode, a \$100 "synth," compensated delay filters and so on, to accomplish the goals of the "good radio" as per Uli's paper. The radio will cost too much.

I do not believe that any designers of ham-radio gear will use (in the near future) a DSP with a clock of 400 MHz or more to achieve "real-time" processing, with good SFDR and so on, even when the technology is there. I do not believe that any manufacturer will use casting and better shielding for PC boards, to stop the bleed-through in RF and IF stages: It will cost too much. The trend is to use little building blocks or ASICs, not only for ham radio, but for the commercial market.

In conclusion, I do not see a "good" receiver in the ham-radio market coming forth specifically because of concerns about cost. Cornell [KW7CD] will build one, I will build one, and maybe some hardened old guys—but not the mass of ham-radio operators.

Doug, keep up the good work with *QEX*. Maybe one day we'll have a radio with real good receiver in the market.—73, Costel Popescu, KG6NK, 1659 Rogers St, Long Beach, CA 90805; Cdp1@aol.com

Doug,

I read the article in the *May/June '99*

QEX with interest, and have two remarks concerning the article. First, little mention was made of synthesizer phase noise as a strong-signal performance limiter. I think many of the recent Product Reviews in *QST* indicate that the strong-signal performance of many modern receivers is limited by the synthesizer phase noise rather than the quality of the RF front end. Modern receivers that provide wide frequency coverage have little or no RF selectivity ahead of the mixer, except perhaps a low-pass filter. Any signal that gets past this minimal selectivity has a chance to be mixed down to the IF by synthesizer noise components. These very low-level noise components may be present megahertz away from the actual synthesizer output frequency. High on my wish list are improved synthesizer designs that offer lower phase noise—or else go back to an amateur-band-only receiver design that provides some RF selectivity ahead of the mixer!

Second, the requirement for strong-signal performance at VHF is even more stringent since receivers are more sensitive. A 10- to 15-dB noise figure is completely intolerable on 6 meters, 2 meters and up. A 1- to 3-dB noise figure adds 12-14 dB to the dynamic range there.

As a case in point, take my own situation: I live in an average suburban area. The local channel-2 TV transmitter is perhaps 10 miles away and there is a hospital with a number of paging transmitters atop it about a mile away. There are also some FM broadcast stations around. After a popular-brand 2-meter FM mobile radio was completely desensitized when connected to my attic-mounted ground plane, I borrowed a spectrum analyzer and connected it to my antennas. On the attic ground plane, TV and the 152-MHz pagers averaged -30 dBm. Some of the local FM stations were in the -25-dBm range. The local channel-2 signal came in at -25 dBm off the back corner of my 6-meter beam. Things weren't much better on the 2-meter horizontal beam. What I saw is probably typical of suburban RF environments. The situation is getting worse with time as more and more commercial transmitters are activated.

The newer radios I own (IC-706 MkII and TS-690) both seem to suffer some degradation in VHF performance if no external filtering is used in the feedlines. In light of the measured signal amplitudes, these re-

sults are not surprising. Since MDS is in the -140-dBm range, these out-of-band signals are 110 to 120 dB above MDS, which is more than these receivers can handle.

Meanwhile, my old TS-700A shrugs off the interference as if it weren't present. For 6 meters, I once used a homebrew transverter with a TS-820 as IF and had no problems with channel 2 (the transverter passband rolled off very sharply above 51 MHz). These two are non-synthesized radios with some selectivity in the RF amplifiers ahead of the mixer.

I think the noise and interference problems in the newer radios—usually lumped under the term “intermod”—are caused at least in part by the wide-open front ends coupled with phase-noise components (or even low-level discrete spurs) in the synthesizers. An 80-dB-down synthesizer spur can still mix with a 100-dB-above-MDS signal from an out-of-band source and produce a readable signal.

At the present state of the art (including affordable cost as part of the state), bells and whistles (such as broadband receive coverage, scanning capability, many memories and digital VFOs) directly conflict with the ability to reject strong signals. Perhaps someday, cleaner synthesizer designs (or an all-digital receiver where the antenna hooks to an A/D converter!) will permit the bells and whistles to be incorporated without compromising strong-signal performance. We are not there yet.—*Joe Fleagle, W0FY; 320 S Greentrails Dr, Chesterfield, MO 63017; jfleagle@SEISTL.COM*
Gentlemen,

Thank you for the letters. It's interesting to read all those in-depth comments. So we really do have a technical point that is being seriously considered by very many amateurs.

As far as sideband noise is concerned, I clearly pointed out that blocking dynamic range as limited by reciprocal mixing (LO sideband noise) must be at least 10 dB greater than spurious-free dynamic range. Especially in wide-band systems, blocking effects may be caused by single strong signals with large frequency offsets; IMD products need at least two strong signals with the proper frequency relationship to cause problems. Certainly, an improvement in oscillator sideband noise is only feasible with voluminous, high-Q resonant circuit elements and sophisticated loop design.

Most amateurs believe an improved

receiver will not be realizable because of the high cost of parts. This is the argument perennially used by manufacturers. It is not true! Relays for shortwave frequencies are available for much less than the cost of good PIN diodes. The super-high-level MOSFET mixer does not cost more than the quad-JFET mixer and is not inherently more complex. It requires much less LO power than a diode mixer with an IP_3 of +30 dBm and has far-superior isolation performance. A narrow-band roofing filter may be constructed in a bridge configuration from four crystals with performance comparable to that of monolithic filter blocks, and it has better IMD characteristics at hardly higher cost. Finally: Why not invest all the money and engineering effort now expended on useless gimmicks in an improved synthesizer, instead? Analog technology still has a high potential for improvement. We should use the well-known circuitry now instead of waiting many more years for the all-digital receiver to come.

I wonder how Joe could buy the transceiver he did knowing all the facts about blocking and IMD so well. Look at these radios band by band: They are all (and must be!) worse than their single-band counterparts. I think manufacturers will regretfully return to single-band radios with a higher degree of RF performance in the near future.—*73, Uli Graf, DK4SX, Seidlheck 19, D-89081 Ulm, Germany; ulrich.graf@ulmail01.europe.nokia.com*

Measuring Distortion in Linear Amplifiers (May/June '99)

◇ Although two-tone testing has been popular for many years, it doesn't tell anything like the whole truth. Power-supply deficiencies that appear when a signal is modulated at the syllabic rate aren't seen with a two-tone test using tone spacing of 1 kHz or more.

There are a number of approaches to get around this:

- Three-tone testing, suggested many times by Tom Rauch, W8JI, where two of the three tones are very close in frequency (20 Hz or so)

- Two-tone testing with very narrow tone spacing (20 Hz or so);

- Noise testing, where the transmitter is modulated by audio noise with a notch in the audio passband. Intermodulation products fill up the notch, thus allowing measurement, while the low-frequency components exercise the amplifier under something approximating normal use.

This method has been used for many years in analog, multi-channel telephony and has been suggested a number of times for evaluating HF SSB transmitters.

I believe a caveat is in order: Wide tone spacing is fine for certain evaluations, but it will not necessarily tell the whole truth.—*Peter Chadwick, G3RZP*

On Pi and Pi-L Networks

◇ I did not yet send in my article "Some Characteristics of Pi and Pi-L Networks." A couple of my friends who are both amateurs and retired professionals offered the opinion that pi and pi-L networks are not timely topics. The reason being the changes that have taken place in power-amplifier circuit design brought on primarily by the availability of solid-state devices.

I recall a statement of purpose that was published in the very first issue of *QEX* to the effect that it was to be a means for the exchange of ideas that were at the "cutting edge" of technology. Perhaps this has changed over the years. I don't know. Please give me your thoughts.—73, *Vince Bartell, WOMFK, 4424 Jansa DR, St Paul, MN 55126-2102; vbartell@isd.net*

Hi Vince,

I would suggest that an extremely broad range of subjects worth publishing. This is especially so if one or more of the following is true: (1) you present a new way of looking at things, (2) you intend to clarify or simplify matters, (3) you want to inform readers about something that isn't commonly known, or (4) you relate your own unique experiences.

We're trying to broaden the scope of *QEX* to reflect Amateur Radio's diversity. This means covering a profusion of interests and points of view. It doesn't always mean cutting-edge, highly esoteric stuff. Sometimes it involves lots of suggestions and discussion, making "boo-boos" and so forth. In keeping with our current mission statement, we'll continue to run state-of-the-art material; we also want to encourage experimentation at all skill levels.—*Ed.*

Doug,

Jul/Aug '99 is another great *QEX*. *QEX* offers excellent material to the

ham who still has technical competence. Lord knows, you're about all that's left.

How about putting a homebrew rig or two per year through the ARRL Lab for at least spot performance numbers? Or, set some broad specifications—say a single-band, 20-meter SSB rig that is within the capability of a large number of homebrewers—and have people submit their designs. That could create a massive amount of work for you when those rigs come together, though.

I can envision a "competition" between rigs submitted by premier designers wherein the tradeoffs between design philosophies are explained. It would include a page of measured IP₃, NF, MDS, SFDR etc. I know, it's not practical within the scope of *QEX*. Still, it would certainly be an incredible undertaking.—*Regards, Bill Carver, W7AAZ, 690 Mahard Dr, Twin Falls, ID 83301; bearver@magiclink.com*

Hi Bill,

Thank you. It would be easy to take the credit, but every one of the staff listed on p 1 works hard on this magazine. You writers are the real stars: Without your input, *QEX* would not exist.

The League publishes measurements on production gear in *QST* as a service to its members. It seems to follow that *QEX* should render the same type of service, but we tend to prefer that authors present and substantiate their own claims. We retain that approach because we are experimenters: We want to keep the flow of ideas as free as possible. We reserve the option of inviting an author to submit equipment for ARRL Lab testing, but that would be quite unusual. In any case, it is easy to challenge the data (or lack of it) proffered in *QEX*: Just write the author or us!

I believe our contributors are giving us their best work without much intercession by me. This is your forum; it is largely what you make it. I will, however, encourage the development of realistic performance goals and the incorporation of technology that helps achieve them. If more hard data are what we want, then you and I shall insist on getting them.—*Ed.*

Doug,

I have a major problem with *QEX*: The articles published are too good. Mandlekern, Sabin, Hayward, Graf, Rohde, Zavrel and the rest are what *QST* has been missing. Now, my previously dormant interest in the hobby has revived.

I can't put *QEX* down; I read it at breakfast, dinner, whenever. Now I'm going to have to spend a fortune re-equipping my shop, retire 17 years early and risk poverty so I can get started on a new receiver, new antennae, new transmitters—paring down a to-do list that grows by the issue. Thanks a bunch.—73, *Dave French, AA4WD, 5305 Deep Valley Run Rd, Raleigh, NC 27606; dfrench@ipass.net*

A Switching Power Supply for Beginners (Jul/Aug '99)

◇ I moved recently and finally have e-mail and snail mail here in Austin. My snail mail is: Ray Mack, PO Box 200671, Austin, TX, 78720-0671.—*Ray, WD5IFS; ray.mack@conexant.com*

Hi Ray,

Thanks for the update. By the way, I found that the inductor labeled L5 in your Fig 7 (p. 14) should have been L3. Sorry about that.—*Ed.*

Creating 3-D Antenna Radiation-Pattern Plots (Jul/Aug '99)

◇ Eq 3 should read:

$$z = \rho \sin \phi \quad (\text{Eq 3})$$

The derivation that followed is unaffected by the error.—*Ed.*

A Regulated 2400-V Power Supply (Jul/Aug '99)

◇ I just got an e-mail from Ray Heaton, NJ0G, who pointed out a small error that could be a big error for somebody. He pointed to Fig 7 at the right-hand end and a 300-Ω resistor, 25-μF capacitor, and the coil of RY2. It is labeled as "+2400 V", whereas it should read "+24 V." If someone connects 2400 V to that point, I suspect the 4th of July would come early for next year!—73, *Al Williams, VE6AXW, 13436 114 St, NW, Edmonton, AB T5E 5E6, Canada; al.williams@gte.net* □□

Upcoming Technical Conferences

18th Annual ARRL and TAPR Digital Communications Conference

Make your arrangements now if you wish to attend. The conference will be held September 24-26, 1999, in Phoenix, Arizona. For more information, contact TAPR at tel 940-383-0000, fax 940-566-2544; e-mail tapr@tapr.org or visit www.tapr.org.

The 17th Space Symposium and AMSAT-NA Annual Meeting

The 17th Space Symposium and AMSAT-NA Annual Meeting will be held October 8-11, 1999 at the Hanalei Hotel in San Diego, California. Whether you are new to satellites or have been working them for years this year's symposium will allow you to expand your horizons in amateur satellite communications. The weekend will be full of technical presentations that range from Friday evening's "Getting Started" introduction to Amateur Radio satellites to presentations on microwave operation, the International Space Station, recently launched and upcoming satellites along with other satellite related topics.

The symposium begins with technical sessions Friday morning. After a break for lunch, technical sessions resume in the afternoon. Friday evening there is a choice between the "Getting Started" session and the IARU Satellite meeting. There will be more technical sessions on Saturday followed by the AMSAT-NA Annual Meeting. The annual banquet Saturday evening will conclude the day's activities. Sunday morning there will be an optional field trip to visit Qualcomm Globalstar labs and SpaceDev, Inc. The AMSAT-NA board will meet Sunday afternoon to discuss business matters and this meeting will continue on Monday October 11.

Spouses and families may choose to visit some of San Diego's many nearby attractions during your stay. For enter-

tainment, there is Sea World or the world famous San Diego Zoo. History buffs can "discover" San Diego at Cabrillo National Monument or experience periods of San Diego's history by visiting Mission San Diego de Alcala, Presidio Park, Old Town San Diego State Park and Balboa Park. Golfers will enjoy playing on any of San Diego's many fine golf courses. Of course there is no shortage of shopping with Mission Valley Center, Fashion Valley Mall, Seaport Village and Horton Plaza a short ride away. If relaxation is more your style visit scenic La Jolla, Mission Bay Park, Coronado Island or any of San Diego's beautiful beaches.

If you're interested in an Amateur Radio vacation, visit the ARRL Southwestern Division Convention (HAMCON) on the Queen Mary in Long Beach, California, October 1-3. Then see some of Southern California's sights before attending the 17th Space Symposium and AMSAT-NA Annual Meeting in San Diego October 8-11.

Registration information may be obtained by telephone, fax, e-mail or on the Web. Please contact the AMSAT business office at 301-589-6062 (voice), 301-608-3410 (fax) or e-mail martha@amsat.org. For additional information visit <http://www.amsat.org>. Symposium registration is \$25 before September 15, \$30 after September 15 and \$35 at the door. Tickets for Saturday's banquet are \$25. The optional field trip Sunday morning is \$10. Please send your registration form and check, money order or VISA/MC (in US funds) payable to AMSAT-NA addressed to AMSAT, 850 Sligo Ave, #600, Silver Springs, MD 20910-4703.

Microwave Update '99

W5LUA, WA5VJB and the North Texas Microwave Society welcome you to Microwave Update 99, which will be held at the Harvey Hotel in Plano, Texas, on October 21-23, 1999. Plano is located north of Dallas on US 75,

about 30 minutes drive from downtown Dallas and 40 minutes drive from the Dallas-Fort Worth airport. The Harvey Hotel is located on the northeast corner of Fifteenth Street and US 75. Fifteenth Street is exit #29 from US 75.

Accommodations

We have negotiated a special rate at the Harvey Hotel for both single and double occupancy. Make room reservations by calling the Harvey Hotel directly at 972-578-8555. Identify yourself as part of the Microwave Update group to receive the specially negotiated room rates (\$63 plus taxes per night). Make your reservations no later than three weeks prior to your arrival date because any vacant rooms in our block will be released three weeks prior to the conference. Additional reservation requests will be honored on a space-available basis.

Topics

The list of speakers includes well-known microwave figures from coast to coast and around the world. Some of the topics to be presented include:

Microwave basics; Qualcomm conversions at 10 and 24 GHz; Microwave beacons; Quad-loop Yagis; 24 GHz power amplifiers; New 10 GHz transverter designs; New MMICs for 2 GHz through 24 GHz; Low noise amplifiers; Working with TWTs; Amateur satellites; Microwave tube power amplifiers; Millimeter waves; Atmospheric-scatter propagation on 10 GHz; LASER systems and working VUCC on 76 GHz; and installation of a 5-meter dish for 23 and 3 cm EME from California.

Other speakers and topics are in the works. If you would like to present a paper at the conference, please contact W5LUA.

Proceedings

The proceedings will again be published by the ARRL. W5ZN is

coordinating the collection of technical material for the proceedings. Please send Joel any material that you wish to have published even if you do not plan to present a paper. Cut-off date for paper submission to Joel is September 7, 1999, the day after Labor Day.

Entertainment

There will be no formal spouse's program at the conference. However, the area is full of antique shops and shopping malls. The hotel is very close to the South Fork Ranch for those that remember the TV show *Dallas*. Please indicate if your spouse is coming. We will compile a list and coordinate a meeting place for the spouses where they can gather and make plans.

The Saturday night banquet will be held at the Harvey Hotel. We will again have a Texas-style-barbecue buffet for \$20 per person. Spouses are welcome and a short program is being planned. Everyone is encouraged to attend.

Registration and Information

Please register for the conference as soon as possible. Pre-registration cost is \$40 and is due to W5LUA by October 1. Regular registration after October 1 and at the door will be \$45. Make checks payable to the North Texas Microwave Society. We will have special prize drawings for pre-registered attendees. For more information, visit the North Texas Microwave Society page www.ntms.org or contact the following:

Al Ward, W5LUA, 2306 Forest Grove Estates Rd, Allen, TX 75002; tel 972-562-6018; al_ward@hp.com.

Kent Britain, WA5VJB, 1626 Vineyard, Grand Prairie, TX 75052-1405; WA5VJB@flash.net.

Joel Harrison, W5ZN, 528 Miller Rd, Judsonia, AR 72081; w5zn@arrl.org.

Tom Whitted, 4641 Port Clinton East Rd, Port Clinton, OH 43452; wa8wzg@wa8wzg.com.

EME 2000 Brazil Conference

The ninth bi-annual International Amateur Radio Moon-Bounce Conference will take place on August 18-20, 2000, in Rio de Janeiro, Brazil. The conference is dedicated to Earth Moon Earth (EME) Amateur Radio activities at 432 MHz and higher frequencies. Many technical papers are already

scheduled for this conference, covering all technical aspects of EME. For more details visit the Web page at www.eme2000.com.br. Information courtesy of D. W. Murden, PY5ZBU. □□

Strays

New Amateur Radio DX Information Page

◇ URL <http://www.dxbands.com> is designed to give amateurs throughout the world the opportunity to find up-to-the-moment Amateur Radio news, details on DXpeditions, contests and pages of ham-radio links.

The site includes a unique "dx-diary" that lists large and small DXpeditions the world over, in a month-by-month format. The style shows the start and finish date of each event, together with details, QSL manager and other information.

Updated each day with the latest Amateur Radio news, [dxbands.com](http://www.dxbands.com) is destined to become an important online resource. E-mail news@dxbands.com.

Write for QEX?

◇ Thousands of radio amateurs and professionals interested in technical work at all skill levels read *QEX*. It is an open forum for the exchange of ideas and information as well as projects with results. Staff writers provide only a small fraction of the material appearing in *QEX*; we count on *you* to supply the stuff that keeps us going. We welcome all letters, queries, and article submissions.

Authors of published feature articles are compensated at \$50 per printed magazine page, but that payment pales in comparison with the satisfaction of knowing that you've contributed to Amateur Radio's growing body of knowledge. Are you building something that others might want to duplicate? Do you have a new technique or suggestion? Do you want to reach a sophisticated readership with your advertisement or announcement? Will you comment on what you see in *QEX*? Contact us using the addresses shown on p 1. For more information, visit us at www.arrl.org/qex/. □□

Next Issue in QEX

We have a fine article by John Stephenson, KD6OZH, that begins by defining the needs of microwave- and millimeter-band enthusiasts for good frequency stability, low phase noise and low noise floor. John furnishes a thorough analysis of the requirements, then goes on to provide his solution: a very-low-noise VCXO locked to an atomic standard. The results come quite close to theoretical minima in several categories.

Bruce Pontius returns with ideas about replacing some of those hot, current-hungry signal generators in your lab with something smaller and cooler. One generator covers 0 through 50 MHz, the other 2.1 to 2.4 GHz. He makes good use of widely available 50-Ω modules, where possible. He is not afraid to compare the performance of his designs to that of the older, professional gear he is replacing.

Harke Smits, PA0HRK, contributes an analyzer design that lets you measure the noise figure and gain of a device under test simultaneously. It allows measurements up to at least 500 MHz directly and at much higher frequencies using a transverter. Don't miss this last issue of the 1900s as we help you add some relatively sophisticated gear to your arsenal. □□

Surface Mount Chip Component Prototyping Kits—
Only **\$49.95**

CC-1 Capacitor Kit contains 365 pieces, 5 ea of every 10% value from 1pF to 33μF. CR-1 Resistor Kit contains 1540 pieces, 10 ea of every 5% value from 10Ω to 10 megΩ. Sizes are 0805 and 1206. Each kit is ONLY \$49.95 and available for Immediate One Day Delivery!

Order by toll-free phone, FAX, or mail. We accept VISA, MC, COD, or Pre-paid orders. Company PO's accepted with approved credit. Call for free detailed brochure.

COMMUNICATIONS SPECIALISTS, INC.
426 West Taft Ave. • Orange, CA 92665-4296
Local (714) 998-3021 • FAX (714) 974-3420
Entire USA 1-800-854-0547



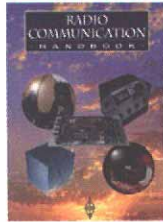
Radio Society of Great Britain Products Imported by ARRL!



Communication Reference

Packed with technical information!

Radio Communication Handbook



Covers semiconductors, HF and VHF/UHF receivers, transmitters and transceivers, microwaves, propagation, HF and VHF/UHF antennas, amateur satellites and space communications, image techniques, power supplies, and much more. PCB layouts included. 760 pages.

ARRL Order No. 5234—\$38



The RSGB Guide to EMC

Diagnose and cure unwanted RF interference and achieve electromagnetic compatibility (EMC). Also covers filters and braid-breakers. 204 pages.

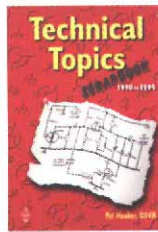
ARRL Order No. 7350—\$30

RadCom 1998 on CD-ROM



All of the words, diagrams and photographs of the technical articles, news and reviews published in RadCom magazine during 1998. Includes a fully searchable keyword index covering all 12 issues; over 1000 pages including all advertisements; and Adobe® Acrobat® Reader for Windows.

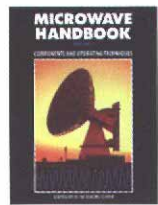
ARRL Order No. 7415—\$30



Technical Topics Scrapbook 1990 to 1994

An invaluable collection of experimental HF/VHF antennas, circuit ideas, radio lore, general hints and comments...all from the popular *RadCom* magazine column, *Technical Topics*. 314 pages.

ARRL Order No. 7423—\$20



Microwave Handbook, Volume 1

Operating techniques, system analysis and propagation, microwave antennas, transmission line and components, microwave semiconductors and tubes. 200 pages.

ARRL Order No. 2901—\$35

Microwave Handbook, Volume 2

Construction techniques, common equipment, microwave beacons and repeaters, test equipment, safety, filters and additional circuit data. 244 pages.

ARRL Order No. 3606—\$35

Microwave Handbook, Volume 3

Microwave theory and practice, reference information, practical designs, hints and tips. Covers 1.3-24 GHz. 284 pages.

ARRL Order No. 3975—\$35



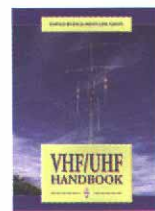
Calling All LowFERs!

The LF Experimenter's Source Book

Food for the dedicated Low Frequency experimenter! In the US, unlicensed "Lowfers" may operate 1-watt between 160 and 190 kHz. Are you up

for the challenge? Antennas, propagation, receivers, transmitters, special modes and test equipment. Plenty of detail for the LF beginner! 146 pages (comb bound).

ARRL Order No. 7148—\$15



VHF/UHF Handbook

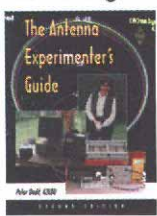
A guide to the theory and practice of VHF/UHF operating and transmission lines. Includes essential background on antennas, EMC, propagation, receivers and transmitters, together with construction details for many projects. Plus, information on specialized modes such as data and TV. 317 pages.

ARRL Order No. 6559—\$35.95

Order Toll Free
1-888-277-5289

Antennas

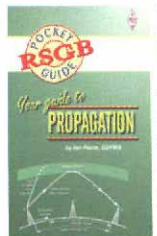
Take the guesswork out of experimenting!



The Antenna Experimenter's Guide

Build and use simple RF equipment to measure antenna impedance, resonance and performance. General antenna construction methods, how to test theories, and using a computer to model antennas. 158 pages.

Order No. 6087—\$25



NEW! Pocket Guide!

Your Guide to Propagation

This handy, easy-to-read guide takes the mystery out of radio wave propagation. It will benefit anyone who wants to understand how to get better results from their station. ARRL Order No. 7296—\$10



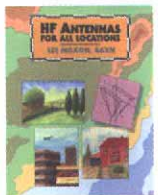
Outstanding Antennas!

HF Antenna Collection

Articles from RSGB's *RadCom* magazine. Single- and multi-element horizontal and vertical antennas, very small transmitting and receiving antennas, feeders, tuners and more. 240 pages.

ARRL Order No. 3770—\$18

Antennas for every situation!

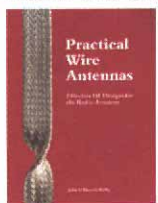


HF Antennas for All Locations

Design and construction details for hundreds of antennas, including some unusual designs. Don't let a lack of real estate keep you off the air! 322 pages.

ARRL Order No. 4300—\$35

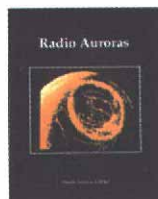
Build the antenna that's right for you!



Practical Wire Antennas

Dive into the practical aspects of HF wire antennas: how the various types work, and how to buy or build one that's right for you. Marconis, Windoms, loops, dipoles and even underground antennas—they're all covered!

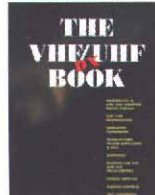
The final chapter covers matching systems. 100 pages. ARRL Order No. R878—\$14



Radio Auroras

Explore the world of Amateur Radio communications via auroral propagation. What causes auroras, how they are forecast and how to best use them to work DX. You'll find an abundance of tables and charts. 96 pages. Order No. 3568—\$18

Operating



The VHF/UHF DX Book

Assemble a VHF/UHF station, and learn about VHF/UHF propagation, operating techniques, transmitters, power amplifiers and EMC. Includes designs for VHF and UHF transverters, power supplies, test equipment and much more. 448 pages. Order No. 5668—\$28

Complete guide to country identification!



RSGB Prefix Guide

DXCC listings by prefix, useful data such as CQ/ITU Zones, hours +/- on UTC and latitude/longitude. Ed 4, October 1998. Order No. 7237—\$12.95

The official IOTA award sourcebook!

RSGB IOTA Directory and Yearbook - 1998/99

Try your hand at island expeditioning! The entire IOTA (Islands on the Air) award material, much statistical information and features many national island programs. ARRL Order No. 6079—\$15

Shipping:

US orders add \$4 for one item, plus \$1 for each additional item (\$9 max). International orders add \$1.50 to US rate (\$10.50 max). US orders shipped via UPS.

ARRL

225 Main St, Newington, CT 06111-1494 tel: 860-594-0355

fax: 860-594-0303 e-mail: pubsales@arrl.org World Wide Web: <http://www.arrl.org/>

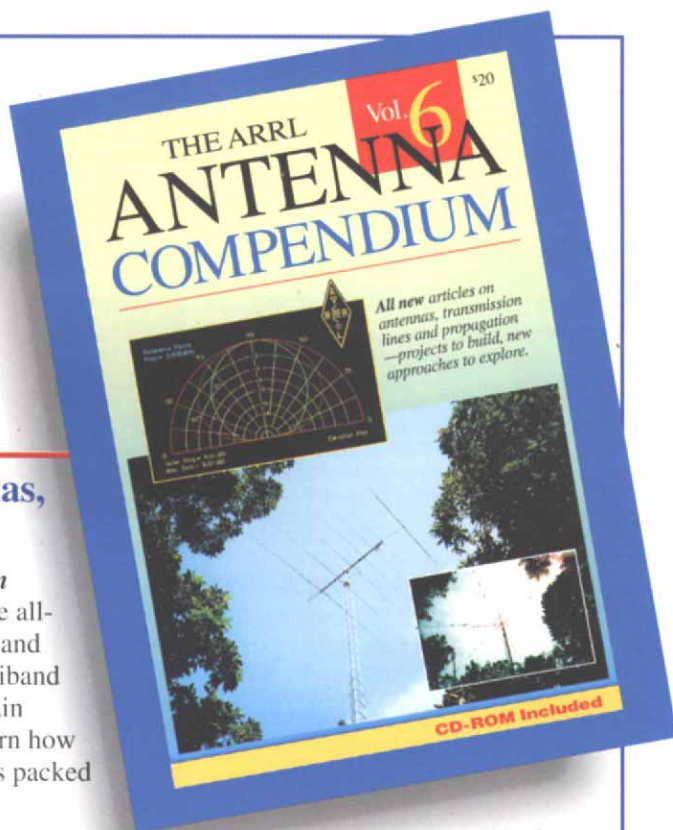
All NEW! 43 Articles

The ARRL Antenna Compendium **VOLUME 6**

More new articles and projects on antennas, transmission lines and propagation.

This latest volume in the popular *ARRL Antenna Compendium* series covers a wide range of antenna-related topics. Among the all-new articles, you'll find nine that deal with low-band antennas and operating, four articles on antennas for 10 meters, four on multiband antennas, and four heavy-duty articles on propagation and terrain assessment. You'll even learn how to motorize a tower, and learn how to safely put up a through-the-roof antenna system. Volume 6 is packed with **Antennas, Antennas and More Antennas**:

- 10-Meter Antennas
- 40, 80 and 160-Meter Antennas
- Antenna Modeling
- Measurements and Computations
- Multiband Antennas
- Propagation and Ground Effects
- Quad Antennas
- Special Antennas
- Towers and Practical Tips
- Tuners and Transmission Lines
- Vertical Antennas
- VHF/UHF Antennas

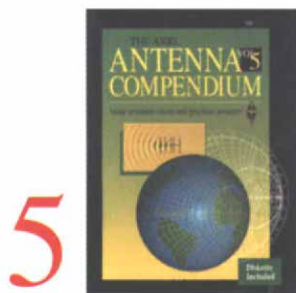


ARRL Order No. 7431 \$20*

*plus shipping \$4 US (UPS)
/\$5.50 International (surface)

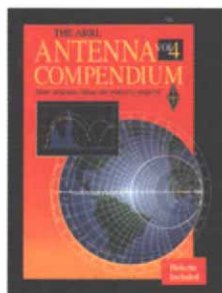
CD-ROM included with N6XMW's innovative propagation prediction program, *XMW*, and input data files for use with commercial modeling software.

ARRL Antenna Compendiums have more antennas — ideas and practical projects



Enjoy excellent coverage of baluns, an HF beam from PVC, low-band Yagis, quads and verticals, curtain arrays, and more!

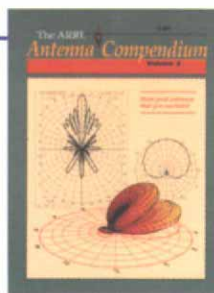
Volume 5—ARRL Order No. 5625 \$20*—Includes software



Loaded with antennas for 80-160 meters, articles for mobile work, portable or temporary antennas, and modeling by computer.

Volume 4—ARRL Order No. 4912 \$20*—Includes software

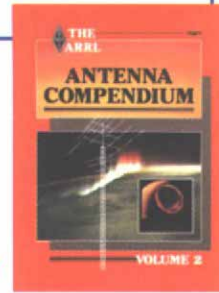
3



Quench your thirst for new antenna designs, from Allen's Log Periodic Loop Array to Zavrel's Triband Triangle. Discover a 12-meter quad, a discone, modeling with MININEC and VHF/UHF ray tracing.

Volume 3
—ARRL Order No. 4017 \$14*

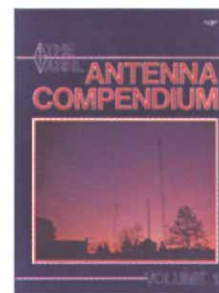
2



Covers a wide range of antenna types and related topics, including innovative verticals, an attic tri-bander, antenna modeling and propagation.

Volume 2
—ARRL Order No. 2545 \$14*

1



The premier volume includes articles on a multiband portable, quads and loops, baluns, the Smith Chart, and more.

Volume 1
—ARRL Order No. 0194 \$10*

ARRL

*Shipping: US orders add \$4 for one volume, plus \$1 for each additional volume (\$9 max.). Orders shipped via UPS. International orders add \$1.50 to US rate (\$10.50 max).